Role of a novel TrkB agonist antibody in positively modulating the architecture and synaptic plasticity of hippocampal neurons in health and disease

Von der Fakultät für Lebenswissenschaften
der Technischen Universität Carolo-Wilhelmina zu Braunschweig
zur Erlangung des Grades einer
Doktorin der Naturwissenschaften
(Dr. rer. nat.)
genehmigte

D i s s e r t a t i o n

von Charlotte Dorothea Alma Judith Tacke
aus Salzgitter

1. Referent:	Prof. Dr. Martin Korte
2. Referent:	Prof. Dr. Reinhard Köster
eingereicht am:	15.12.2020
mündliche Prüfung (Disputation) am:	10.02.2021

Druckjahr 2021

Vorveröffentlichungen der Dissertation

Teilergebnisse aus dieser Arbeit wurden mit Genehmigung der Fakultät für Lebenswissenschaften, vertreten durch den Mentor der Arbeit, in den folgenden Beiträgen vorab veröffentlicht:

Posterbeiträge

Tacke C, Xie J, DiStefano PS , Zagrebelsky M and Korte M. Role of a novel TrkB agonist antibody in modulating the architecture and plasticity of hippocampal neurons. *12th FENS Forum of Neuroscience*, Virtual Meeting (2020).

Tacke C, Xie J, DiStefano PS , Zagrebelsky M and Korte M. Role of a novel TrkB agonist antibody in modulating the structure and function of murine hippocampal neurons. *4th Brainswick Meeting*, Braunschweig (2019).

Tacke C, Xie J, DiStefano PS , Zagrebelsky M and Korte M. Role of a novel TrkB agonist antibody in modulating the structure and function of murine hippocampal neurons. *13th Meeting of the German Neuroscience Society*, Göttingen (2019).

”Awareness Is The Greatest Agent For Change”

(Eckhart Tolle)

Contents

Abstract

Brain derived neurotrophic factor (BDNF), signaling via its receptor Tropomyosin receptor kinase B (TrkB) plays a pivotal role in establishing and maintaining the structure and function of neurons within the central nervous system. Deficits in BDNF/TrkB signaling are reported to contribute to the pathogenesis of multiple major disorders, such as Alzheimer's disease. While manipulating the BDNF/TrkB signaling has been shown to be a viable approach to ameliorate some of the symptoms in a variety of neurological and psychiatric disorders, effective delivery of BDNF into the brain is challenging due to its poor pharmacokinetic profile and clinical translation has fallen short. This triggered the development of BDNF mimetics which specifically activate the TrkB receptor. This work investigated whether a recently identified fully human TrkB agonist antibody (ZEB85) exerts similar biological functions to BDNF. It was shown that treatment with ZEB85 leads to TrkB phosphorylation and increases expression of the activity-dependent immediate early gene c-Fos. Further, ZEB85 significantly increases the neurite complexity of developing hippocampal neurons. Parvalbumin positive interneurons from hippocampal cultures deprived of BDNF have a severely altered dendritic phenotype which can be completely rescued by the TrkB agonist antibody. Moreover, ZEB85 leads to changes in spine number and morphology in mature neurons. Under pathological conditions, treatment with ZEB85 completely prevents amyloid-β induced dendritic spine loss. Lastly, prolonged application of ZEB85 over several days in hippocampal organotypic slice cultures prepared from heterozygous *bdnf* knockout mice, known to have deficits in the induction and maintenance of long-term potentiation (LTP) improved these parameters.

Taken together, ZEB85 indeed exerts some of the biological functions of BDNF as seen in TrkB activation and structural and functional changes of healthy and diseased neurons. However, when directly compared to BDNF, the effect of ZEB85 is less pronounced. Thus, this work provides an initial characterization of a new promising TrkB agonist suggesting its potential value for therapeutical applications.

Zusammenfassung

Der neurotrophe Faktor BDNF, mit seinem über den TrkB Rezeptor nachgeschalteten Signalweg, spielt eine zentrale Rolle bei der Etablierung und Aufrechterhaltung der neuronalen Struktur und Funktion. Defizite in der BDNF/TrkB Signalkaskade stehen im Zusammenhang mit der Pathogenese unterschiedlichster schwerwiegender Erkrankungen, wie der Alzheimer-Krankheit. Die Manipulation dieser Signalkaskade hat sich als wirkungsvoller Ansatz zur Linderung diverser Symptome erwiesen, ist jedoch auf Grund schlechter pharmakokinetischen Eigenschaften und der daraus resultierenden limitierten Verfügbarkeit von BDNF im Gehirn eine Herausforderung. Ein Lösungsansatz bietet die Entwicklung von BDNF Mimetika, die spezifisch den TrkB Rezeptor aktivieren. Die vorliegende Arbeit fokussiert sich auf die Analyse eines kürzlich identifizierten menschlichen TrkB-Agonist-Antikörper (ZEB85) und die Vergleichbarkeit dessen biologischer Funktionen mit BDNF. Ich konnte in dieser Arbeit zeigen, dass eine Behandlung von hippocampalen Neuronen mit ZEB85 neben der TrkB-Phosphorylierung und erhöhter Expression des *immediate early genes* c-Fos zu komplexeren Neuriten in sich entwickelnden Neuronen führt. Darüber hinaus wurde eine erhöhte Anzahl der dendritischen Spines und Reifung der Spinemorphologie gezeigt. In einem Alzheimer-Krankheitsmodellsystem konnte ich zeigen, dass ZEB85 einen pathologischen Spine-Verlust verhindern kann. Funktionelle Defizite in der synaptischen Übertragung bei heterozygoten *bdnf* Knockout-Mäusen wurden durch ZEB85 reduziert, wie durch eine Verbesserung der Induktion und Aufrechterhaltung der Langzeitpotenzierung (LTP) gezeigt werden konnte.

Zusammengefasst übt ZEB85 einige der biologischen Funktionen von BDNF aus; z.B. die TrkB-Aktivierung und strukturelle sowie funktionelle Veränderungen von unterschiedlichen Neuronen. Im direkten Vergleich zu BDNF ist der Effekt von ZEB85 jedoch weniger stark ausgeprägt. Die vorliegende Arbeit stellt eine erste Charakterisierung eines neuen vielversprechenden TrkB-Agonisten mit potentiell hohem Wert für die therapeutische Anwendung dar.

1. Introduction

The human brain looks rather inconspicuous examined from the outside, but is in fact one of the most fascinating and complex organs of the human body. This 1.4 kg heavy jello-like structure is the command center for our physiological and psychological behavior and thus controls our every thought and movement. While the brain had been the focus of study for centuries, it was not until Santiago Ramón y Cajal's detailed descriptions that neurons were identified as the cellular functional and structural units of the brain. This discovery paved the way for modern neuroscience. While the often used statement that there are as many neurons in the human brain as stars in the Milky Way might be exaggerated, the human brain still contains a staggering $\sim$86 billion neurons. Neurons are not a homogenous cell population but can vastly vary both in structure and function. The neurons form intricately complex interconnected neuronal circuits via tiny structures called synapses. The neuronal networks are not static but rather quite plastic. Indeed, one of the many fascinating characteristics of the brain is its capacity to change throughout life. A learning experience can modulate the structure and function of existing synapses, communication junctions between neurons, and even lead to the formation of new synapses. This process, termed synaptic plasticity is indispensable for learning and memory processes and is dependent on plasticity-related proteins such as neurotrophins, in particular Brain derived neurotrophic factor (BDNF). Moreover, due to its organization the hippocampus, a brain region involved in the consolidation of different types of memory, has long been used as a model system to study synaptic plasticity events. Besides for its role as a strong mediator of structural and functional plasticity BDNF is also important for the survival and development of neurons. Due to these crucial functions, alteration in this neurotrophin signaling has been also implicated in the pathogenesis of several neurological diseases.

1.1. The Hippocampus

The hippocampus, a curved bilateral structure is an evolutionary old part of the cortex and is located deep within the medial temporal lobe. The hippocampus is involved in the formation of memories, particularly in those related to declarative memory. This knowledge came mostly from studying patients with hippocampal lesions. The famous patient H.M. suffered of anterograde and partial retrograde amnesia after removal of the medial temporal lobe, including large parts of both hippocampi (Squire, 2009; Augustinack et al., 2014). However, H.M. was still able to retrieve older memories, demonstrating that the hippocampus is not the storage site for long-term memories but rather serves for the processing of memories enabling the storage into higher cortical brain areas (Korte and Schmitz, 2016). Hence, the dependence of a memory on the hippocampus decreases over time (Frankland and Bontempi, 2005). Thus, the hippocampus is involved in the transition from short-term to long-term memory and therefore in the consolidation of information. Further studies have confirmed that the hippocampus is not only essential for the formation of episodic, spatial and contextual memory but also for their recall (Burgess et al., 2002; Eichenbaum, 2004). Interestingly, the functions differ based on location throughout the dorsal-ventral axis of the hippocampus. While the dorsal part of the hippocampus has been associated with spatial learning and memory, the ventral part seems to be associated more to anxiety-related behaviors (Bannerman et al., 2004)

The hippocampus has a unique laminar organization of its neurons and neural pathways, (Figure 1.1 A) making it an ideal model for techniques such as *ex vivo* extracellular recordings for the study of synaptic plasticity, as neuronal projections in hippocampal slices remain largely intact. The hippocampus can be divided into two main anatomical regions: the dentate gyrus (DG) and the cornu ammonis (CA). The latter region is further subdivided into CA1, CA2 and CA3 due to the morphological differences and density of its prevalent excitatory cell type, the pyramidal neurons. The signaling pathway that connects the different anatomical regions of the hippocampus can be depicted as a simplified trisynaptic circuit (Figure 1.1 B). The major input enters the hippocampus from the perforant pathway which projects from the enthorhinal

cortex (EC) to the granule cells of the dentate gyrus. The axons of the granule cells, called mossy fibers, project onto pyramidal neurons of the CA3 area and these in turn are the major input onto neurons of the CA1 area through the Schaffer collaterals pathway. The CA1 neurons then project back to the EC (Andersen et al., 2006; Neves et al., 2008). Besides the region-specific excitatory neurons, the hippocampal formation also contains a vast heterogeneity of inhibitory neurons mediating local inhibition through feedforward and feedback connections (Booker and Vida, 2018) and thus, being important regulators of activity patterns (Gulyas et al., 1999). In contrast to the tightly organized arrangement of both pyramidal neurons and granule cells (Figure 1.1), whose cell bodies are located in densely packed, few cell-layers thick bands (Amaral et al., 2007), the cell bodies of inhibitory neurons are scattered throughout the hippocampus (Pelkey et al., 2017). The axons of most inhibitory neurons, called interneurons, remain local in the subfield However, a small subset also projects to other subareas or even outside the hippocampus (Pelkey et al., 2017; Booker and Vida, 2018).

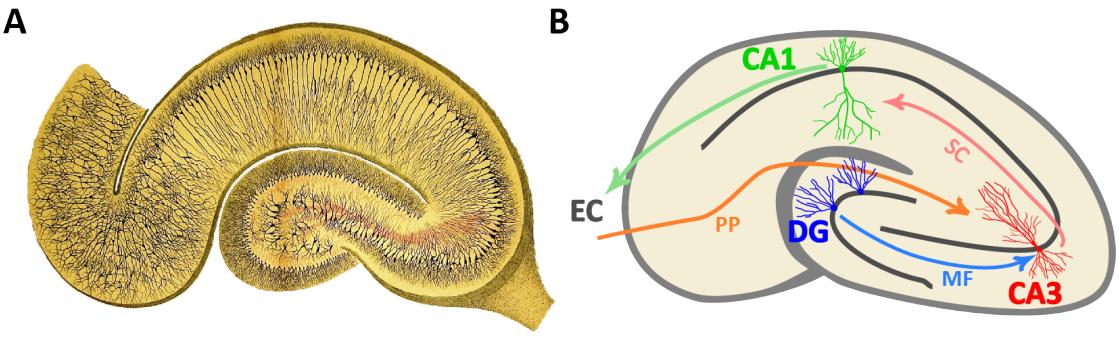

Figure 1.1.: Anatomy and circuitry of the hippocampus.
A, Drawing of a silver chromate stained hippocampal section by Camillo Golgi published in 1903. The hippocampus is organized in transverse lamellae. The cell bodies of the excitatory pyramidal and granule cells are tightly aligned and form an interlocking C-shaped arrangement. ***B,*** Schematic depiction of the hippocampal trisynaptic circuit. Input starts from the enthorhinal cortex (EC) via the perforant path (PP; orange) to the granule cells of the dentate gyrus (DG; blue) and the pyramidal neurons of the CA3 region (red). The granule cells project via their axons, the mossy fibers (MF) to the CA3 neurons. Signals are then transferred via the Schaffer collaterals (SC) to CA1 neurons (green) which then project back to the EC. (Adapted from Korte and Schmitz, 2016; Catani et al., 2013).

1.2. A Brief Insight into Hippocampal Excitatory and Inhibitory Neurons

As mentioned above the principal cell type in the hippocampus are the excitatory pyramidal neurons, which are responsible for transmitting and integrating information for long-term storage in different areas of the brain, putting them at the center-stage of many cognitive processes (Graves et al., 2012). Pyramidal neurons are characterized by a unique pyramidal-shaped soma and two distinct dendritic trees. From the apex of the soma arises typically a main apical dendrite from which smaller oblique dendrites emanate, ending in an apical tuft and several short basal dendrites emerge from the base of the soma (Figure 1.2) as well as the long axon (Benavides-Piccione et al., 2020). While sharing this basic organization, pyramidal neurons differ morphologically from each other depending on the hippocampal sub region (Figure 1.2). Moreover, differences in structure can be even seen within a single region (Raus Balind et al., 2019). The granule cells of the dentate gyrus only have a short apical cone-shaped dendritic tree and are therefore clearly differentiable from the pyramidal neurons.

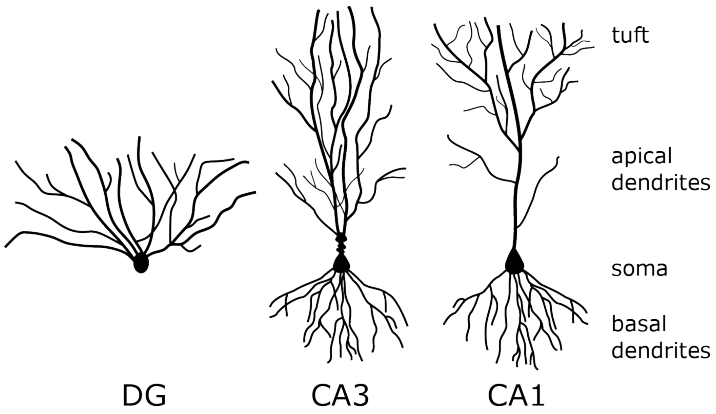

Figure 1.2.: Hippocampal neurons.
Drawings of neurons from different hippocampal regions. Depicted is a granule cell from the dentate gyrus (DG; *left*) and pyramidal neurons from the CA3 and CA1 area. Granule cells only have short apical dendrites, while pyramidal neurons share the basic organization of a triangular soma, basal and apical dendrites. However, the dendritic trees of pyramidal neurons display numerous differences depending on the hippocampal subregion and even within a subregion.

Although making up only about 10-20% of neurons in the hippocampus there is an exceedingly greater heterogeneity in inhibitory neurons in terms of morphology, connectivity and intrinsic and synaptic properties (Maccaferri and Lacaille, 2003;

Booker and Vida, 2018). This is emphasized in the description of 21 classes of interneurons for the CA1 area alone (Klausberger and Somogyi, 2008). The vast majority of interneurons are characterized by the synthesis and release of the neurotransmitter GABA (gamma-aminobutyric acid). One broad subtype of interneurons residing in the hippocampus expresses the calcium-binding protein parvalbumin (PV). This interneuron type preferentially targets the perisomatic region of a postsynaptic neuron and is a critical regulator of pyramidal neuronal activity (Murray et al., 2011; Udakis et al., 2020).

1.2.1. Dendritic Spines and Synaptic Plasticity

The dendrites of excitatory neurons receive the overwhelming majority of excitatory inputs. Specifically dendritic spines, small protoplasmic membrane protrusions, are the primary recipients of excitatory glutamatergic input (Niesmann et al., 2011) and thus form the postsynaptic side of most excitatory synapses. In contrast, synapses of GABAergic interneurons connect directly to the dendritic shaft, the cell body or the axon initial segment (Markram et al., 2004; Mullner et al., 2015; Kwon and Sabatini, 2011). They cover the dendritic tree at high densities, and typically receive input from one excitatory synapse (Nimchinsky et al., 2002). Therefore, the number of spines of a dendritic segment is used to estimate synapse density (Alvarez and Sabatini, 2007). A typical spine consists of a bulbous head connected to the dendritic shaft by a narrow neck (Figure 1.3 A). Due to this structure dendritic spines can control synaptic transmission locally by serving as biochemical micro-compartments (Muller and Connor, 1991; Yuste and Denk, 1995; Bourne and Harris, 2008). The spine head contains the postsynaptic density (PSD), a multiprotein complex consisting of neurotransmitter receptors, ion channels, and signaling systems involved in synaptic transmission (Nimchinsky et al., 2002). Dendritic spines have astonishingly diverse shapes and sizes (Figure 1.3 A), suggesting functional diversity (Nimchinsky et al., 2002). The finding that the size of the spine head, the area of the PSD and the number of neurotransmitter receptors correlate with synaptic enhancement underpins the view that the architecture of spines is coupled to their function (Hering and Sheng, 2001;

Matsuzaki et al., 2004; Kwon and Sabatini, 2011; Bosch and Hayashi, 2012). In addition, dendritic spines are dynamic structures that undergo activity-dependent structural reorganization linking them to processes of synaptic plasticity (Figure 1.3 B). This includes changes in morphology, the elimination of existing and the generation of new spines (Alvarez and Sabatini, 2007; Niesmann et al., 2011; Rochefort and Konnerth, 2012) leading to changes in synaptic connectivity between neuronal partners, affecting the efficacy of synaptic communication and thus ultimately learning and memory (Harms and Dunaevsky, 2007; Holtmaat and Svoboda, 2009). In contrast to excitatory neurons, GABAergic interneurons are mostly devoid of dendritic spines with only a few spiny interneuronal subpopulations reported. It has been reported that these spines also receive excitatory inputs however they present only a fraction of all excitatory synapses made on dendrites of interneurons (Guirado et al., 2014; Foggetti et al., 2019). There is in general little information about dendritic spines of interneurons and therefore not relevant for this study, and not described further.

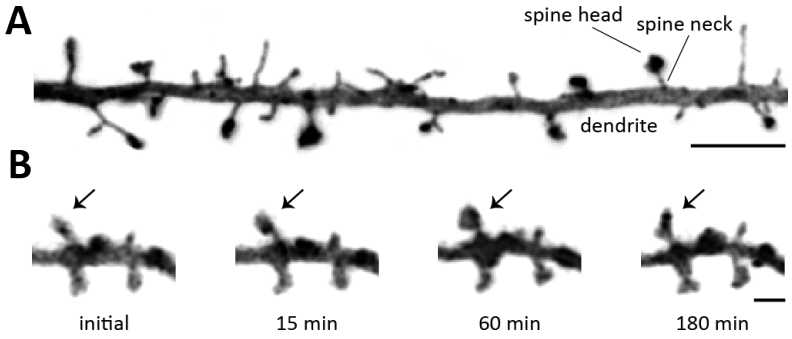

Figure 1.3.: Dendritic spines.
Dendritic spines are small protoplasmic membrane protrusions that are the primary recipients of excitatory glutamatergic input. ***A,*** Spines come in diverse shapes and sizes and typically consist of a bulbous head connected to the dendritic shaft by a narrow neck. Scale bar, 5 µm. ***B,*** Moreover, dendritic spines are dynamic structures that can undergo structural reorganization within minutes (most visibly in the spine indicated by the arrow). Scale bar, 1 µm.

1.2.1.1. Long-Term Potentiation

Synaptic plasticity is considered the cellular basis for learning and memory. Synaptic strength at excitatory synapses is bidirectionally modifiable, hence synaptic transmission can be potentiated or depressed depending on the pattern of stimulation (Lisman, 1989; Shouval et al., 2002; Citri and Malenka, 2008). Induction of long-term

potentiation (LTP) is a widely used experimental model to study synaptic plasticity and is thought to provide an insight into the mechanisms involved in memory formation (Citri and Malenka, 2008). LTP has been investigated most commonly in hippocampal slices, as the organization of the neurons leave the relevant circuit intact when sectioned (section 1.1). LTP is an enduring enhancement of synaptic transmission following a brief, high-frequency stimulation or other induction protocol (Bliss and Lomo, 1973). This phenomenon can persist beyond the period of exposure to the stimulus and can last for hours or even days. Moreover, LTP is input-specific, meaning it is restricted to activated synapses and does not spread to inactive ones on the same neuron (Zhang et al., 2008; Bliss and Cooke, 2011; Hao et al., 2018). Stimulation of the presynapse causes the release of neurotransmitters, i.e. glutamate, which bind to AMPA receptors, triggering the influx of Na^+ and subsequently leading to the depolarization of the postsynapse (Figure 1.4). This leads to the ejection of Mg^{2+} ions which, at near-resting membrane potentials block the ion pore of NMDA receptors. The simultaneous binding of glutamate then allows Ca^{2+} and Na^+ influx into the postsynaptic neuron (Jahr and Stevens, 1993; Garaschuk et al., 1996). Thus, the NMDA receptor functions as a coincidence detector due to the requirement for pre- and post-synaptic depolarization for its activation (Kumar, 2011). The degree of depolarization determines the amount of Ca^{2+} influx into the postsynaptic neuron. The rise in intracellular Ca^{2+} leads to the activation of Ca^{2+}-dependent protein kinases, that mediate the induction of LTP by recruiting AMPA receptors as synaptic sites which results in an increase in the synaptic current (Mammen et al., 1997; Sweatt, 1999; Park, 2018). Long-lasting LTP requires gene transcription and is dependent upon protein synthesis (Frey and Morris, 1997; Kelleher et al., 2004) of factors, such as the plasticity-related protein BDNF (Lu et al., 2008). These functional changes leading to altered synaptic transmission are accompanied by changes in spine morphology (Figure 1.4), leading to spine enlargement (termed structural LTP) and can even lead to an increase in spine number (Van Harreveld and Fifkova, 1975; Matsuzaki et al., 2004; Stewart et al., 2005; Fortin et al., 2010; Bosch et al., 2014). The structural alterations of the synapse, enforcing long-term changes in synaptic strength, might be the basis of circuit reorganization during learning and memory (Zhou et al., 2004; Yang

et al., 2009; Kasai et al., 2010). LTP can be regulated by and is dependent on a variety of molecules including those that also mediate functional changes into structural changes such as Ca^{2+}/calmodulin - dependent protein kinase (CaMKII) and in particular the neurotrophin BDNF (Kang and Schuman, 1995; Figurov et al., 1996; Korte et al., 1998; Xie et al., 2010a; Korte and Schmitz, 2016).

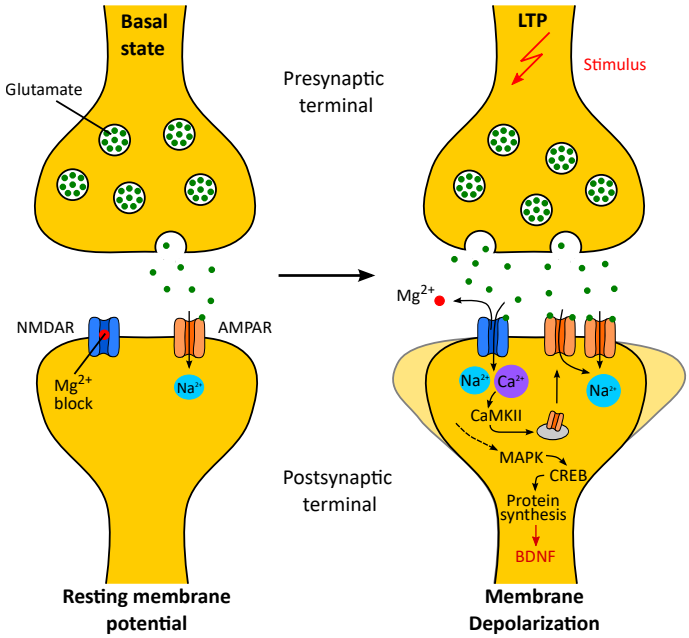

Figure 1.4.: Long-Term Potentiation mediated functional and structural synaptic plasticity.
Simplified illustration of cellular processes at resting membrane conditions and following stimulation. Under resting membrane potential *(left)* Na^+ influx in the postsynaptic terminal is regulated by AMPA receptors (AMPAR), while influx into NMDA receptors (NMDAR) is blocked by Mg^{2+} ions. AMPAR are activated by glutamate, thus the amount of released glutamate determines Na^+ influx. The arrival of an action potential *(right)* at the presynaptic terminal results in increased glutamate release which results in increased Na+ influx through AMPAR in the postsynaptic terminal. The resulting membrane depolarization and glutamate binding to the NMDAR results in the removal of the Mg^{2+} block in the ion channel and allows entry of Na^+ and Ca^{2+} ions. The elevation in cytosolic Ca^{2+} activates Ca^{2+}-dependent enzymes (e.g., CaMKII) facilitating AMPAR trafficking, thereby increasing synaptic strength. The long lasting form of LTP (late LTP) requires protein synthesis of molecules like BDNF. In addition to the functional changes, the potentiated dendritic spine can undergo structural remodeling, such as spine enlargement. (Adapted from Korte and Schmitz, 2016; Kauer and Malenka, 2007).

1.3. BDNF - A Versatile Regulator of Neuronal Function

Brain-derived neurotrophic factor (BDNF) is a secreted protein, belonging to the family of neurotrophins and was first described in 1982 as a factor promoting neuronal survival in the central nervous system (Barde et al., 1982). However, it soon became

apparent that BDNF is essential for multiple aspects of neuronal development and function (Lewin and Barde, 1996; Korte and Bonhoeffer, 1997; McAllister et al., 1999). Among the neurotrophin family members, including nerve growth factor, neurotrophin 3 and 4/5, BDNF has the most abundant and widespread expression in the developing and adult mammalian brain (Murer et al., 2001). Furthermore, BDNF has a particular high expression in the hippocampus (Kawamoto et al., 1996). BDNF has been postulated to be produced exclusively by glutamatergic excitatory neurons in the past but recent studies have indicated that BDNF is released from GABAergic inhibitory neurons as well (Barreda Tomas et al., 2020). In addition, BDNF has been shown to act in a highly localized manner via autocrine and paracrine mechanisms (Murer et al., 2001; Horch and Katz, 2002; Rauti et al., 2020) and the transport and local synthesis of BDNF in dendrites and spines happens in an activity-dependent manner (Aicardi et al., 2004). Fascinatingly, it has been shown that autocrine BDNF/ TrkB signaling can even occur at a single dendritic spine (Harward et al., 2016). These characteristics may serve as a mechanism to precisely regulate BDNF function in space and time (Tongiorgi, 2008).

BDNF is initially synthesized as a precursor proBDNF and then cleaved to form the mature form. While the extent of the intracellular and extracellular processing of proBDNF is still under debate, the majority of studies indicate that proBDNF is secreted in an activity-dependent manner as it is the case for BDNF (Mowla et al., 2001; Nagappan et al., 2009; Gibon and Barker, 2017). BDNF and its precursor bind and activate both pre- and postsynaptically two transmembrane receptors with different affinities: the tropomyosin receptor tyrosine kinase B and the pan neurotrophin receptor p75 ($p75_{NTR}$). BDNF has a higher affinity for TrkB, while $p75_{NTR}$ preferentially binds proBDNF (Teng et al., 2005; Gibon et al., 2016; Gibon and Barker, 2017). Overall, the picture has emerged that TrkB and $p75_{NTR}$ signaling elicit opposing biological effects by promoting survival and facilitating neuronal activity or by initiating pro-apoptotic signaling cascades and suppressing neuronal activity, respectively (Woo et al., 2005; Gibon et al., 2016). However, the $p75_{NTR}$ can have a dual role by either forming a complex with TrkB, leading to an increased affinity of BDNF for the TrkB receptor thereby promoting neuronal survival (Lee et al., 2001; Nykjaer et al., 2005;

Zanin et al., 2019) or by forming a complex with the sortilin receptor which interacts with proBDNF initiating apoptotic signaling (Nykjaer et al., 2005; Teng et al., 2005; Meeker and Williams, 2015; Gibon and Barker, 2017). The role of $p75_{NTR}$ is even more complex and diverse effects have been reported (Chao, 2003; Nykjaer et al., 2005; Yamashita et al., 2005). In general the cross-talk between TrkB and $p75_{NTR}$ is important for the development, maintenance and repair of the nervous system (Haddad et al., 2017).

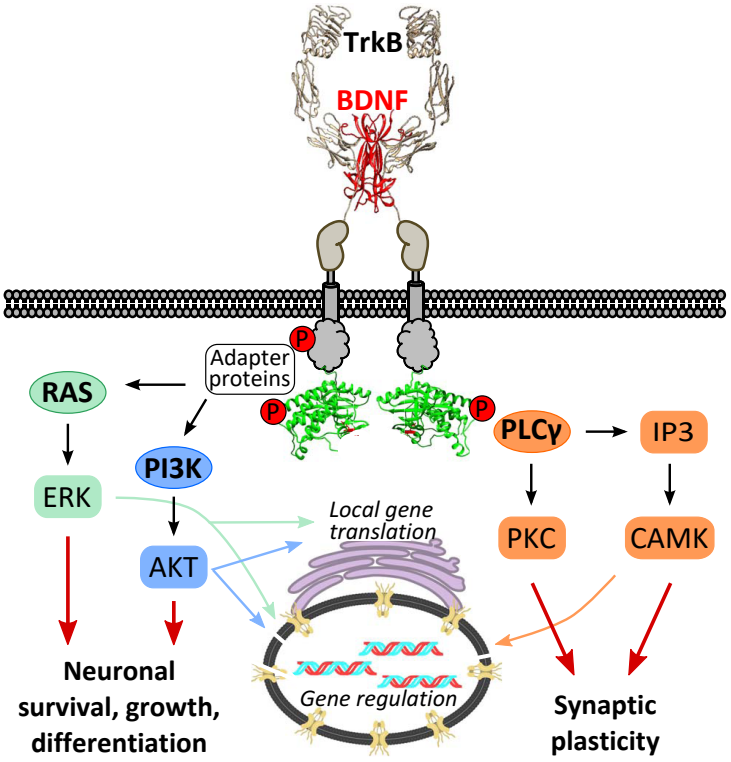

Figure 1.5.: BDNF/TrkB signaling. The binding of BDNF to TrkB results in receptor dimerization and autophosphorylation of specific tyrosine residues in its cytoplasmic kinase domain. This triggers the activation of three major signaling cascades involving the PI3K pathway, the PLCγ pathway and the RAS-ERK pathway. These signaling pathways regulate neuronal survival, growth, differentiation, synaptic plasticity and collectively mediate local protein synthesis and regulate gene expression. (Adapted from Boltaev et al., 2017).

TrkB is a single-pass transmembrane receptor, consisting of a ligand binding site in the extracellular domain, a transmembrane domain and an intracellular tyrosine kinase domain. Binding of BDNF homodimers to TrkB induce receptor dimerization and autophosphorylation of specific tyrosine residues leading to kinase activation. Signaling and adaptor proteins are then recruited to the receptor triggering the activation of three major signaling cascades (Figure 1.5), including the PI3K (phosphatidylinositol 3-kinase) pathway, the PLCγ (phospholipase Cγ) pathway and the RAS-ERK (RAS-extracellular signal-regulated kinase, member of the mitogen-activated protein kinase (MAPK) family) pathway (Boltaev et al., 2017). These pathways account for different cellular responses but collectively mediate local protein

synthesis and regulate gene expression via transcription factors such as cAMP response element binding protein (CREB) (Mayr and Montminy, 2001; Cunha et al., 2010), that ultimately lead to increased neuronal survival, neurogenesis, neuronal growth and differentiation, synaptogenesis and structural and functional plasticity (Kang et al., 1997; Barco et al., 2003; Minichiello, 2009; Cunha et al., 2010; Park and Poo, 2013; Zagrebelsky and Korte, 2014; Boltaev et al., 2017).

1.3.1. BDNF - Long-Term Potentiation

BDNF potentiates excitatory synaptic transmission via pre- and postsynaptic mechanisms. Presynaptically BDNF increases neurotransmitter release of glutamatergic neurons, increasing AMPA receptor-mediated miniature excitatory postsynaptic currents (mEPSCs) (Tyler and Pozzo-Miller, 2001; Rauti et al., 2020). Postsynaptically BDNF seems to strengthen excitatory (glutamatergic) synapses and weaken inhibitory (GABAergic) synapses by altering the activation kinetics of glutamatergic NMDA receptors and inhibitory GABA receptors (Tanaka et al., 1997; Rose et al., 2004; Holm et al., 2009; Kim et al., 2017; Porcher et al., 2018; Rauti et al., 2020). BDNF is one of the crucial mediators of long-term potentiation in the CNS. BDNF knockout mice show severe deficits in the initiation (Korte et al., 1995) and maintenance (Korte et al., 1998) of LTP in the CA1 region of the hippocampus. Similar results were obtained by applying function-blocking BDNF antibodies or TrkB receptor bodies, molecular scavenger of endogenous BDNF, leading to attenuation of LTP (Figurov et al., 1996; Kang et al., 1997; Korte et al., 1998). By using methods to re-express BDNF in BDNF knockout mice the LTP impairment could be restored (Korte et al., 1996; Patterson et al., 1996). BDNF activates distinct mechanisms to regulate the induction and early phase of LTP (Kang and Schuman, 1995; Messaoudi et al., 2002), as well as the maintenance of LTP (Kang et al., 1997; Korte et al., 1998). A recent study compared the roles of presynaptic and postsynaptic BDNF and TrkB to LTP, by selectively deleting them in the CA3 and CA1 regions of the Schaffer collateral pathway (Lin et al., 2018). Presynaptic BDNF is involved in LTP induction, while postsynaptic BDNF contributes to LTP maintenance. The opposite was shown for

TrkB, here presynaptic TrkB is required to maintain LTP, while postsynaptic TrkB is essential for LTP formation. Moreover, a presynaptic role of TrkB in basal neurotransmission was shown (Lin et al., 2018). As mentioned above (section 1.2.1.1) LTP is associated with the enlargement of dendritic spines and it has been demonstrated that postsynaptic BDNF/TrkB signaling is necessary for both functional and structural LTP (Tanaka et al., 2008; Harward et al., 2016).

1.3.2. BDNF - Neuronal Morphology

BDNF is not only a crucial mediator of functional plasticity but is also critical for the fine-tuning of the neuronal network during development (McAllister et al., 1995). In fact, homozygous mice lacking BDNF (Ernfors et al., 1994) or TrkB (Klein et al., 1993) die before the third postnatal week or directly after birth, respectively. Moreover, BDNF is involved in the maintenance of dendritic architecture and can additionally modulate the shape and number of dendritic spines (Murphy et al., 1998; Horch et al., 1999; Ji et al., 2005; Chakravarthy et al., 2006; Gao et al., 2009). The influence of BDNF on the architecture of developing neurons has been mostly demonstrated in culture. For instance it has been shown that BDNF can modulate dendritic growth of developing neurons in the visual cortex, depending on the cortical layer (McAllister et al., 1995, 1997; Lom and Cohen-Cory, 1999). While BDNF promotes neurite growth and complexity in primary developing hippocampal neurons (Ji et al., 2010; Kellner et al., 2014) and demonstrated a highly localized effect in modulating neuronal architecture in brain slices of the visual cortex (Horch and Katz, 2002), the loss of BDNF did not influence neurite architecture in developing hippocampal neurons (Kellner et al., 2014). In addition, knocking out BDNF at early stages of the culturing of primary hippocampal neurons had no influence on the dendritic complexity of mature pyramidal neurons (Zagrebelsky et al., 2018). Further, conditional knockout mice lacking BDNF (Rauskolb et al., 2010) or TrkB (Luikart et al., 2005) showed only minimal (Rauskolb et al., 2010) or no changes at all in dendritic arborization of mature pyramidal neurons of the CA1 region (Luikart et al., 2005). In contrast, substantial evidence points towards the fact that the survival and the dendritic development and maintenance of particularly

GABAergic interneurons strongly depends on BDNF (Mizuno et al., 1994; Kohara et al., 2003; Zagrebelsky et al., 2018) and its receptor TrkB (Zheng et al., 2011; Tan et al., 2018). For example, different types of mature GABAergic interneurons showed severe alterations in dendritic morphology in hippocampal and cortical primary cultures deprived of BDNF at the start of culturing (Zagrebelsky et al., 2018). Furthermore, in the main olfactory bulb dendritic development of PV^+ interneurons was both affected *in vivo* and *in vitro* by deletion of BDNF or by inhibiting the TrkB signaling cascades, respectively (Berghuis et al., 2006). Specifically, PI3K signaling was detrimental for the survival of GABAergic neurons (Berghuis et al., 2006). In addition, BDNF promotes the maturation of GABAergic synapses (Yamada et al., 2002) and by blocking BDNF/TrkB signaling the number of inhibitory synapse, formed on excitatory neurons, is reduced as well (Zheng et al., 2011; Chen et al., 2016a; Yuan et al., 2016), altering the network excitation/ inhibition balance (Huang et al., 1999; Cohen-Cory et al., 2010; Zheng et al., 2011; Tan et al., 2018; Xenos et al., 2018).

1.3.3. BDNF - Dendritic Spines

As already mentioned above, BDNF/TrkB signaling does not only influence neurons on the gross anatomy level but also modulates the shape and number of dendritic spines of excitatory neurons (Murphy et al., 1998; Horch et al., 1999; Chakravarthy et al., 2006; Gao et al., 2009). Previous studies have reported that BDNF application *in vitro* leads to an increase in dendritic spine number (Tyler and Pozzo-Miller, 2001; Ji et al., 2005, 2010) and that BDNF/TrkB signaling is important for the maintenance of dendritic spines as removal of BDNF (Kellner et al., 2014) or blocking TrkB (Tyler and Pozzo-Miller, 2001; Ji et al., 2010) leads to a reduction in spine number and/or prevents the BDNF induced increase in spine number. In an elegant study the influence of TrkB in synapse formation was analyzed by specifically ablating TrkB expression in the presynapse, postsynapse or both at the hippocampal Schaffer collateral pathway. The study provides evidence that TrkB is necessary both at the presynapse and postsynapse for the formation of synapses especially in the temporal window of activity-dependent synapse formation via cell-autonomous mechanisms (Luikart et al., 2005).

BDNF/TrkB signaling does not only influence spine number but is a modifying factor for spine morphology as well. A loss of BDNF resulted in a less mature spine phenotype both *in vitro* (Kellner et al., 2014; Zagrebelsky et al., 2018) and *in vivo* (Rauskolb et al., 2010). Interestingly, acute application of BDNF leads to a spine head enlargement, whereas gradual and slow BDNF application facilitates spine neck elongation (Ji et al., 2010). Furthermore, using two-photon uncaging of glutamate paired with postsynaptic spikes in single dendritic spines of CA1 pyramidal neurons induces a gradual long-term enlargement of spine heads that is mediated by BDNF and dependent on protein synthesis (Tanaka et al., 2008). Surprisingly, by blocking $p75_{NTR}$ signaling, the effects of BDNF on spine density and morphology were prevented (Chapleau and Pozzo-Miller, 2012) further pointing towards a supportive role of the $p75_{NTR}$in BDNF/TrkB signaling. However, not all studies could reproduce the same effect on spine density with BDNF application *in vitro* and reported no change in spine number with the application or overexpression of BDNF (Horch and Katz, 2002; Kellner et al., 2014; Zagrebelsky et al., 2018). For an extensive review on the effects of BDNF on dendritic spines see Zagrebelsky et al. (2020).

Besides the above mentioned functions (Figure 1.6), BDNF also regulates cell fate decisions (Turner et al., 2006; Waterhouse et al., 2012), such as the differentiation and phenotype of GABAergic interneurons (Waterhouse et al., 2012). Moreover BDNF regulates axon growth (Cheng et al., 2011), the patterning of innervation and the expression of proteins crucial for normal neuronal function (Huang and Reichardt, 2001). Furthermore, BDNF/TrkB signaling has been also implicated to be involved in learning and memory processes (Figure 1.6). Indeed, a selective increase in BDNF mRNA and protein (Kesslak et al., 1998; Hall et al., 2000; Mizuno et al., 2000) and TrkB mRNA (Gomez-Pinilla et al., 2001) expression, as well as activation of TrkB (Gooney et al., 2002) was found in the hippocampus following contextual spatial learning. In line with these findings, BDNF and TrkB loss-of-function experiments impaired spatial learning in mice and retention of memory for inhibitory avoidance in mice (Linnarsson et al., 1997; Mu et al., 1999; Alonso et al., 2002; Heldt et al., 2007; Petzold et al., 2015; Blank et al., 2016).

In summary, BDNF production and secretion is highly localized and happens in an activity-dependent manner. In addition, the kinetics of TrkB activation via BDNF seems to be critical for cell signaling and function. Furthermore, BDNF/TrkB signaling has been shown to play a pivotal role in establishing and maintaining the structure and function of neurons within the central nervous system (Figure 1.6). Due to these versatile roles perturbations in BDNF/TrkB signaling may have adverse effects and is correlated to the pathogenesis of several neurological disorders.

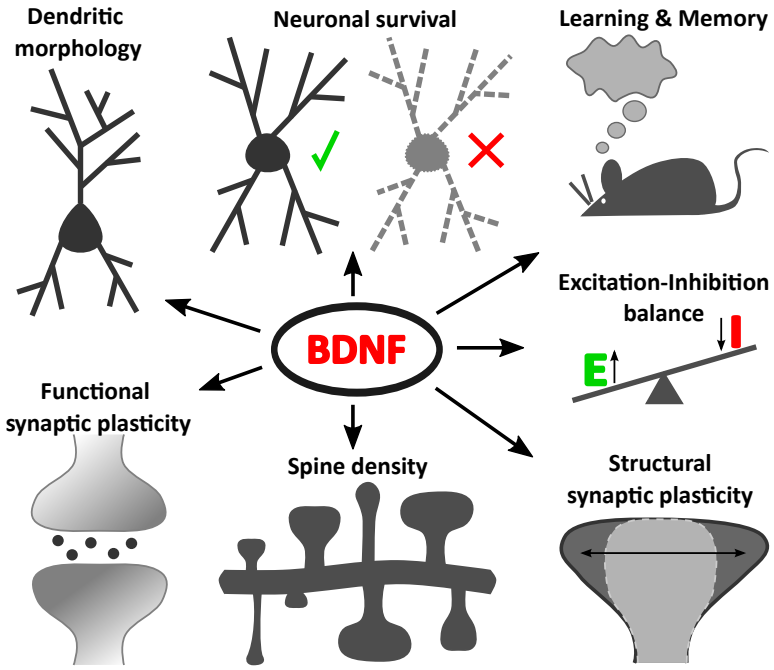

Figure 1.6.: The versatile functions of BDNF.
Among other functions, BDNF/TrkB signaling promotes neuronal survival and is a major player in functional synaptic plasticity thereby changing synaptic properties. BDNF is also involved in the transformation of functional into structural changes and as such modulates spine morphology and spine number. In addition, BDNF affects dendritic morphology, especially of GABAergic interneurons. Moreover, BDNF is implicated in influencing the excitation-inhibition balance by decreasing the strength of inhibitory synapses made onto excitatory neurons. Taken together, BDNF/TrkB signaling is involved in activity-dependent synaptic plasticity (e.g. LTP) and thus affects learning and memory processes.

1.3.4. BDNF - Implications in Neurological Diseases

Alterations in BDNF and TrkB protein or mRNA levels have been observed in brains of postmortem patients and mouse models neuropsychiatric disorders, such as depression (Castren and Rantamaki, 2010), and in the neurodevelopmental disorder Rett syndrome (Chang et al., 2006) as well as in neurodegenerative diseases such as

Parkinson's disease (Mogi et al., 1999; Parain et al., 1999; Howells et al., 2000; Scalzo et al., 2010), Huntington's disease (Ferrer et al., 2000; Zuccato et al., 2001, 2008) and Alzheimer's disease (Phillips et al., 1991; Murray et al., 1994; Ferrer et al., 1999; Narisawa-Saito et al., 1999; Ginsberg et al., 2010; von Bohlen und Halbach, 2010; Jiao et al., 2016). Furthermore, a single-nucleotide polymorphism in the BDNF gene (Val66Met), impairing BDNF release from neurons, has been associated with abnormalities in episodic memory in older adults (Canivet et al., 2015; Kennedy et al., 2015). In addition, some studies suggest that the Val66Met polymorphism confers susceptibility to AD (Fukumoto et al., 2010; Lim et al., 2013; Boots et al., 2017; Franzmeier et al., 2019). Furthermore, higher levels of BDNF were linked to a slower cognitive decline in AD patients (Laske et al., 2011; Buchman et al., 2016). The fact that there is currently no cure for these diseases, especially neurodegenerative diseases, has encouraged the study of the therapeutic potential of BDNF. However, effective delivery of BDNF into the brain is challenging due to its poor pharmacokinetic profile. In particular, BDNF has marginal blood–brain barrier permeability and a short half-life in blood (Poduslo and Curran, 1996; Sakane and Pardridge, 1997; Soderquist et al., 2009) making systemic intravenous delivery of BDNF inefficient. In addition, BDNF diffuses very poorly in and into tissue which also limits the effectiveness of direct injections of BDNF into the central nervous system. These delivery methods are furthermore associated with side effects (Zuccato and Cattaneo, 2009; Weissmiller and Wu, 2012; Kerkis et al., 2020). Thus, alternative BDNF delivery strategies have been explored, such as methods that enable BDNF the crossing of the BBB (Baseri et al., 2012; Chen et al., 2016b; Khalin et al., 2016) or to express BDNF in cells via gene delivery (Yoshimoto et al., 1995; Chang et al., 2006; Xie et al., 2010b; Jiao et al., 2016; de Pins et al., 2019). Alternative approaches use pharmacological agents to increase endogenous BDNF expression (Deogracias et al., 2012) or to directly target the TrkB receptor. The approach of using TrkB agonists that mimic the activation profile of BDNF circumvents the possibility of the undesired production of proBDNF.

1.4. TrkB Agonists - Therapeutic Potential

Several recent studies reported the identification of small-molecule mimetics of BDNF that supposedly act specifically on TrkB (Jang et al., 2010a,b; Massa et al., 2010). Numerous studies have investigated the effect of these small TrkB agonists in the treatment of several neurological disorders in animal models such as Rett Syndrome (Johnson et al., 2012; Li et al., 2017), Alzheimer's disease (Devi and Ohno, 2012; Castello et al., 2014; Gao et al., 2016; Aytan et al., 2018; Chen et al., 2018), Parkinson's Disease (Sconce et al., 2015; Li et al., 2016) and Huntington's disease (Jiang et al., 2013; Simmons et al., 2013; Garcia-Diaz Barriga et al., 2017) and have indeed seen promising therapeutic potential. However, some studies have reported seemingly contradictory results (Park et al., 2012, 2014) and found TrkB-independent mode of actions. Importantly, two independent studies investigating these small molecule TrkB agonists could not detect activation of TrkB or its intracellular signal transduction pathway (Todd et al., 2014; Boltaev et al., 2017), raising doubts about their specificity and potential therapeutic use. TrkB agonist antibodies are another class of BDNF mimetics and have gained recent attention as they have been shown to induce receptor activation consistent with the activation profile upon binding of BDNF (Qian et al., 2006; Todd et al., 2014; Merkouris et al., 2018; Guo et al., 2019; Wang et al., 2020) and have shown therapeutic potential as well, like the recently identified fully human TrkB agonist antibody ZEB85 (Merkouris et al., 2018). ZEB85 was shown to mimic BDNF application both in its potency and effects in human cell lines and, with a slightly lower efficacy also in mouse cortical neurons. Moreover, ZEB85 has been shown to promote, in a similar fashion to BDNF the maintenance of dendritic arbors of axotomized adult mouse retinal ganglion cells in explant cultures (Merkouris et al., 2018), a well-established assay known to depend on BDNF/TrkB signaling.

To sum up, the modulation of BDNF/TrkB signaling has shown to be of relevance as a potential therapeutic strategy in a multitude of neurological disorders and TrkB agonists could provide a powerful therapeutic tool for amelioration/treatment of the aforementioned diseases.

1.5. Aim of the Thesis

Compounds are being developed that specifically bind and activate TrkB which possess a better pharmacokinetic profile than BDNF. These BDNF mimetics, intended to be used as therapeutics in neurological diseases, need to be investigated for their specificity for TrkB as well as for their effects and mechanism of action. This work describes the effects of a treatment with ZEB85, a recently identified fully human TrkB agonist antibody and compares its biological functions to BDNF, the best studied natural TrkB ligand.

First, the specificity of ZEB85 for the TrkB receptor and the activation of downstream signaling was investigated. Previous work showed that ZEB85 application leads to TrkB phosphorylation and activation of downstream signaling molecules with a similar potency to BDNF in a human cell line and with a slightly lower efficacy also induced TrkB activation in mouse cortical neurons (Merkouris et al., 2018).

- This study investigated whether a 5 times or even 50 times lower concentration of ZEB85 still results in TrkB phosphorylation in primary hippocampal cultures.
- Further, the expression of the downstream immediate early gene c-Fos was analyzed following treatment with ZEB85.

As BDNF/TrkB signaling has been shown to be important for the formation, maturation and maintenance of different aspects of neuronal architecture (see 1.3.2 and 1.3.3), the ability of ZEB85 was analyzed to modulate dendritic morphology and dendritic spines.

- The effect of ZEB85 on the dendritic architecture was analyzed in developing excitatory and mature inhibitory primary hippocampal neurons.
- Further, the actions of ZEB85 in modulating spine density and morphology were analyzed in healthy and diseased primary hippocampal neurons.

BDNF is a modulator of activity-dependent synaptic plasticity and has been shown to be a crucial mediator for LTP (see 1.3.1). Whether ZEB85 reproduces the effects of BDNF in regulating the induction and maintenance of LTP was investigated using different slice preparation methods both in wild-type mice and in a BDNF knockout mouse showing deficits in LTP.

2. Material and Methods

2.1. Mouse Strains

Wild-type, floxed BDNF and BDNF knockout mice were kept under a C57Bl/6J background and were bred in the mouse facility of the TU Braunschweig. The floxed BDNF mouse was created in the group of Yves-Alain Barde (University of Basel) by inserting LoxP sites flanking exon IX (5′ loxP at bp 906, 5′ loxP at bp 3449 locus AY057907), the single protein coding exon of *bdnf* (Rauskolb et al., 2010). The heterozygous BDNF knockout mouse were generated by replacing a 560 bp fragment from the BDNF protein-coding exon with a selection marker, thus deleting most of the mature BDNF coding sequence. By injection of embryonic stem cells carrying the altered *bdnf* gene into mouse blastocysts chimeric mice were generated which were further crossed with NMRI females to produce heterozygotes (Korte et al., 1995). Genotypes of the mice were assessed by PCR using genomic DNA purified from tail biopsies as previously described (Rauskolb et al., 2010). The mice were housed on a 12 h light/dark cycle in a temperature-controlled environment (21 $\pm$ 2°C) with food and water provided *ad libitum*. All experimental procedures were approved by the animal welfare representative of the TU Braunschweig and the LAVES (Oldenburg, Germany, Az. §4 (02.05) TSchB TU BS).

2.2. Primary Hippocampal Cultures

2.2.1. Solutions and Media

Borate buffer (pH 8.5)

0.31 g boric acid (Sigma) and 0.475 g sodium tetraborate decahydrate (Sigma) were dissolved in 100 ml sterile MilliQ water.

Poly-L-Lysine stock solution

10 mg/mL Poly-L-Lysin hydrobromide (Sigma) in MilliQ water.

Gey's balanced salt solution (GBSS)

NaCl (Roth)	8.00 g
D(+)-Glucose (Roth)	1.00 g
KCl	0.37 g
KH_2PO_4	0.03 g
$MgCl_2 \cdot 6H2O$	0.21 g
$MgSO_4 \cdot 7\ H2O$	0.07 g
$NaHCO_3$ (Roth)	0.227 g
Na_2HPO_4	0.12 g
$CaCl_2$	0.22 g

Filled up with MilliQ water to 1 l and stored at $4°$C.

The chemicals used were acquired from AppliChem if not stated otherwise.

Preparation solution (pH 7.2)

GBSS	49.5 ml
Glucose (50 %)	0.5 ml

Serum medium

DMEM (Invitrogen)	10 ml
FCS	200 µl

Culture medium for dissociated hippocampal cultures

Gibco Neurobasal medium (Invitrogen)	45 ml
N_2 (10x)	5 ml
B27 (Invitrogen)	1 ml
L-Glutamin (200 mM) (Invitrogen)	125 µl

2.2.2. Preparation of Poly-L-Lysine Coated Coverslips

Glass coverslips (⌀ 13 mm, VWR) were incubated in 10 M NaOH for 3-5 h at $100°$C and afterwards washed multiple times with MilliQ water. The coverslips were sterilized at $255°$C for 8 h and then coated with 0.5 mg/ml poly-L-lysine in boric acid buffer for 2-3 h at $37°$C. Afterwards the coverslips were washed 5 times with MilliQ water, dried and stored in 24-well plates at $4°$C until further use.

2.2.3. Preparation of Primary Hippocampal Cultures

Primary mouse hippocampal cultures were prepared at embryonic day 18 (E18). Therefore, the pregnant mouse was sacrificed by cervical dislocation and the embryos were removed from the uterus and rapidly decapitated. The brains were immersed in ice-cold Gey's Balanced Salt Solution (GBSS), the skin and skull were removed and the upper half of the brain was separated from the lower one (along a line running parallel to the skull base starting below the cerebellum) and kept in fresh ice-cold GBSS. The cerebellum and the colliculi were removed and the two hemispheres were separated. The hippocampi were dissected and incubated in Trypsin/EDTA (Sigma) at $37°$C for 30 min. The digestion was stopped my removing the Trypsin/EDTA solution and by subsequently adding 1 ml of serum medium, followed by multiple washing steps with serum medium. The neurons were further mechanically dissociated with a fire polished Pasteur pipette and centrifuged at 1500 rpm for 5 min. After removing the supernatant and re-suspension in culture medium the neurons were plated at a high density (7×10^4/cm^2), middle density (3.5×10^4/cm^2; TrkB phosphorylation fluorescence) or low density (1×10^4/cm^2; morphology of developing neurons) on poly-L-lysine-coated coverslips. The cultures were incubated at $37°$C, 5% CO_2 and 99% humidity. Once a week 20% of the medium was exchanged.

2.3. Transfection of Primary Hippocampal Cultures

Cultured mature hippocampal neurons were transfected at DIV20 with a DNA plasmid encoding the enhanced green fluorescent protein tagged with a farnesylation

sequence (feGFP, Clonetech) or with the red fluorescent monomeric derivative of DsRed pmApple-N1 (mApple) using Lipofectamine2000 (ThermoFisher Scientific) according to the manufacturer's protocol. Neurobasal (NB) medium was pre-incubated at $37°$C, 5% CO_2 and 99% humidity. In the meantime, 0.8 µg/ well feGFP or mApple and 2 µl/ well Lipofectamine2000 were each diluted in 50 µl/ well NB medium and incubated at room temperature (RT) for 5 min. Afterwards, the two solutions (DNA and Lipofectamine2000) were combined and incubated at RT for further 20 min. The old culture medium was collected and exchanged for 300 µl/ well of fresh NB medium. 100 µl of the transfection solution was added dropwise into each well. After incubating the cultures for 50 min at $37°$C, 5% CO_2 and 99% humidity the transfection medium was exchanged back to the old, previously collected culture medium. After 24 h the neurons were treated for different time periods, depending on the experiment.

2.4. Amyloid-β Oligomer Preparation

The stock solution of soluble Amyloid-$\beta_{1\text{-}42}$ oligomers was prepared as previously described (Takata et al., 2003). The lyophilized 1,1,1,3,3,3-hexafluoro-2-propanol (HFIP)-treated human A$\beta_{1\text{-}42}$ peptides (Bachem) were dissolved in Dimethyl Sulfoxide (DMSO; Invitrogen), sonicated for 20 min, aliquoted, and stored at $70°$C. For the oligomerization process the A$\beta_{1\text{-}42}$ peptides were incubated in PBS (see section 2.6.1) to a final concentration of 33 µM at $4°$C for 24 h. The control contained no peptide but an equal amount of DMSO, incubated in PBS at $4°$C for 24 h as well. After the incubation time the A$\beta_{1\text{-}42}$ oligomers were used for the experiment (see section 2.5).

2.5. Pharmacological Treatments of Primary Dissociated Cultures

The reported small molecule TrkB agonist 7,8-DHF (Tocris) and the TrkB antagonist ANA-12 (Tocris) were dissolved in DMSO at stock concentrations of 10 mM and 50 mM, respectively. 7,8-DHF was used at a final concentration of 0.5 µM and ANA-12

at 50 µM. The TrkB agonist antibody ZEB85 and the control-antibody (GGVV-FC) were provided by Merkouris et al., 2018 at a stock concentration of 1 µg/µl. Both antibodies were used at a final concentration of either 1 µg/ml or 10 µg/ml. Recombinant human BDNF protein (R&D systems) was dissolved in sterile PBS with 0.1% BSA at a stock concentration of 50 ng/µl. BDNF was used at a final concentration of 40 ng/ml. An equal amount of solvent (PBS with 0.1% BSA) was used as a control for BDNF. BDNF and the antibodies were stored at $-70°$C. The following treatments were performed:

Treatment of developing neurons

- Developing primary hippocampal neurons were treated from DIV3 until DIV7 in fresh culture medium with 1 µg/ml and 10 µg/ml of ZEB85-antibody or control-antibody. In addition, as a positive control BDNF (40 ng/ml) was used and the control to BDNF.

Treatment of BDNF deprived cultures

- **Treatment over the entire culturing time with ZEB85-antibody:**
  Primary dissociated hippocampal neurons derived from BDNF floxed mice were either transduced with an AVV-Cre-GFP (Stock titer: 1.5×10^{12} genome copies/ml, multiplicity of infection (MOI): 3×10^4, dilution: 1:354 in culture medium; Addgene Catalog#: 68544) at the day of preparation (DIV0) or not transduced and were treated with 10 µg/ml of ZEB85-antibody or control-antibody on the same day in culture medium. 20% of the culture medium was exchanged once a week in addition to a treatment with ZEB85-antibody or control-antibody. The cultures were fixed at DIV21.
- **Treatment at DIV14 until DIV21 with BDNF:**
  Primary cultures derived from BDNF floxed mice were either transduced with an AVV-Cre-GFP (see above) or not at DIV14 and were treated with BDNF on the same day in culture medium. The cultures were fixed at DIV21.

Treatment with TrkB antagonists and TrkB agonists for c-Fos analysis

- For the analysis of the immediate early gene c-Fos mature cultured hippocampal

neurons (DIV21) were treated with 0.5 µM 7,8-DHF, an equal amount of DMSO, BDNF and 50 µM ANA-12 for 90 min. Or cultures were pretreated with ANA-12 for 30 min after which BDNF was co-applied and cultures were treated for another 90 min in Neurobasal medium.

- Cultures were treated with BDNF, ZEB85-antibody and control-antibody (1 µg/ml and 10 µg/ml) for 2 h or 24 h in Neurobasal medium.

Treatment of mature neurons for spine analysis

- **Treatment with ZEB85-antibody over 24 h:**
  In order to analyze changes in dendritic spine number and spine morphology mature hippocampal neurons (DIV22) expressing feGFP (see 2.3) were treated for 24 h in Neurobasal medium.
- **Pretreatment of Amyloid-β exposed neurons with ZEB85-antibody:**
  In another experiment mature hippocampal neurons (DIV22) expressing feGFP were pretreated with 10 µg/ml of ZEB85-antibody or control-antibody for 15 min in Neurobasal medium, after which oligomerized $A\beta_{1\text{-}42}$ peptides (see 2.4) or the respective control (DMSO in PBS) was added directly into the medium at a final concentration of 500 nM. The cultures were then co-treated for 6 h.

After the respective treatments the hippocampal cultures were fixed with PFA (see section 2.6.1).

2.6. Immunocytochemistry

2.6.1. Solutions and Antibodies

Phosphate buffer (PB; 0.2 M, pH 7.4)

$NaH_2PO_4 \cdot 2H_2O$ (AppliChem)	6.24 g
$Na_2HPO_4 \cdot 2H_2O$ (AppliChem)	24.48 g

Solved in 1 l MilliQ water.

4% Paraformaldehyde (PFA; in 0.1 M PB)

40 g PFA solved in 500 mL 70°C MilliQ water, cooled down, filtrated. 500 mL of 0.2 M PB were added.

10x Phosphate-buffered saline (PBS; pH 7.4)

NaCl	80.0 g
KCl	2.0 g
KH_2PO_4	2.0 g
$Na_2HPO_4 \cdot 2H_2O$	14.4 g

Solved in 1 l MilliQ water. For experiments 1 x PBS was used (referred to as PBS).

Table 2.1.: Primary and secondary antibodies

Primary Antibody	**Species**	**Dilution**	**Reference**
anti-MAP2 IgG1	mouse	1:1000	Sigma-aldrich
anti-c-Fos	rabbit	1:10000	Synaptic Systems
anti-Phospho-MAPK/Erk1/2	rabbit	1:1000	Cell Signaling Technology
Phospho-TrkA (Tyr674/675)/ TrkB (Tyr706/707) (C50F3)	rabbit	1:500	Cell Signaling Technology
anti-parvalbumin	rabbit	1:5000	Swant
Secondary Antibody	**Species**	**Dilution**	**Reference**
anti-mouse IgG-Cy2	goat	1:500	Jackson ImmunoResearch
anti-rabbit IgG-Cy3/Cy5	goat	1:500	Jackson ImmunoResearch

2.6.2. Immunocytochemical Staining of Primary Cultures

The cultures were fixed with 4% PFA for 10 min at room temperature (RT) and washed multiple times with PBS. To block unspecific binding sites and to permeabilize the neuron's membrane, the primary cultures were incubated in blocking solution containing 0.2% Triton X-100 and 1.5% Normal Goat Serum (ThermoFisher) in PBS for 1 h at RT. Subsequently, the cultures were incubated overnight at 4°C with the respective primary antibodies (see table 2.1) diluted in blocking solution. The next day, the cultures were kept for 30 min at RT, followed by washing with PBS (3x for 10 min).

The cultures were then incubated for 2 h at RT in the dark with secondary antibodies conjugated with appropriate cyanine fluorophores (Cy; see table 2.1) diluted in PBS. The cultures were counterstained with 4′,6-diamidino-2-phenylindole (DAPI) diluted 1:1000 in PBS for 10 min and washed with PBS (3x for 10 min). Finally the coverslips were mounted onto glass slides using anti-fading Fluoro-Gel embedding medium (Electron Microscopy Sciences). Slides were stored at 4°C in the dark.

2.7. Image Acquisition and Analysis

Images were obtained using a Zeiss Axio Imager M2 microscope equipped with an ApoTome.2 module and a Zeiss Axiocam 702 mono camera (Carl Zeiss AG). All analysis was performed blind to the treatment.

2.7.1. Dendritic Complexity

Isolated developing MAP2 positive or mature hippocampal neurons expressing mApple were imaged using a 20x (0.8 NA) objective. For analysis of neuronal complexity, the soma and dendrites (or neurites for developing neurons) of neurons were traced with Neurolucida 9 (MicroBrightField) and analyzed with the Neurolucida explorer (MicroBrightField). Different parameters were used to investigate neuronal complexity such as Sholl analysis (Sholl, 1953) which quantifies the number of dendritic intersections at 10 µm incremental intervals starting from the soma (Figure 2.1), the number of branching points, the number of primary dendrites and the total dendritic length.

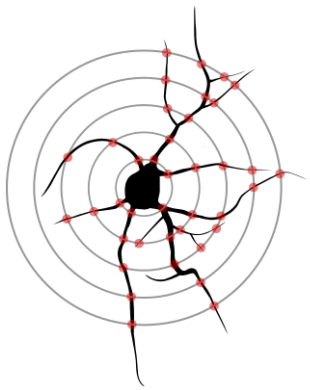

Figure 2.1.: Scheme of Sholl analysis.
Sholl analysis is a method of quantitative analysis of neuronal dendritic morphology. This analysis quantifies the number of dendritic crossings that occur at defined distances from the soma in concentric circles, as indicated by the red circles.

2.7.2. Dendritic Spine Density and Spine Morphology

Second to third order dendritic branches from feGFP expressing hippocampal neurons were imaged with a 63x (1.4 NA, oil) objective using the ApoTome.2 module to acquire 3D-stacks sectioned at 0.25 µm intervals. Spines were counted and measured using the multipoint and the segmented line tools of ImageJ (National Institutes of Health). Spine density was calculated by dividing the number of dendritic spines per the length of dendritic segment. For dendritic spine morphology the length (measured from the spine base at the dendrite to the spine tip), the head width (at the largest diameter) and the neck width (at the thinnest diameter) of dendritic spines were measured. These parameters were used to categorize them into three subtypes: thin, stuby, mushroom and filopodia (see Figure 2.2), as previously described (Zagrebelsky et al., 2005). Spines with a filopodia-like structure were excluded from analysis, as this spine type usually lacks a PSD and is not apposed by a presynaptic axon, thus often considered a precursor of a dendritic spine (Berry and Nedivi, 2017; Furutani and Yoshihara, 2018).

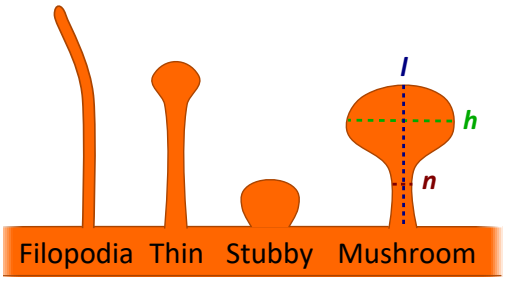

Figure 2.2.: Dendritic spine types.
Dendritic spines can be categorized into 4 subtypes depending on their shape: filopodia, thin, stubby and mushroom. Therefore the **spine length** (**l**; measured from the the spine base at the dendrite to the spine tip), the **head width** (**h**; measured at the largest diameter) and the **neck width** (**n**; measured at the thinnest diameter) of individual spines was measured.

2.7.3. Canonical Signal Transduction

For the analysis of the immediate early gene downstream of the TrkB receptor c-Fos positive neurons, identified over MAP2 positive neurons were imaged with a 10× (NA 0.3) objective. Areas with a similar neuronal density were chosen and the selection was based on the MAP2 staining alone. Moreover, the exposure time for each excitation wavelength, set to the control of BDNF or to the control-antibody, was kept constant across different treatments within the same experimental repetition. For the analysis all MAP2 positive neurons were counted first using the multipoint selection

tool in ImageJ. The c-Fos antibody show low staining in almost all neurons but with different intensities. Therefore, in order to count c-Fos positive neurons a threshold was set. Thus, the mean gray value from nuclei with a low fluorescent intensity but still considered to be c-Fos positive was measured from multiple neurons and averaged. Then, only neurons that were above the chosen threshold, kept constant across one experimental set, were counted as positive. The percentage of c-Fos positive neurons was calculated by dividing the number of c-Fos positive neurons by the number of MAP2 positive neurons.

2.7.4. TrkB Phosphorylation

TrkB activation was analyzed for the TrKB phosphorylation site Tyr706/707 (pTrkB). Therefore, primary isolated dendrites from mature MAP2 labeled hippocampal neurons were randomly chosen and imaged with a 63x (1.4 NA, oil) objective. The exposure time for the pTrkB and MAP2 immunostaining, set to the control of BDNF, was kept constant across different treatments within the same experiment. Background fluorescence for pTrkB was calculated for each neuron individually by placing small regions of interest (ROIs) in ImageJ along the dendrite in areas with no pTrkB fluorescence and by averaging the mean grey value of the ROIs per dendrite. Puncta density, area and fluorescence intensity of pTrkB was detected in SynPAnal (Danielson and Lee, 2014) after subtraction of 2x background.

2.8. Electrophysiology

The hippocampal circuit organization enables the study of activity-dependent synaptic plasticity *ex vivo*, as the transversal hippocampal slice preparation keeps the synaptic circuits and the cytoarchitecture of the hippocampus largely intact.

2.8.1. Artificial Cerebrospinal Fluid

Artificial cerebrospinal fluid (ACSF) mimics the extracellular fluid of the brain and provides vital conditions for neuronal tissue (i.e. brain slices) by maintaining

Table 2.2.: Composition of Artificial cerebrospinal fluid (ACSF)

Substance	**Low Mg^{2+} ACSF [mM]**	**High Mg^{2+} ACSF [mM]**
NaCl	125	125
KCl	2.5	2.5
$NaH_2PO_4 \cdot H_2O$	1.25	1.25
$MgCl_2 \cdot 6H_2O$	1	2
$NaHCO_3$	26	26
D(+)-Glucose	25	25
$CaCl_2 \cdot 2H_2O$	2	2

homeostasis, osmolarity and pH at physiological levels. In order to supply the brain slices with enough oxygen and to reach a physiological pH of 7.3 the ACSF was constantly carbogenated (95% O_2, 5% CO_2). For the preparation of acute hippocampal slices an ACSF containing a high Mg^{2+} concentration (2 mM; see table 2.2) was used to prevent a pre-potentiation of the slices by inhibiting the Mg^{2+} block release from the NMDAR during slice preparation. For the resting period and during recording of the acute slices a low Mg^{2+} concentration (1 mM) was used. For the recording of organotypic hippocampal slices high Mg^{2+} ACSF was used.

2.8.2. Preparation of Acute Hippocampal Slices

Male 6-8 week old C57Bl/6J wild-type mice were briefly anesthetized with Isoflurane (Baxter Healthcare Corporation) and subsequently rapidly decapitated. The brain was quickly, in less than 90 s, removed from the skull and transferred into ice-cold (4°C), carbogenated (95% O_2 and 5% CO_2) high Mg^{2+} ACSF for 3 min. To reduce oxidative stress ice-cold ACSF was used in the following preparation steps as well. After removal of the cerebellum and prefrontal cortex, the two hemispheres were separated. The surrounding striatal tissue was removed from the hippocampus at the medial side. By placing a rounded spatula underneath the fimbria hippocampi and by using another spatula to free the hippocampus from the subiculum, the hippocampus could be folded out of the remaining cortical tissue. In all preparation steps stretching and direct touching of the hippocampus was avoided. Both hippocampi were glued with their

ventral end on a specimen plate leaning upright against an agar block (2%; AppliChem) with the dentate gyrus facing the agar. Using a vibrating microtome (VT 1200S; Leica) the hippocampi were sectioned into 400 µm thick transversal slices while being submerged in ice-cold ACSF. The slices were transferred directly into a custom-made holding submerged chamber constantly perfused with carbogenated low Mg^{2+} ACSF at RT. The slices were allowed to rest and recover for at least 90 min before starting the electrophysiological recordings.

2.8.3. Organotypic Hippocampal Slice Cultures

The organotypic brain slice cultures derived from neonatal brains have the advantage over acute brain slices that they can be maintained *in vitro* over multiple weeks and therefore enable a prolonged treatment with drugs.

2.8.3.1. Solutions and Media

Kynurenic acid

0.946 g kynurenic acid (Sigma) dissolved in 5 ml 1 M NaOH, 45 ml MilliQ water added, filtered sterile, and stored in fractions at $-20°$C.

Preparation solution (pH 7.2)

GBSS	98 ml
Glucose (50 %)	1 ml
Kynurenic acid	1 ml

Culture medium for Organotypic Hippocampal Slice Cultures

BME Medium (Invitrogen)	100 ml
HBSS (Invitrogen)	50 ml
Horse serum (Hyclone)	50 ml
L-Glutamine (200 mM; Sigma)	1 ml

Mitotic inhibitors

Uridin 2.422 mg in 10 ml MilliQ water (1 M).

Cytosine-β-D-arabinofuranoside * hydrochloride 2.79 mg in 10 ml MilliQ water (1 M).

5-fluoro-2′-deoxyuridine 2.462 mg in 10 ml MilliQ water (1 M).

Stock solutions were mized 1: 1, sterilized by filtration and freezed fractions at $-20°$C.

The mitotic inhibitors were acquired from Sigma.

2.8.3.2. Preparation of Organotypic Hippocampal Slice Cultures

Organotypic hippocampal cultures were prepared as previously described (Stoppini et al., 1991; Michaelsen-Preusse et al., 2014). Heterozygous BDNF knockout mice of either sex were decapitated on postnatal day 4/5 (P4/5) and the dorsal part of the brain was dissected and removed. Further preparation steps were performed in a petri dish placed on a cooling pad, filled with ice-cold preparation solution. After removing the remaining cerebellum and meninges from the brain, the hemispheres were separated and the hippocampi were isolated. Transversal slices were cut using a tissue chopper (McIlwain) at a thickness of 400 µm. Slices were transferred back to the petri dish and kept at $4°$C for 15-30 min. Afterwards the slices were positioned on Millicells© membrane inserts (Millipore), which were placed into wells filled with 1.1 ml pre-warmed medium, and cultivated at $37°$C, 5% CO_2 and 99% humidity. Three days after preparation 15.4 µl of a mixture of mitotic inhibitors (see Mitotic inhibitors, 2.8.3.1) was added into the medium for 24 h followed by a complete medium exchange. Every seven days half of the medium was exchanged.

2.8.4. Technical Equipment for Extracellular Field Recordings

For all electrophysiological recordings two submerged setups with similar technical equipment were used. Hippocampal slices were electrically stimulated with a lacquer coated monopolar tungsten electrode (WPI, USA) with a resistance of 0.1 MΩ. An Ag/AgCl pellet (E201, WPI), being suspended in ACSF in the recording chamber, served as an indifferent electrode by a connection to the positive pole of the stimulation electrode. Stimuli, programmed in the master pulse generator Master 8

(A.M.P.I.), could be given to the slices via a connection of the negative pole of the stimulation electrode to a stimulus isolator (A360 or A365, WPI). The hippocampal slices were stimulated with rectangular current pulses lasting 200 µs at a frequency of 0.1 Hz with different stimulus currents, dependent on the slice preparation (acute hippocampal slices or organotypic hippocampal slice cultures; see 2.8.5 and 2.8.6) and slice quality. The generated field excitatory postsynaptic potentials (fEPSPs) were recorded with a borosilicate glass capillary (0.58 x 1.00 x 100 mm, Biomedical Instruments) with a resistance of 1-3 MΩ, filled with 3 M NaCl. The recording electrodes were pulled with a Flaming/Brown Micropipette Puller (P-97, Sutter Instruments). The submerged recording chamber (RC-22, Warner instruments), the electrical micromanipulator (SM-5, Luigs and Neumann or Nano-Stepper, WSE Electronics) for the recording electrode, the mechanical micromanipulator (Leitz) for the stimulation electrode and a stereo microscope (SMZ 654, Nikon or Leica Microsystems) were fixed onto a vibration dampened table (Spindler & Hoyer and TMC). The recording chambers were fixed onto an aluminum heating base (PH-1, Warner Instruments) connected to a thermistor. In addition, a preheating element (in-line solution heater SC-20, Warner Instruments) as well as the heating base were connected to an adjustable Dual Channel Heater Controller (TC-334B, Warner Instruments) to ensure a constant temperature of 32 $\pm$ 0.2°C. Hippocampal slices were constantly perfused with carbogenated ACSF at a flow rate of 1.5 ml/min adjusted with a peristaltic pump (Ismatech, Switzerland). Silicon tubings (PharMed® Ismaprene, Ismatec) were used to prevent sticking of the antibodies to the tubing walls.

2.8.5. Extracellular Field Recordings of Acute Hippocampal Slices

Acute hippocampal slices were placed in a submerged recording chamber after the resting time of 90 min. They were treated with 1 µg/ml of ZEB85-antibody or the control-antibody diluted in 40 ml low Mg^{2+} ACSF, circulating in a closed loop. Field excitatory postsynaptic potentials (fEPSPs) were recorded in the stratum radiatum of the CA1 region in hippocampal slices after 1 h of pretreatment. The Schaffer collaterals were

electrically stimulated and fEPSPs were recorded at a depth of ∼130-170 µm. At the beginning of each recording the maximal stimulus strength in which a population spike in the fEPSP slope started to appear was identified. In order to investigate long-term synaptic changes in synaptic plasticity, the stimulus strength for the recordings was set to 40% of the maximal fEPSP slope. The stimulus current ranged from 25-40 µA. After 20 min of stable baseline recordings, long-term potentiation (LTP) was induced in the hippocampal slice by theta-burst stimulation (TBS; 10 trains of 4 pulses at 100 Hz in a 200 ms interval, repeated 3x) and measured for 60 min.

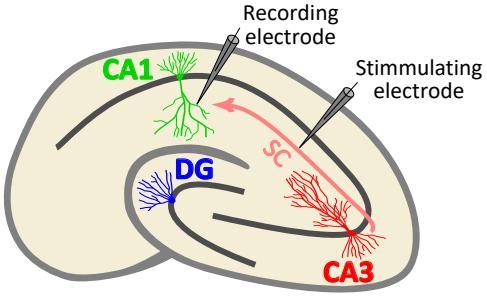

Figure 2.3.: Electrode positioning in a hippocampal slice.
The stimulation electrode was placed in the CA3 region of the hippocampus to stimulate the Schaffer collateral pathway (SC). The recording electrode was positioned in the stratum radiatum of the CA1 region. (Adapted from Korte and Schmitz, 2016).

2.8.6. Extracellular Field Recordings of Organotypic Hippocampal Slices

Organotypic hippocampal slices from heterozygous BDNF knockout mice were treated on DIV16 with 10 µg/ml of ZEB85-antibody or control-antibody added to the culturing medium, and were recorded on DIV21-22. The organotypic hippocampal slices were recorded similar to the acute hippocampal slices (see section 2.8.5) with a few adjustments. The organotypic slices were individually cut out of the membrane and placed into the submerged recording chamber with circulating high Mg^{2+} ACSF. To keep the slice into place a small grid (Warner Instruments) was placed onto the surrounding membrane, without it touching the slice itself. As the organotypic hippocampal slice cultures flatten over the culturing time, fEPSPs were recorded at a depth of only ∼35–70 µm. Moreover, these slices were hyperexcitable and often times did not recover after increasing the stimulus intensity shortly. Therefore the maximal stimulus strength in which a population spike in the fEPSP slope started to appear could not be defined. Instead the stimulation intensity was adjusted to an equal fEPSP slope of -0.2 mV/ms for all measured slices on the same recording day. The stimulus current ranged from 7-10 µA and LTP was recorded for only 30 min.

2.8.7. Data Acquisition and Analysis

The fEPSP response was recorded in bridge mode and 200x amplified by the Axoclamp2B differential amplifier (Axon Instruments Molecular Devices). Furthermore the signal was filtered (LHBF-48X, NPI Electronic and Hum Bug, Quest Scientific). For online monitoring during recording and analysis, programs written by M. Korte and V. Staiger (DAP Version 4.751 and ANA-DAP version 4.755 respectively) based on the National Lab View Software (National Instruments) were used. For analysis the negative slope of the elicited fEPSP signal was measured in a defined manually set window with the analyzing software, generating Microsoft Excel files containing the single values of each fEPSP slope measurement per 10 s. For the LTP recordings the mean value for 1 minute was calculated out of 6 values of fEPSP slopes. To plot the LTP data as an increase compared to basal synaptic activity, all fEPSP slopes for the baseline (20 min for acute slices; 10 min for organotypic slices) were averaged and set to 100%. The slope sizes obtained after TBS induction were normalized to baseline and calculated as following:

$$\frac{SlopefEPSP_{\text{minute}}}{SlopefEPSP_{\text{baseline}}} \times 100$$

For the experiments on acute slices only recordings that lead to an induction of LTP were analyzed while for the organotypic slices all recordings were included, even if LTP could not be induced. Experiments with an unstable baseline (variability $> \pm$ 10% for acute slices and $> \pm$ 20% for organotypic slices) were excluded.

2.9. Statistical Analysis

Statistical analysis and graph plotting was done with GraphPad Prism 6 (GraphPad Software Inc.). Data is presented as mean $\pm$ SEM. A two-tailed unpaired Student's t-test was used to compare two treatment groups. For the comparison of more than two groups a one-way ANOVA followed by a Bonferroni's multiple comparisons post-hoc test was used. For Sholl analysis and spine phenotype analysis, a regular two-way ANOVA

and for electrophysiological measurements a two-way ANOVA with repeated measures was performed, each followed by a Bonferroni's multiple comparisons post-hoc test. Minimum significance was considered for p value < 0.05. Each statistical test used for an experiment is stated in the respective figure legend.

3. Results

BDNF mimetics that specifically activate the TrkB receptor are being developed to be used as tools for basic research as well as potential therapeutics in neurological diseases. This thesis investigated the effects of ZEB85, a recently identified fully human TrkB agonist antibody, on the structure and function of primary hippocampal murine neurons under physiological and pathological conditions and compared its biological functions to BDNF.

3.1. c-Fos Expression as a Readout for TrkB Activation

The small-molecule compound 7,8-dihydroxyflavone (7,8-DHF), reported to act specifically on the TrkB receptor (Jang et al., 2010b), has shown promising effects in the treatment of several neurological diseases in animal models (Johnson et al., 2012; Zhang et al., 2014; Garcia-Diaz Barriga et al., 2017; Aytan et al., 2018). However, two recent independent studies investigating 7,8-DHF among other compounds, could not detect activation of TrkB or its intracellular signal transduction pathways (Todd et al., 2014; Boltaev et al., 2017). This first experiment investigated if the latter findings could be confirmed or refuted by testing if 7,8-DHF is able to induce the expression of c-Fos.

The activity-dependent immediate early gene *c-fos* is implicated in influencing excitability and survival of hippocampal neurons (Dong et al., 2006) and has been shown to be important for some forms of learning tasks and memory consolidation (He et al., 2002; Gallo et al., 2002). As the transcription of c-Fos is upregulated upon BDNF-mediated TrkB signaling (Marty et al., 1996; Pizzorusso et al., 2000; Gascon et al., 2005; Ohba et al., 2005; Meier et al., 2011), the analysis of c-Fos expression can be used as a tool to quickly investigate compounds that supposedly modulate TrkB activity. Thus, primary hippocampal cultures DIV21 were treated for 90 min with 7,8-DHF (0.5 µM dissolved in DMSO), DMSO as a negative control and BDNF

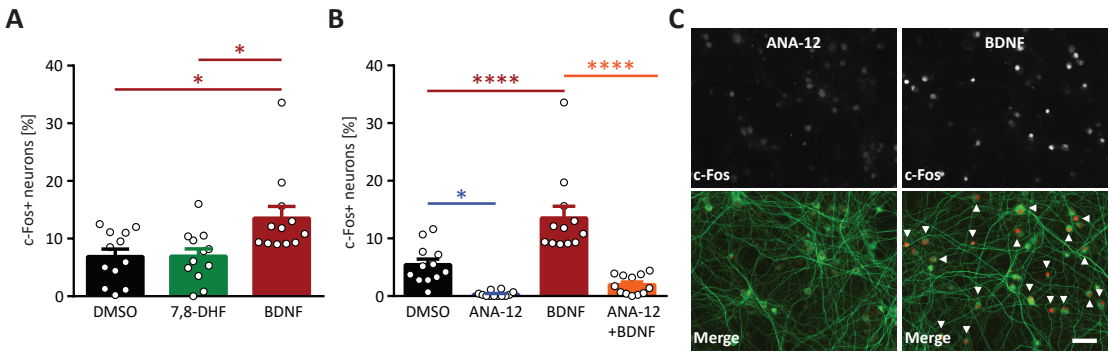

Figure 3.1.: c-Fos expression as a readout for TrkB activity.
Primary hippocampal cultures DIV21 were treated with BDNF, a suggested TrkB agonist (7,8-DHF) and a TrkB antagonist (ANA-12). ***A and B***, Graphs show the number of c-Fos positive neurons calculated over total MAP2 positive neurons. ***A***, Cultures were treated for 90 min and **B**, for a total of 120 min.**C**, Representative image details of neurons immunostained for MAP2 and c-Fos (above) and with the corresponding merged images (below). Examples of two treatment groups (ANA-12 and BDNF) are shown. The arrows (white) in the merged image indicate c-Fos expressing MAP2 positive neurons. Scale bar, 50 µm. Data in graphs is represented as mean + SEM and circles show the number of coverslips (CS) analyzed. Per CS 7 fields of view were analyzed. Data is obtained from 12 CS from 4 independent experiments. Statistics used: One-way ANOVA followed by Bonferroni's multiple comparisons post-hoc test. *$p < 0.05$, ****$p < 0.0001$.

(40 ng/ml; diluted in DMSO) as a positive control. The analysis was performed by counting c-Fos positive nuclei over MAP2 positive neurons. The quantification revealed that application of 7,8-DHF did not result in any increase in c-Fos expression compared to control treated cultures (Figure 3.1 A), while treatment with BDNF resulted in a significant increase in the number of c-Fos positive neurons compared to the control and 7,8-DHF (Figure 3.1 A; $p < 0.05$; Table B.1). In a second experiment the sensitivity of this approach to detect changes in c-Fos expression was tested with the application of a TrkB antagonist (Cazorla et al., 2011). Primary hippocampal cultures were pre-treated with the low-molecular weight TrkB antagonist ANA-12 (50 µM) for 30 min after which BDNF was co-applied and cultures were treated for another 90 min. Treatment with ANA-12 markedly decreased the number of c-Fos positive neurons compared to the control treatment (Figure 3.1 B; $p < 0.05$; Table B.1). Moreover, the co-treatment of ANA-12 together with BDNF prevented the increase in c-Fos positive neurons significantly compared to BDNF treatment alone (Figure 3.1 B; $p < 0.0001$; Table B.1). The difference in c-Fos expression between the TrkB antagonist ANA-12 and the ligand of the TrkB receptor, BDNF, is also clearly visible in the exemplary images (Figure 3.1 C; Table B.1).

In summary, the results support the finding that 7,8-DHF does not lead to the activation of the signaling downstream of the TrkB receptor as evaluated by c-Fos expression. Moreover, both the application of BDNF and a TrkB antagonist have proven that this method is adequate to detect changes in c-Fos expression.

3.2. Concentration and Time-Depended Effect of ZEB85-Antibody on c-Fos Expression

As the results from the previous experiment suggest, the previously reported TrkB agonist 7,8-DHF most likely does not lead to receptor activation. Therefore, a different compound, i.e. ZEB85-antibody, was tested for its ability to induce c-Fos expression. First, it was analyzed whether a 24 h treatment with ZEB85-antibody results in an increase in c-Fos expression. Thus, DIV21 primary hippocampal neurons were stimulated with a low (1 µg/ml) and a high (10 µg/ml) concentration of ZEB85-antibody or control-antibody. BDNF served as a positive control. Representative images are shown in Figure 3.2 A. The analysis was performed by counting c-Fos positive nuclei over MAP2 positive neurons. Treatment with either 1 µg/ml ZEB85-antibody (Figure 3.2 B; $p < 0.05$; Table B.2) or BDNF ($p < 0.001$) resulted in a significant increase in the number of c-Fos positive neurons compared to the control-antibody. Moreover, the number of c-Fos positive neurons between the BDNF and ZEB85-antibody treatments did not differ significantly. In contrast, a 24 h treatment with 10 µg/ml of ZEB85-antibody did not lead to an increase in c-Fos positive neurons compared to the respective concentration of the control-antibody, but rather even to a significant decrease (Figure 3.2 C; $p = 0.036$; Table B.2). As the peak activation time of c-Fos upon BDNF stimulation is around 90-120 min (Kovacs, 2008; Chowdhury and Caroni, 2018), it was assessed if a more acute application of ZEB85-antibody resulted in an increase of c-Fos expression as well and if there were any differences between the two concentrations of ZEB85-antibody. In contrast to the longer treatment, a short treatment of 2 h showed the opposite results. The high concentration of ZEB85-antibody resulted in a significant increase in c-Fos positive neurons (Figure 3.2 D, $p = 0.01$; Table B.3) while the low concentration had no effect compared to the

respective concentrations of the control-antibody. However, the two concentrations of the control-antibody differed significantly (Figure 3.2 D, p = 0.01; Table B.3).

In summary, ZEB85-antibody increases c-Fos expression differently depending on treatment duration and antibody concentration.

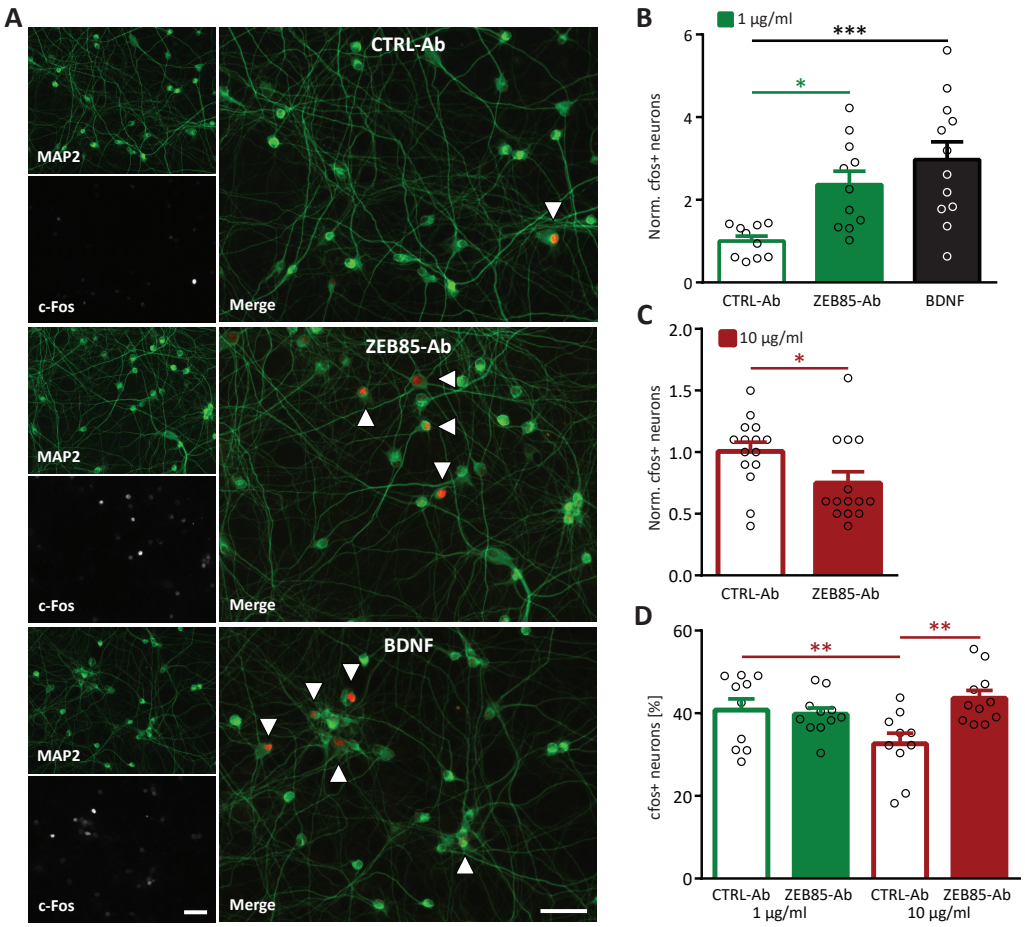

Figure 3.2.: ZEB85-Antibody induces c-Fos expression in a time- and concentration-dependent manner.
Primary hippocampal cultures DIV21 were treated with two concentrations of ZEB85-antibody (ZEB85-Ab) and control-antibody (CTRL-Ab) or with BDNF for either 24 h or 2 h. ***A***, Representative image details of neurons immunostained for MAP2 (left insert above) and c-Fos (left insert below) and with the corresponding merged images (right). The cultures were treated with 1 µg/ml of ZEB85-Ab and CTRL-Ab or BDNF for 24 h. The arrows (white) in the merged images indicate c-Fos expressing MAP2 positive neurons. Scale bars, 50 µm. ***B and C***, Graphs show the normalized number of c-Fos positive neurons calculated over total MAP2 positive neurons. ***B***, Cultures were treated with 1 µg/ml of ZEB85-Ab and CTRL-Ab or BDNF or ***C***, with 10 µg/ml of ZEB85-Ab and CTRL-Ab for 24 h. ***D***, Graph shows the percentage of c-Fos positive neurons. Hippocampal cultures were treated with 1 µg/ml and 10 µg/ml of ZEB85-Ab and CTRL-Ab for 2 h. Data in graphs is represented as mean + SEM and circles show the number of coverslips (CS) analyzed. Data is obtained from ***B and D***, 10-12 CS from 4 independent experiments and ***C***, 14-15 CS from 5 independent experiments. Statistics used: ***B and D***, One-way ANOVA followed by Bonferroni's multiple comparisons post-hoc test, ***C***, Unpaired Student's t-test. *$p < 0.05$, **$p < 0.01$, ***$p < 0.001$.

3.3. ZEB85-Antibody Induces TrkB Activation in a Concentration-Dependent Manner

ZEB85-antibody has been shown to lead to TrkB phosphorylation at site Tyr706/707 in a human derived cell line at a concentration of 5 µg/ml and at a 10 times higher concentration of 50 µg/ml also in cultured mouse cortical neurons, as detected by Western-Blot (Merkouris et al., 2018). Here it was tested if lower concentrations of ZEB85-antibody are also able to activate the TrkB receptor in primary mouse hippocampal neurons via immunocytochemistry. Therefore, DIV21 primary hippocampal cultures (3.5 x 10^4/cm^2) were treated with 1 µg/ml ZEB85-antibody or the control-antibody and immunostained for MAP2 and the phosphorylated TrkB site Tyr706/707. To confirm that this method is sensitive enough to detect an increase in TrkB phosphorylation BDNF served as a positive control. Cultures were first treated for 1 h as it seemed from the previous publication that this treatment duration with ZEB85-antibody leads to the strongest TrkB activation in mouse cortical neurons (Merkouris et al., 2018). Isolated single primary dendrites were selected based on the MAP2 immunostaining. TrkB activation was then analyzed based on the fluorescence intensity, area and number of positive puncta for phosphorylated TrkB (pTrkB). The 1 h

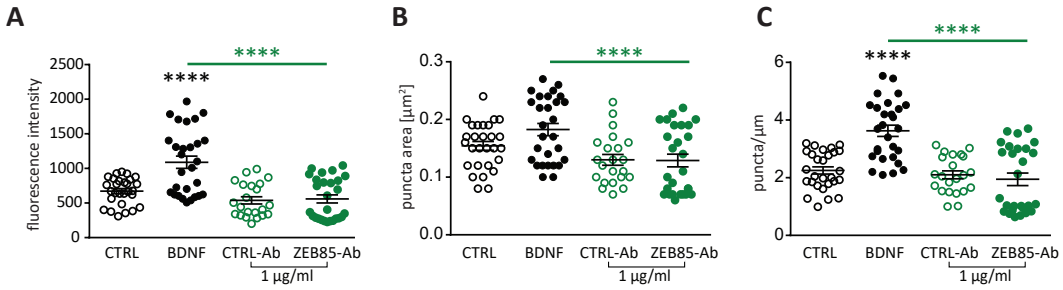

Figure 3.3.: 1 µg/ml of ZEB85-Antibody has no effect on TrkB phosphorylation.
Primary hippocampal cultures DIV21 were treated for 1 h with 1 µg/ml of ZEB85-antibody (ZEB85-Ab) and control-antibody (CTRL-Ab) or with BDNF and its respective control (CTRL). ***A***, Quantification of pTrkB fluorescence intensity, ***B***, pTrkB puncta area and ***C***, pTrkB puncta density [puncta/ µm]. Data in graphs is represented as mean ± SEM and is obtained from 22-28 neurons per group from 2 independent experiments. Statistics used: One-way ANOVA followed by Bonferroni's multiple comparisons post-hoc test. Star significance directly above the bar refers to the CTRL ****$p < 0.0001$.

treatment with BDNF led to a significant increase both in the pTrkB fluorescence intensity (Figure 3.3 A; $p < 0.0001$; Table B.4) and pTrkB puncta density (Figure 3.3 C;

p $<$ 0.0001; Table B.4) by over 60%. Further, the pTrkB puncta area increased by 18%, although not significantly (Figure 3.3 B; Table B.4). However, the application of 1 µg/ml of ZEB85-antibody had no effect on any of the analyzed parameters for TrkB phosphorylation. Thus, ZEB85-antibody and BDNF differ significantly from each other (Figure 3.3 A-C; p $<$ 0.0001; Table B.4). But, the two controls did not significantly differ from each other (Figure 3.3 A-C). Because the 1 h treatment with the low concentration (1 µg/ml) of ZEB85-antibody did not lead to TrkB activation, in a second experiment the higher concentration (10 µg/ml) of ZEB85-antibody was used and a shorter treatment duration of 15 min was chosen, at which the maximum of TrkB activation induced by BDNF application was previously reported (Ji et al., 2010; Guo et al., 2014). Treatment with 10 µg/ml of ZEB85-antibody significantly increased pTrkB puncta fluorescence intensity and pTrkB puncta density by 52% (Figure 3.4 A; p = 0.0002; Table B.5) and 57% (Figure 3.4 C; p $<$ 0.0001; Table B.5) respectively. In addition, the pTrkB puncta area was increased by 17%, although not significantly (Figure 3.4 B; p = 0.065; Table B.5).

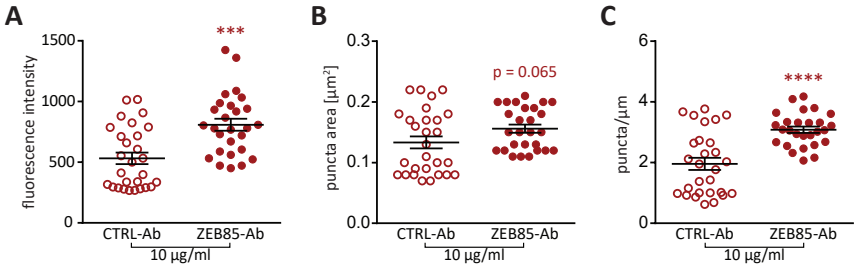

Figure 3.4.: 10 µg/ml of ZEB85-Antibody increases TrkB phosphorylation.
Primary hippocampal cultures DIV21 were treated for 15 min with 10 µg/ml of ZEB85-antibody (ZEB85-Ab) and control-antibody (CTRL-Ab). ***A***, Quantification of pTrkB fluorescence intensity, ***B***, pTrkB puncta area and ***C***, pTrkB puncta density. Data in graphs is represented as mean ± SEM and is obtained from 27-28 neurons per group from 2 independent experiments. Statistics used: Unpaired Student's t-test. ***p $<$ 0.001, ****p $<$ 0.0001.

As the higher concentration of ZEB85-antibody induced TrkB activation within 15 min, the same experiment was repeated with the inclusion of the low (1 µg/ml) concentration of ZEB85-antibody and BDNF, in order to compare them to each other. The treatment with BDNF as well as with 10 µg/ml of ZEB85-antibody visibly showed a stronger staining for the TrkB phosphorylation site Tyr706/707 compared to the respective controls (Figure 3.5 A). However, the effect with BDNF seemed to be more pronounced. This was confirmed by analysis. Both BDNF and 10 µg/ml of

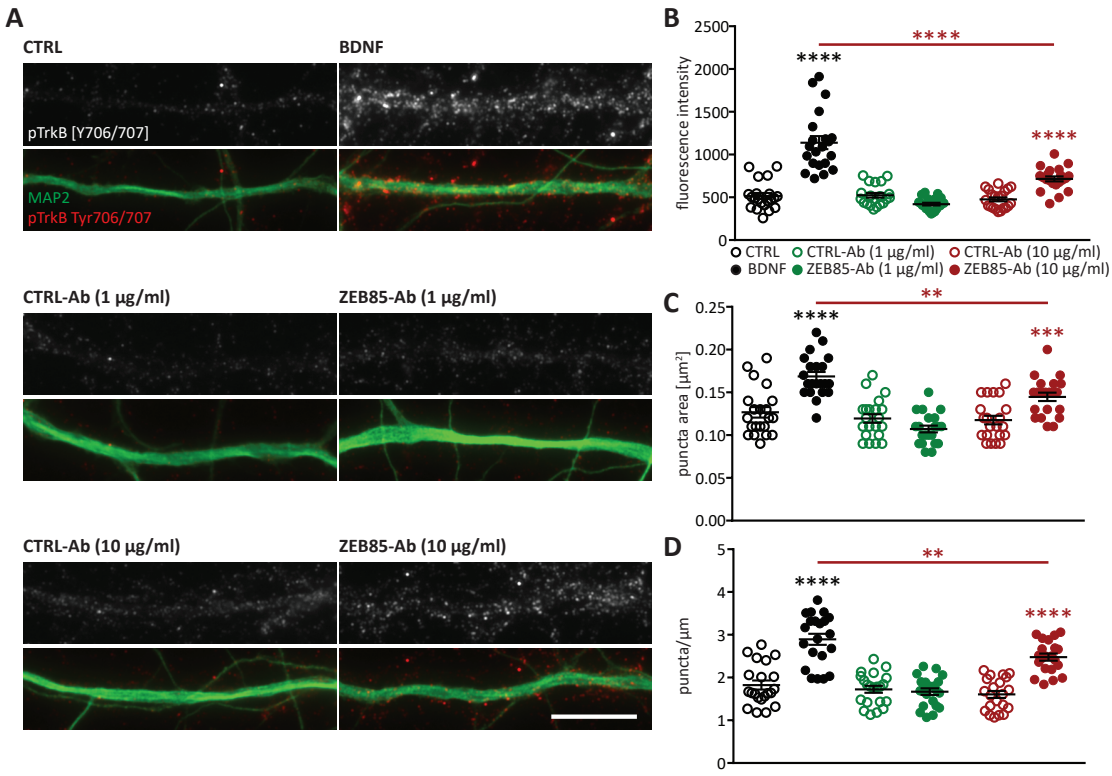

Figure 3.5.: ZEB85-Antibody activates TrkB in a concentration-dependent manner. Primary hippocampal cultures DIV21 were treated for 15 min with ZEB85-antibody (ZEB85-Ab; 1 µg/ml and 10 µg/ml) and control-antibody (CTRL-Ab) or with BDNF and its respective control (CTRL). ***A***, Representative dendritic segments immunostained for MAP2 and the TrkB phosphorylation site Tyr706/707 (pTrkB) for the different treatment groups. The upper image of a panel shows the pTrkB immunostaining and the image below displays the merged image which includes the MAP2 immunostaining. Scale bar, 10 µm. ***B***, Quantification of pTrkB fluorescence intensity, ***C***, pTrkB puncta area and ***D***, pTrkB density. Data in graphs is represented as mean ± SEM and is obtained from 21 neurons per group from 2 independent experiments. Statistics used: One-way ANOVA followed by Bonferroni's multiple comparisons post-hoc test. Star significance directly above the bar refers to the respective control (color coded). **$p < 0.01$, ***$p < 0.001$, ****$p < 0.0001$.

ZEB85-antibody led to a significant increase in all analyzed parameters. The results obtained again for the 15 min treatment with the high concentration of ZEB85-antibody are in agreement with the previous results (see Figure 3.4). While the pTrkB fluorescent intensity increased by 121% with BDNF (Figure 3.5 B, $p < 0.0001$; Table B.6), 10 µg/ml of ZEB85-antibody treatment resulted in a significantly lower increase by 51% (Figure 3.5 B; $p < 0.0001$; Table B.6). The pTrkB puncta area increased by 33% with BDNF treatment (Figure 3.5 C; $p < 0.0001$; Table B.6) and by 23% with ZEB85-antibody application (Figure 3.5 C; $p < 0.001$; Table B.6). Moreover, the number of pTrkB puncta increased by over 50% for both treatments compared to the respective controls (Figure 3.5 D; $p < 0.0001$; Table B.6). However, in contrast to

10 µg/ml of ZEB85-antibody the lower concentration of 1 µg/ml did not induce any detectable TrkB activation at the phosphorylation site Tyr706/707. Worth mentioning is that the different controls did not differ from each other significantly for any of the three parameters (Figure 3.5 B-D; Table B.6).

The results demonstrate that treatment with ZEB85-antibody induces TrkB activation at the TrkB phosphorylation site Tyr706/707 in mouse primary neurons even at a 10 times lower concentration than previously tested (50 µg/ml vs. 10 µg/ml). The effect is however not as pronounced as with BDNF application. As a side note, the two different treatment durations of 60 min and 15 min confirm the well-established observation that BDNF application results in a fast TrkB receptor activation.

3.4. ZEB85-Antibody Promotes Neurite Complexity in Developing Neurons

BDNF has been shown to promote neurite growth and complexity in hippocampal neurons particularly during development (Kellner et al., 2014). Specifically, the treatment with BDNF of primary hippocampal neurons DIV3 over a period of 3 days resulted in an increase in the total neurite length, the number of branch points and the number of primary neurites (Ji et al., 2010; Kellner et al., 2014). Therefore, it was here tested if the TrkB agonist antibody ZEB85 has a similar effect on the neurite architecture of developing hippocampal neurons. Thus, low-cell density primary hippocampal cultures DIV3 were treated for 4 days with ZEB85-antibody (ZEB85-Ab, 1 µg/ml and 10 µg/ml) and control-antibody (CTRL-Ab) or with BDNF and the respective control (CTRL). Noteworthy, the experiment with the higher concentration of ZEB85-antibody was performed separately and to a later time point, which is why the concentration of 10 µg/ml of ZEB85-antibody is not compared to BDNF or the concentration of 10 µg/ml of control-antibody to the other controls. Cultures were fixed at DIV7 and immunostained for MAP2 to visualize the neurites (Figure 3.6 A). Morphometric analysis, performed using the Sholl analysis revealed that the total number of neurite intersections was 27% higher in BDNF treated developing neurons

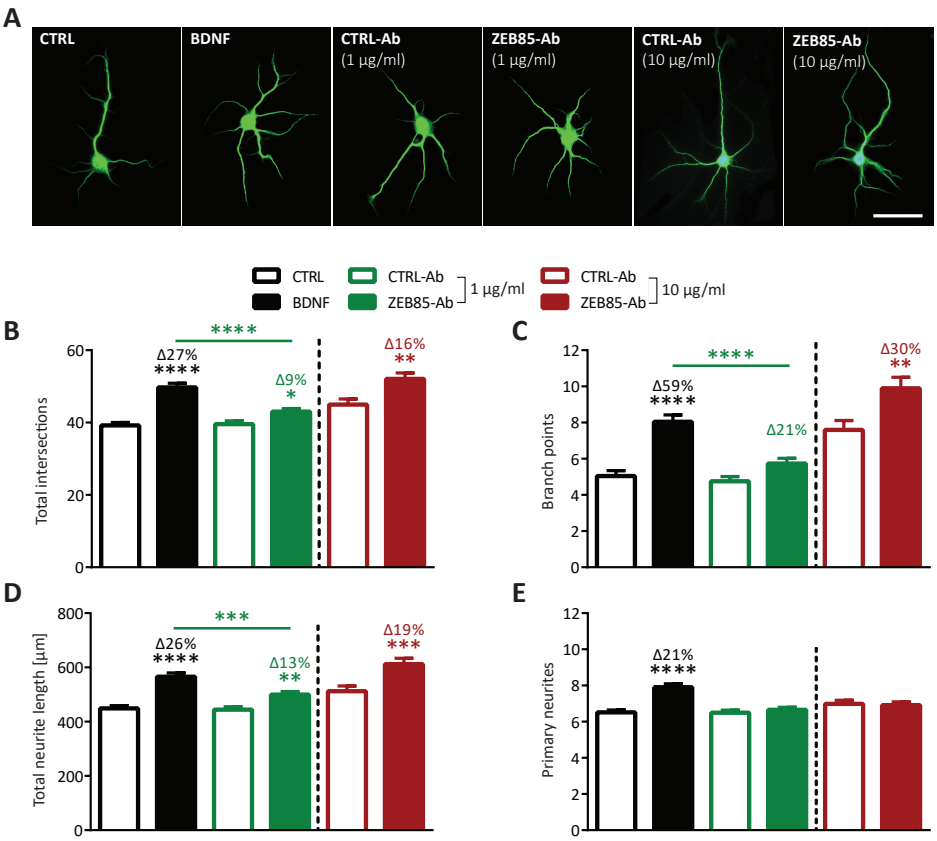

Figure 3.6.: ZEB85-Antibody modulates neurite morphology in developing hippocampal neurons.
Primary hippocampal neurons were treated for 4 days, starting at DIV3, with ZEB85-antibody (ZEB85-Ab; 1 µg/ml and 10 µg/ml) and control-antibody (CTRL-Ab) or with BDNF and its respective control (CTRL). ***A***, Representative images of developing hippocampal neurons DIV7 immunostained for MAP2 for the different treatment groups. Scale bar, 50 µm. ***B***, Total intersections, ***C***, number of branch points, ***D***, total neuritic length and ***E***, number of primary neurites are plotted for the differently treated neurons. Data in graphs is represented as mean + SEM and is obtained from 120-141 neurons per group from 3 independent experiments. Statistics used: BDNF and 1 µg/ml ZEB85-Ab, One-way ANOVA followed by Bonferroni's multiple comparisons post-hoc test, 1 µg/ml ZEB85-Ab, Unpaired Student's t-test. Star significance directly above the bars refers to the respective controls (color coded). *$p < 0.05$, **$p < 0.01$, ***$p < 0.001$, ****$p < 0.0001$.

compared to its control (Figure 3.6 B; $p < 0.0001$; Table B.7). Both the low (1 µg/ml) and the high (10 µg/ml) concentration of ZEB85-antibody led to a significant increase in the total number of intersections compared to the respective control-antibody, albeit to a smaller extent than BDNF, respectively of 9% and 16% (Figure 3.6 B; 1 µg/ml: $p < 0.05$; 10 µg/ml: $p = 0.0023$; Table B.7). A similar result was obtained for the number of branch points and for the total neuritic length. BDNF treated neurons had a 59% higher number of branch points (Figure 3.6 C; $p < 0.0001$; Table B.7) while neurons treated with either 1 µg/ml or 10 µg/ml of ZEB85-antibody showed an increase of 21%

(Figure 3.6 C; p = n.s.; Table B.7) and 30% (Figure 3.6 C; p = 0.0041; Table B.7) respectively compared to the corresponding controls. Moreover, the total neurite length was increased by 26% with BDNF (Figure 3.6 D; $p < 0.0001$; Table B.7), by 13% with 1 µg/ml of ZEB85-antibody (Figure 3.6 D; $p < 0.01$; Table B.7) and by 19% with 10 µg/ml of ZEB85-antibody (Figure 3.6 D; p = 0.0007; Table B.7) compared to the respective controls. Interestingly, only BDNF treatment promoted the outgrowth of new primary neurites (Figure 3.6 E; $p < 0.0001$; Table B.7). Moreover, the control of BDNF and the low concentration of the control-antibody did not differ from each other for any morphometric parameter analyzed (as mentioned above the higher concentration of 10 µg/ml was not compared to the other groups).

In summary previous studies showing that exogenous BDNF application promotes neurite complexity could be reproduced. Importantly, ZEB85-antibody increases the growth and complexity of developing hippocampal neurons as well. While both concentrations of ZEB85-antibody influence neurite morphology, the higher concentration of ZEB85-antibody has shown the stronger effect.

3.5. ZEB85-Antibody Modulates Dendritic Spine Density and Spine Morphology

While the role of exogenous BDNF application in modulating neurite architecture of developing neurons *in vitro* has been confirmed in multiple studies, the role of BDNF in modulating the dendritic spine number and spine morphology of mature neurons is less clear. In fact some studies show that BDNF treatment increases dendritic spine number and leads to a more mature spine phenotype (Tyler and Pozzo-Miller, 2001; Ji et al., 2010) while others report no effect (Kellner et al., 2014; Zagrebelsky et al., 2018). Proposed explanations for this discrepancy in literature are different culture conditions and animal species (Chapleau et al., 2008; Kellner et al., 2014). In spite of the discrepancies, spine density and morphology were assessed upon a ZEB85-antibody treatment. Therefore, primary hippocampal cultures were transfected with feGFP and treated with 1 µg/ml and 10 µg/ml of ZEB85-antibody (ZEB85-Ab),

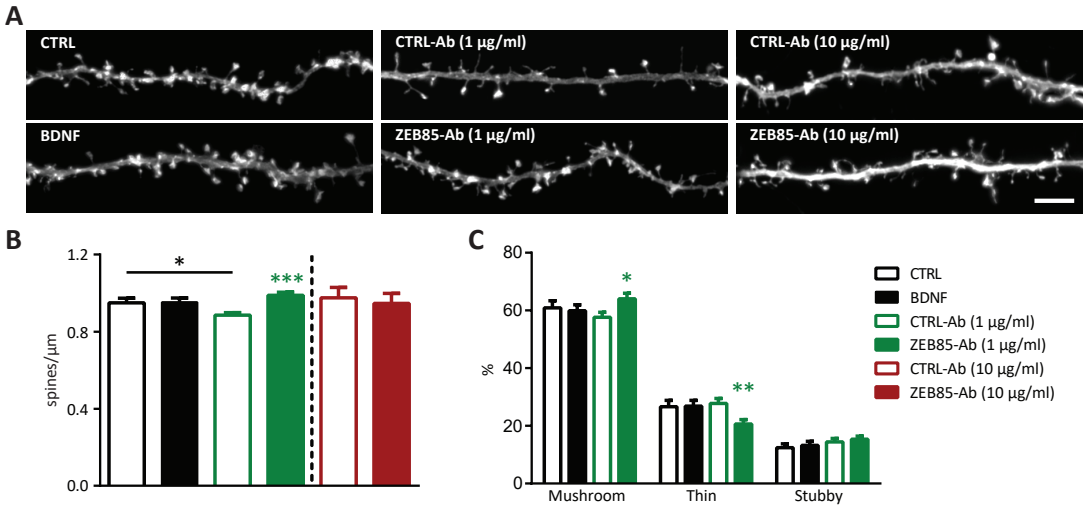

Figure 3.7.: ZEB85-Antibody increases spine density and leads to spine maturation. ***A***, Representative dendritic segments with dendritic spines from feGFP transfected hippocampal neurons treated for 24 h with ZEB85-antibody (ZEB85-Ab; 1 µg/ml and 10 µg/ml) and control-antibody (CTRL-Ab) or with BDNF and its respective control (CTRL). Scale bar, 5 µm. ***B***, Quantification of spine density and ***C***, spine types. Data in graphs is represented as mean + SEM. ***B***, Data is obtained for BDNF and CTRL: 58-60 neurons/ dendrites from 4 independent experiments and for 1 µg/ml ZEB85-Ab and CTRL-Ab: 86-88 from 6 neurons independent and for 10 µg/ml ZEB85-Ab and CTRL-Ab: 15 neurons from one experiment. ***C***, Data is obtained for BDNF and CTRL: 37-40 neurons from 3 independent experiments and for 1 µg/ml ZEB85-Ab and CTRL-Ab: 52 from 4 independent experiments. Statistics used: ***B***, One-way ANOVA followed by Bonferroni's multiple comparisons post-hoc test, ***C***, two-way ANOVA followed by Bonferroni's multiple comparisons post-hoc test and. Star significance directly above the bar refers to the respective control (color coded). *$p < 0.05$, **$p < 0.01$, ***$p < 0.001$.

BDNF and the respective controls. In agreement with Kellner et al., (2014), a BDNF treatment did not affect dendritic spine number (Figure 3.7 B; Table B.8) or the proportion of spine types (Figure 3.7 C; Table B.9). In contrast, treatment with 1 µg/ml of ZEB85-antibody showed a significant increase in dendritic spine number compared to the control-antibody (CTRL-Ab; Figure 3.7 B; $p < 0.001$; Table B.8). However, the spine density in control-antibody treated neurons was significantly reduced compared to the control of BDNF (Figure 3.7 B; $p < 0.05$; Table B.8). Moreover, the spine density upon ZEB85-antibody treatment did not differ between BDNF and its control. In contrast to the low concentration, preliminary data shows that treatment with the higher concentration (10 µg/ml) of ZEB85-antibody did not lead to differences in spine density compared to its respective control (Figure 3.7 B; Table B.8). Further, treatment with 1 µg/ml of ZEB85-antibody shifted the proportion of spine types towards a more mature spine morphology, by increasing the number of mushroom type spines (Figure 3.7 C; $p < 0.05$; Table B.9; spine morphology has not been analyzed for 10 µg/ml of

ZEB85-antibody so far). This indicates that treatment with ZEB85-antibody influences dendritic spine number only at a lower concentration.

3.6. ZEB85-Antibody Restores Amyloid-β Induced Dendritic Spine Loss

The loss of dendritic spines and the correlated loss of synapses is an early inevitable characteristic of Alzheimer's disease (AD), and is directly linked to memory loss and cognitive decline (Dorostkar et al., 2015). Soluble oligomeric amyloid-β (Aβ) is widely assumed to be the major toxic species responsible for the disease development and progression instead of Aβ plaques in the brain (Hefti et al., 2013). Indeed, evidence points in favor of this theory as soluble Aβ oligomers have been linked to dendritic spine loss (Brouillette, 2014; Dorostkar et al., 2015; Kommaddi et al., 2018; Patnaik et al., 2020; Zagrebelsky et al., 2020). Accumulating evidence has shown that BDNF and its receptor TrkB are significantly decreased in AD (Ferrer et al., 1999; Ginsberg et al., 2010) and previous studies have reported that a BDNF treatment is able to restore spine abnormalities in AD mouse models *in vivo* (de Pins et al., 2019) and *in vitro* (Meng et al., 2013). Therefore, to replicate a model that leads to the loss of dendritic spines and to investigate if ZEB85-antibody has any potential in rescuing the spine pathology, feGFP expressing wild-type primary hippocampal neurons (DIV21) were pre-treated with $A\beta_{1\text{-}42}$ oligomers (500 nM) or the respective control (DMSO in PBS) for 15 min and then co-treated with ZEB85-antibody or control-antibody (10 µg/ml) for 6 hours. Hippocampal neurons treated with $A\beta_{1\text{-}42}$ oligomers and control-antibody ($A\beta_{1\text{-}42}$ + CTRL-Ab) displayed a visibly reduced dendritic spine density compared to neurons treated with the respective control (CTRL-Ab, hence referred to as control; Figure 3.8 A). In contrast, the dendritic spine density in neurons treated with $A\beta_{1\text{-}42}$ oligomers together with ZEB85-antibody ($A\beta_{1\text{-}42}$ + ZEB85-Ab) looked similar to that of control neurons (Figure 3.8 A). Indeed, quantification confirmed that $A\beta_{1\text{-}42}$ plus control-antibody treated neurons had a significant reduced spine number by 16% compared to control neurons (Figure 3.8 B; $p < 0.0001$; Table B.10). Remarkably, the treatment of $A\beta_{1\text{-}42}$ plus ZEB85-antibody completely prevented

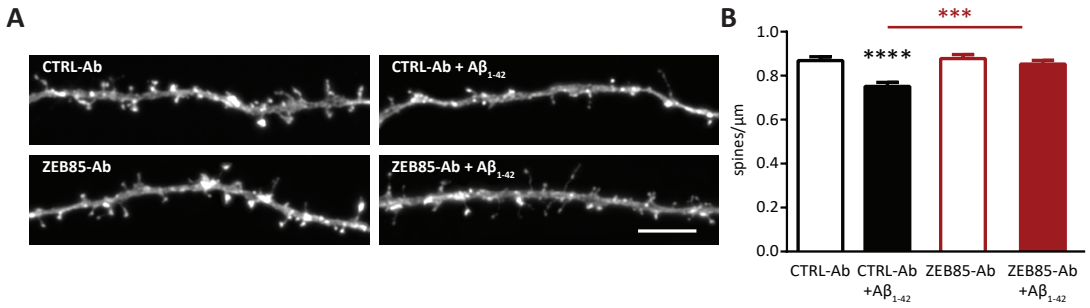

Figure 3.8.: ZEB85-Antibody rescues amyloid-β induced spine loss.
A, Representative dendritic segments with dendritic spines from feGFP transfected hippocampal neurons either pretreated with amyloid-$\beta_{1\text{-}42}$ oligomers ($A\beta_{1\text{-}42}$; 500 nM) for 15 min or not, followed by a 6 h treatment with ZEB85-anitobdy (ZEB85-Ab; 10 µg/ml) or control-antibody (CTRL-Ab). Scale bar, 5 µm. ***B***, Quantification of spine density of dendrites with a length of $\geq$ 60 µm. Data in graphs is represented as mean + SEM and is obtained from 47-49 neurons per group from 3 independent experiments. Statistics used: One-way ANOVA followed by Bonferroni's multiple comparisons post-hoc test. Star significance directly above the bar refers to the respective control (color coded). ***p $<$ 0.001, ****p $<$ 0.0001.

the spine loss compared to $A\beta_{1\text{-}42}$ plus control-antibody treated cultures (Figure 3.8 B; p $<$ 0.001; Table B.10). Thus, the spine density of ZEB85-antibody plus $A\beta_{1\text{-}42}$ treated neurons did not differ from control neurons (Figure 3.8 B; Table B.10).

The results confirm that the application of $A\beta_{1\text{-}42}$ oligomers (500 nM) is a good experimental model to induce dendritic spine loss *in vitro* which allows the screening of potential therapeutics. Indeed, ZEB85-antibody treatment is able to completely rescue the Aβ induced dendritic spine loss in primary hippocampal cultures.

3.7. ZEB85-Antibody Rescues the Dendritic Morphology of BDNF deprived PV$^+$ Interneurons

While it has been convincingly shown that the exogenous application of BDNF in developmental hippocampal neurons strongly promotes neurite complexity (Ji et al., 2010; Kellner et al., 2014), BDNF loss-of function experiments had no effect on the neurite architecture (Kellner et al., 2014). In addition, depriving cultures over 24 h (Kellner et al., 2014) or at the start of culturing of BDNF (Zagrebelsky et al., 2018) does not lead to any alterations in dendritic architecture of mature hippocampal pyramidal neurons *in vitro*. Moreover, conditional knockout mice lacking BDNF throughout the CNS show only minimal morphological alterations in excitatory

pyramidal hippocampal neurons *in vivo* (Rauskolb et al., 2010). However, particularly the dendritic development of GABAergic interneurons has been shown to strongly depend on BDNF (Mizuno et al., 1994; Kohara et al., 2003; Zagrebelsky et al., 2018) and its receptor TrkB (Zheng et al., 2011). Indeed, mature primary hippocampal and cortical GABAergic interneurons deprived of BDNF at the start of culturing were shown to be considerably smaller and less complex. This deficit could be completely rescued by repeated BDNF treatment during the entire culturing time (Zagrebelsky et al., 2018). Thus, as this model could reliably show the promoting effects of BDNF on dendritic architecture of hippocampal GABAergic interneurons, it was used as another prove of principal experiment to test the TrkB agonist antibody ZEB85. Therefore, primary dissociated neurons derived from BDNF floxed mice either transduced (BDNFΔ) with an AVV-Cre-GFP at the day of preparation (DIV0) or not transduced were treated with 10 µg/ml ZEB85-antibody or control-antibody on the same day. Treatment was repeated every week and the cultures were fixed and stained for parvalbumin at DIV21. A transduced parvalbumin-positive (PV^+) interneuron is shown in Figure 3.9 A. Transduced, BDNF depleted PV^+ interneurons treated with control-antibody (BDNFΔ + CTRL-Ab) were visibly smaller and less complex (Figure 3.9 B) compared to non-transduced control neurons (CTRL-Ab), which was also confirmed by morphometric analysis. Sholl analysis showed a significant reduction in the number of intersections of BDNF-depleted PV^+ interneurons treated with control-antibody, especially for the mid-distal part ($\geq$ 60 µm away from the soma) of the dendritic tree compared to the control (Figure 3.9 C; Two-way ANOVA $F_{3,13063}$ = 234.4, $p < 0.0001$; Table B.11). The same trend is reflected in the other parameters analyzed. The total number of intersections of transduced control-antibody treated PV^+ interneurons was reduced by 30% (Figure 3.9 D; $p < 0.0001$; Table B.12) and the number of branch points by 39% (Figure 3.9 E; $p < 0.0001$; Table B.12) compared to control neurons. In line with being less complex they were also significantly smaller and showed a reduction of the total dendritic length by 34% (Figure 3.9 F; $p < 0.0001$; Table B.12). Interestingly, these morphological deficits could be completely rescued by the application ZEB85-antibody in BDNF depleted cultures (BDNFΔ + ZEB85-Ab; Figure 3.9 B-F; $p < 0.0001$; Table B.11 and B.12), hence the dendritic morphology of

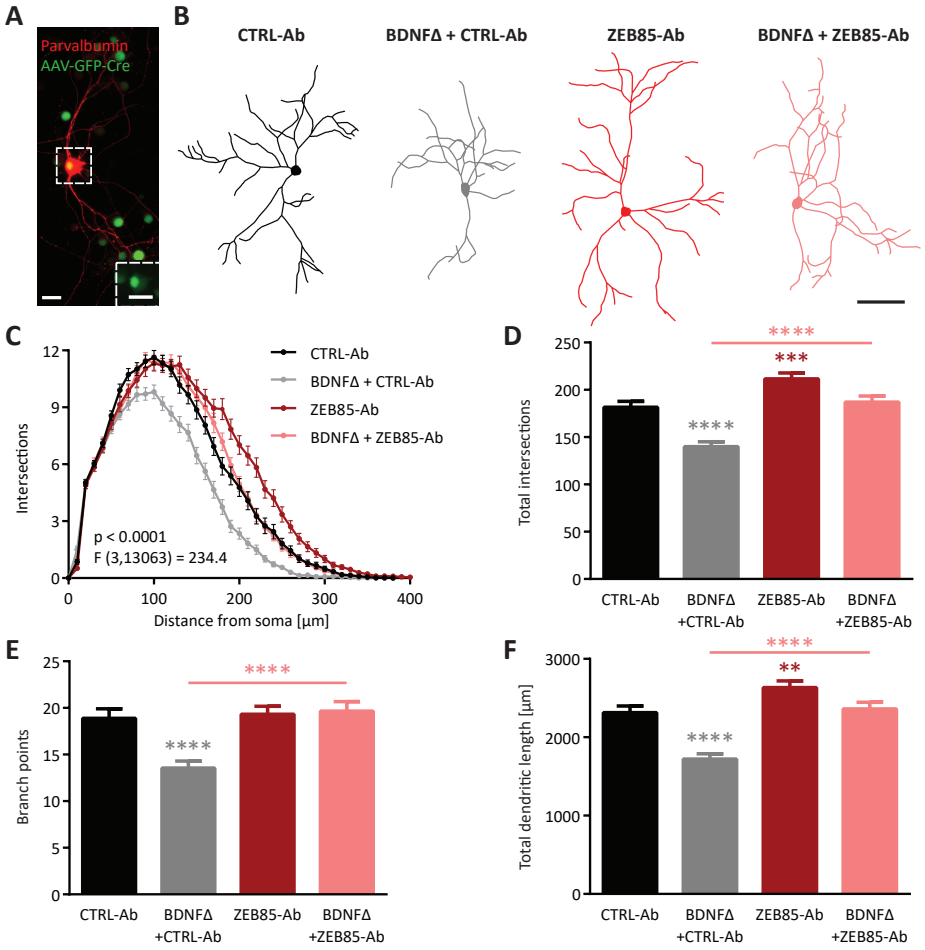

Figure 3.9.: ZEB85-Antibody rescues the complexity of *bdnf*-KO PV$^+$interneurons.
A, Representative image of an AAV-CRE-GFP transduced parvalbumin-positive (PV$^+$) interneuron derived from BDNF floxed mice. The inserted image (dotted square) shows the nuclear GFP expression of the transfected PV$^+$ interneuron. Scale bars, 25 µm. ***B***, Neurolucida tracings used for Sholl analysis from PV$^+$interneurons DIV21 treated at DIV0 with ZEB85-antibody (ZEB85-Ab; 10 µg/ml) or control-antibody (CTRL-Ab) either transduced (BDNFΔ) or not. Scale bar, 100 µm. ***C***, Sholl analysis curves, with the number of intersections plotted against the distance from the cell body, for all 4 treatment groups. ***D***, total intersections, ***E***, number of branch points and ***F***, total neuritic length of PV$^+$interneurons are plotted for the different treatment groups. Data in graphs is represented as mean + SEM and is obtained from 75 neurons per group from 3 independent experiments. Statistics used: ***C***: Two-way ANOVA followed by Bonferroni's multiple comparisons post-hoc test and ***D-F***: One-way ANOVA followed by Bonferroni's multiple comparisons post-hoc test. Star significance directly above the bar refers to the CTRL-Ab. **p $<$ 0.01, ***p $<$ 0.001, ****p $<$ 0.0001.

these PV$^+$ interneurons was indistinguishable compared to non-transduced control neurons (Figure 3.9 B-F; Table B.11 and B.12). Moreover, ZEB85-antibody treatment in non-transduced cultures (ZEB85-Ab) resulted in a longer (Figure 3.9 F; p $<$ 0.01; Table B.12) and more complex (Figure 3.9 D; p $<$ 0.001; Table B.12) dendritic architecture of PV$^+$ interneurons compared to the non-transduced control-antibody treated cultures. The number of intersections was significantly increased for the more

distal part of the dendritic tree ($\geq$ 150 µm away from the soma; Figure 3.9 C; Table B.11). While the number of branch points did not differ between non-transduced control-antibody and ZEB85-antibody treated PV^+ interneurons, the number of total intersections was significantly increased by 16% and the total dendritic length by 14% with ZEB85-antibody treatment.

In conclusion, these results confirm that BDNF is particularly important for the postnatal development of hippocampal PV^+ interneurons. Moreover, it could be shown that ZEB85-antibody treatment completely rescues the structural abnormalities of PV^+ interneurons seen in BDNF depleted cultures. In addition, application of ZEB85-antibody in non-BDNF depleted cultures increases the dendritic complexity and the dendritic length of PV^+ interneurons.

3.8. Long-Term Treatment with ZEB85-Antibody does not alter Spine Density

The knockout of *bdnf* at the start of culturing does not lead to any alterations in the dendritic architecture of mature neurons nor in the dendritic spine density (Zagrebelsky et al., 2018). Even the addition of BDNF in control cultures starting at DIV2 and repeated treatment with BDNF until DIV21 does not influence dendritic spine density of hippocampal excitatory neurons (Zagrebelsky et al., 2018). In the following experiment it was assessed if ZEB85-antibody treatment has any effect on dendritic spine density in primary hippocampal cultures deprived of BDNF at the start of culturing. Therefore, like in the previous experiment, primary dissociated neurons derived from BDNF floxed mice either transduced (BDNF$\triangle$) with an AVV-Cre-GFP at the day of preparation (DIV0) or not transduced were treated with 10 µg/ml ZEB85-antibody or control-antibody on the same day. The cultures were treated every week with ZEB85-antibody or control-antibody. Cultures DIV20 were transfected with mapple and fixed at DIV21. Cultures deprived of BDNF showed no altered spine density compared to control neurons. Also the long-term application of ZEB85-antibody in *bdnf* knockout cultures did not influence the spine number (Figure 3.10 A and B; Table B.13).

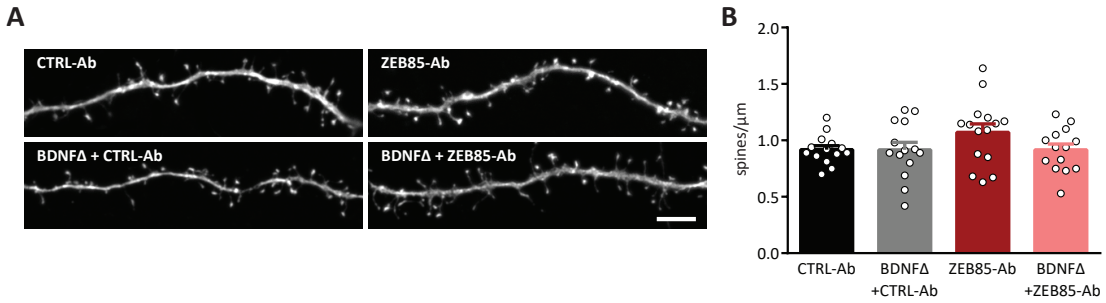

Figure 3.10.: ZEB85-Antibody does not affect spine density if *bdnf* is knocked-out at the start of culturing.
Primary hippocampal cultures either transduced (BDNFΔ) or not were treated at DIV0 with ZEB85-antibody (ZEB85-Ab; 10 µg/ml) or control-antibody (CTRL-Ab). ***A***, Representative dendritic segments with dendritic spines from mapple transfected hippocampal neurons. ***B***, Quantification of spine density for the different treatment groups. Data in graphs is represented as mean + SEM and circles represent the number of analyzed dendrites. Data is obtained from 14-15 neurons per group from one experiment. Statistics used: One-way ANOVA.

However, this data was obtained from only one experiment and although not significant, treatment with ZEB85-antibody in non-transduced cultures increased dendritic spine number by 17% compared to control-antibody treated cultures.

This preliminary set of data confirms, that the knockout of *bdnf* in primary hippocampal cultures at the start of culturing does not affect dendritic spine number. If the repeated treatment with ZEB85-antibody throughout the development of the hippocampal neurons modulates dendritic spine density needs to be evaluated in further experiments.

3.9. BDNF Knockout at a Mature Stage Influences Dendritic Spine Density

Treatment with BDNF during the entire culturing time increases the dendritic complexity but has no influence on the spine density of mature hippocampal neurons (Zagrebelsky et al., 2018). Interestingly, a deprivation of BDNF at the start of culturing influences neither the dendritic architecture nor the spine density (Zagrebelsky et al., 2018). Further, neither the addition nor the loss of BDNF over 24 h has shown any influence on the neuronal morphology of mature hippocampal neurons (Kellner et al., 2014). In contrast, neurons deprived of BDNF for 24 h show a significant reduction in

spine density (Kellner et al., 2014). Thus, the dependence on BDNF/TrkB signaling for the maintenance and modulation of neuronal architecture and dendritic spines seems to differ and might also be influenced by the duration of BDNF availability. Here, in this experiment it was tested whether BDNF gain- or loss-of function over a prolonged period in already mature neurons between DIV14 and DIV21 had any influence on neuronal morphology and spine density. Thus, primary dissociated neurons derived from BDNF floxed mice were either transduced (BDNFΔ) with an AVV-Cre-GFP at DIV14 or not transduced and treated with BDNF or the corresponding control (CTRL) as well. Cultures DIV20 were transfected with mapple and fixed at DIV21. For the analysis only transduced neurons were included (Figure 3.11 A). Unlike a repeated

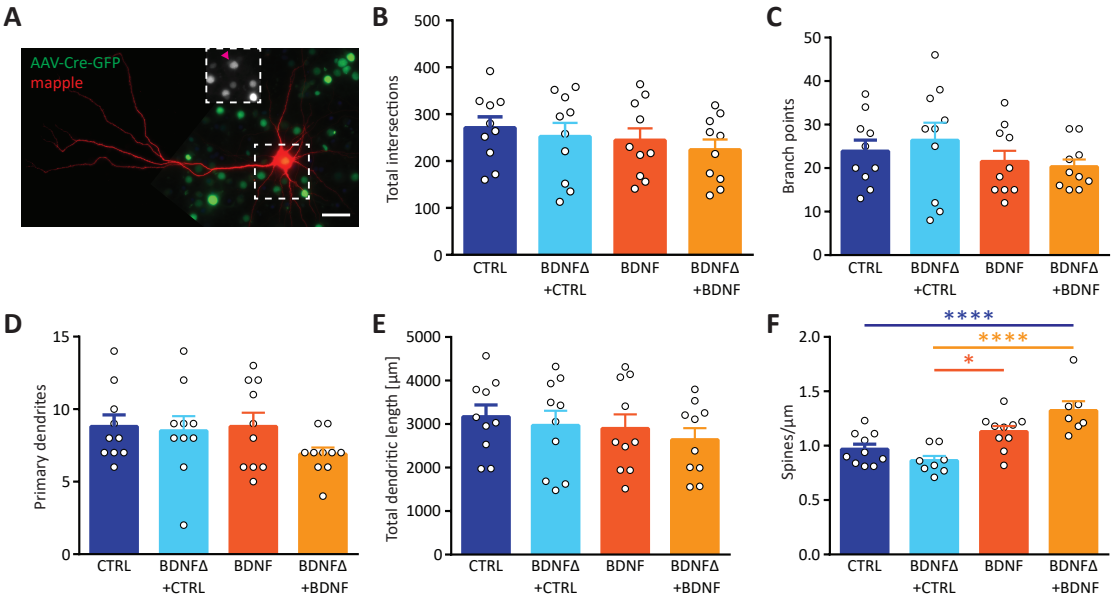

Figure 3.11.: *Bdnf* Knockout in Mature Cultures Influences Dendritic Spine Density. Primary hippocampal cultures were either transduced with AAV-Cre-GFP (BDNFΔ) or not at DIV14 and the cultures were also treated with ZEB85-antibody (ZEB85-Ab; 10 µg/ml) or control-antibody (CTRL-Ab). ***A***, Representative image of a transduced with mapple transfected excitatory hippocampal neuron at DIV21. The inserted image (dotted square) shows the nuclear GFP expression of the transduced neurons. The arrow (pink) indicates the corresponding transfected neuron. Scale bar, 50 µm. ***B-E***, Graphs show the different parameters of the analysis of neuronal morphology and ***F***, shows the quantification of the dendritic spine number. Data in graphs is represented as mean + SEM and circles represent the number of neurons analyzed. Data is obtained from 10 neurons per group from one experiment. Statistics used: One-way ANOVA followed by Bonferroni's multiple comparisons post-hoc test. *p $<$ 0.05, ***p $<$ 0.001, ****p $<$ 0.0001.

treatment with BDNF throughout the development of hippocampal neurons, the treatment with BDNF at DIV14 for a week had no effect on neuronal morphology nor did the knockout of *bdnf* (Figure 3.11 B-E; Table B.14), shown for the parameters of

the number of total intersections (Figure 3.11 B; Table B.14), the number of branch points (Figure 3.11 C; Table B.14), the number of primary dendrites (Figure 3.11 D; Table B.14) and the total dendritic length (Figure 3.11 E). Also the spine density was not significantly reduced in the BDNF deprived cultures. In contrast the treatment with BDNF in *bdnf* knockout cultures significantly increased spine density compared to *bdnf* knockout neurons by 53% (Figure 3.11 F; $p < 0.0001$; Table B.14) and by 37% compared to control neurons ($p < 0.001$; Table B.14). In addition, treatment with BDNF in control neurons significantly increased spine density compared to *bdnf* knockout neurons by 31% (Figure 3.11 F; $p < 0.05$; Table B.14) and by 12% compared to control neurons, although not significantly (Figure 3.11 F; Table B.14).

In summary the results show that the *bdnf* knockout over a week in mature neurons does not lead to any alterations in dendritic morphology nor does the treatment with BDNF. In contrast, the spine density is significantly increased with a BDNF treatment in both non-BDNF depleted and BDNF depleted cultures compared to control treated *bdnf* knockout cultures. However, this experiment needs more repetitions to make a definite statement and the application of ZEB85-antibody would be the next step.

3.10. Long-Term Treatment with ZEB85-Antibody Affects Long-Term Potentiation

The previous results have shown that treatment with the ZEB85-antibody affects the neuronal structure and the dendritic spines. These changes are also correlated to functional changes that ultimately lead to alterations in synaptic connectivity and strength between neuronal partners (Harms and Dunaevsky, 2007). Therefore, it was first investigated if a short treatment with ZEB85-antibody may affect long-term potentiation (LTP) in acute hippocampal slices prepared from 6-8 week old wild-type mice. The Schaffer collaterals were stimulated and field excitatory postsynaptic potentials (fEPSPs) were recorded in the CA1 region (Figure 2.3). The results show that a pre-treatment of 1 h before starting the recordings with 1µg/ml of ZEB85-antibody had no effect on LTP compared to the control-antibody (Figure 3.12 A

and B; A: Two-way ANOVA $F_{1, 35} = 0.3307$, $p = 0.5689$; Table B.15 and Table B.16). As this short-term treatment with ZEB85-antibody had no effect on LTP, it was assessed if a treatment over multiple days would lead to any changes in LTP. Therefore, organotypic hippocampal slice cultures were used, as they have the advantage over acute brain slices that they can be maintained *in vitro* over multiple weeks, enabling a prolonged treatment with drugs furthermore the higher concentration (10 µg/ml) of ZEB85-antibody could be used. In addition, instead of slices from wild-type mice the hippocampal slices were prepared from heterozygous BDNF knockout mice. These mice display a deficit in LTP compared to littermate controls which manifests in a lower number of successful LTP inductions and a lower magnitude of LTP potentiation once induced (Korte et al., 1995). Thus, in the next experiment, organotypic hippocampal

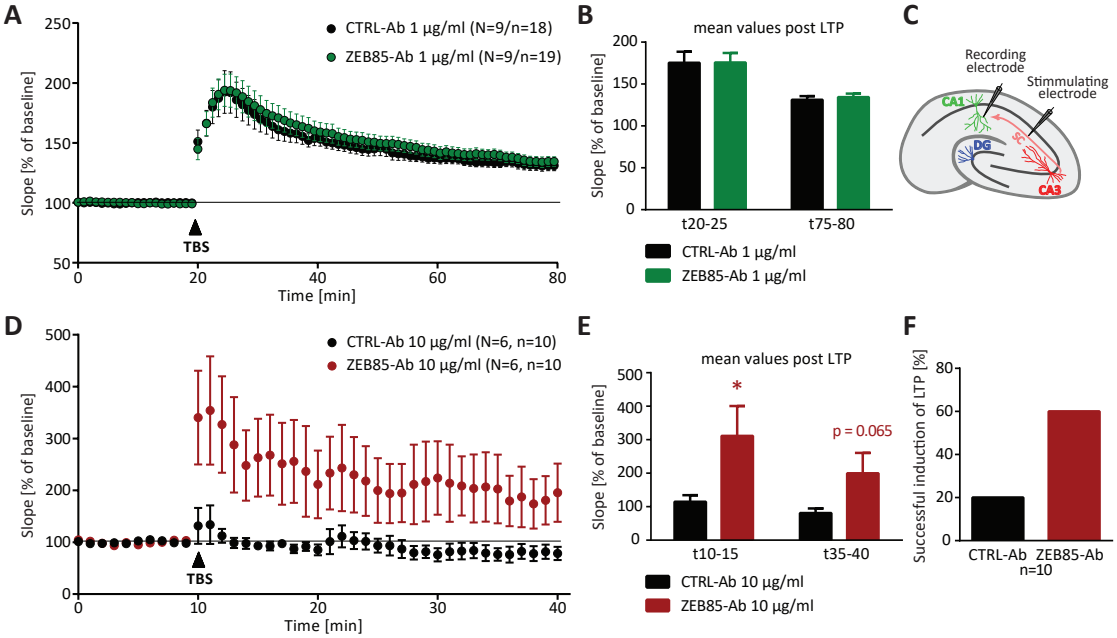

Figure 3.12.: Long-term treatment of ZEB85-Antibody affects LTP in heterozygous BDNF knockout mice.
C, fEPSP were recorded at the CA3-CA1 pathway of either acute slices or organotypic hippocampal cultures. ***A***, Acute hippocampal slices prepared from wild-type mice were treated with 1 µg/ml of ZEB85-antibody (ZEB85-Ab) or control-antibody (CTRL-Ab) for 1 h before starting fEPSP recordings. Baseline was recorded for 20 min after which TBS was applied and LTP was measured for another 60 min. ***B and E***, Graphs show the mean values of the first and last 5 min after LTP induction. ***D***, Organotypic hippocampal cultures DIV16 prepared from heterozygous BDNF-knockout mice were treated for 5-6 days with 10 µg/ml of ZEB85-Ab or CTRL-Ab. Baseline was recorded for 10 min after which TBS was applied and LTP was measured for another 30 min. ***F***, Graph shows the percentage of successful LTP inductions. The criterion for a successful LTP induction was based that fEPSP of the last 5 min after TBS was bigger than 120% of the baseline. Data in graphs is represented as mean ± SEM. The number of mice (N) and the number of slices (n) is shown in graphs ***A and D***. Statistics used: ***A and D***: Two-way ANOVA. ***E***: Unpaired Student's t-test. *$p < 0.05$.

slice cultures DIV16 were treated for 5-6 days with 10 µg/ml of ZEB85-antibody after which fEPSP recordings were performed. In this experiment all recordings with a stable baseline were included, even those that showed no induction of LTP or those where the fEPSP slope decreased after TBS. First of all, LTP could only be induced in 20% of slices treated with control-antibody but interestingly in 60% of slices treated with ZEB85-antibody (Figure 3.12 F). Thus, in slices treated with control-antibody TBS resulted in a low and short potentiation after which the fEPSP slope went slightly below the baseline. Compared to the control-antibody treatment, ZEB85-antibody treated brain slices from heterozygous BDNF-knockout mice displayed a robust potentiation after TBS (Figure 3.12 D; Two-way ANOVA $F_{1, 18}$ = 4.036, p = 0.0598; Table B.17). Both the first 5 min (Figure 3.12 E; p = 0.0444; Table B.18) and also the last 5 min (Figure 3.12 E; p = 0.065; Table B.18) after TBS showed a significant increase in the fEPSP slope relative to the baseline compared to the control-antibody.

To sum up, a short treatment with 1 µg/ml of ZEB85-antibody in acute wild-type hippocampal slices from does not alter long-term potentiation. In contrast, a longer treatment with the higher concentration of 10 µg/ml of ZEB85-antibody in organotypic slice cultures from BDNF knockout mice is able to increase the number of successful LTP inductions and increases the magnitude of potentiation as well.

4. Discussion

Neuronal networks are characterized by a finely tuned system on account of the balanced interplay of many different molecules. Among these, the neurotrophin Brain-derived neurotrophic factor (BDNF), signaling via its receptor Tropomyosin receptor kinase B (TrkB) plays a pivotal role in establishing and maintaining the structure and function of neurons within the central nervous system, thereby regulating learning and memory processes in the brain. A reduction in BDNF mediated TrkB signaling has been associated with many neurological diseases such as the neurodegenerative disorder, Alzheimer's disease. One promising therapeutic approach is to restore the physiological levels of BDNF/TrkB signaling. However, the direct administration of BDNF is not an option due to its poor pharmacological properties. This observation prompted the search for new strategies to increase BDNF/TrkB signaling in the brain, one of which is the use of highly specific TrkB-agonists.

In this thesis a recently identified fully human TrkB agonist antibody (ZEB85) was investigated for its effects on the structure and function of hippocampal healthy and diseased murine neurons and neuronal networks. The results indicate that the ZEB85-antibody indeed reproduces some of the typical effects of BDNF/TrkB signaling regarding structural changes at hippocampal neurons in addition to rescuing the deficit in long-term potentiation in BDNF deficient mice.

4.1. Modulation of Target Genes Downstream of TrkB

BDNF-mediated TrkB signaling is involved in regulating the rapid changes at synapse but has also a long-term effect on the transcription of genes involved in neuronal plasticity such as the immediate early gene *c-fos* (Marty et al., 1996; Pizzorusso et al., 2000; Gascon et al., 2005; Ohba et al., 2005; Meier et al., 2011). Indeed, also this work showed that BDNF treatment leads to a significant increase in c-Fos positive

neurons in primary hippocampal cultures. This effect was visible after both, a 2 h and 24 h application of BDNF. The small-molecule BDNF mimetic 7,8-DHF reported to act specifically on the TrkB receptor (Jang et al., 2010b) which has also been studied extensively for its therapeutic potential in several neurological diseases (Devi and Ohno, 2012; Johnson et al., 2012; Castello et al., 2014; Garcia-Diaz Barriga et al., 2017), was tested in this assay for its use as a positive control as well. The further intention was to use 7,8-DHF as a reference point to compare the ZEB85-antibody to. However, treatment with 7,8-DHF had no effect on c-Fos expression. This result supports the findings of two recent studies (Todd et al., 2014; Boltaev et al., 2017) that could neither detect activation of TrkB nor activation of downstream molecules such as ERK and AKT with 7,8-DHF. Therefore, this compound was not used further. In contrast, the low concentration (1 µg/ml) of the TrkB agonist antibody ZEB85 increased the amount of c-Fos positive neurons after 24 h in a manner comparable to a BDNF treatment. Surprisingly, a 24 h treatment with the high concentration (10 µg/ml) of ZEB85-antibody resulted in a decrease in c-Fos positive neurons. But interestingly, a ZEB85-antibody treatment for 2 h, within the reported activation time peak for c-Fos upon BDNF treatment (Kovacs, 2008; Chowdhury and Caroni, 2018), resulted in the opposite effect. The high concentration of ZEB85-antibody increased the number of c-Fos positive neurons, while the low concentration of ZEB85-antibody showed no difference compared to the respective control-antibody. While this finding is puzzling, it could be theorized that the different concentrations of ZEB85-antibody lead to a different rate of receptor internalization and degradation or receptor desensitization, thus altering the downstream signaling. Indeed, the findings of some studies suggest that the prolonged exposure to BDNF leads to receptor desensitization (Carter et al., 1995) and even TrkB protein and mRNA level decrease (Frank et al., 1996; Knusel et al., 1997), leading to downregulation of downstream signaling cascades. For instance, hippocampal cultures that were pretreated with BDNF for 24 h and that were again acutely stimulated with BDNF after 6 days showed a significant decrease in phosphorylation of TrkB and Erk1/2 and in the number of c-Fos positive neurons, compared to neurons that were stimulated only once on day 6 with BDNF (Frank et al., 1996). The c-Fos levels observed in this study upon a treatment with 10 µg/ml of the

control-antibody are significantly lower compared to those induced by 1 µg/ml, indicating that the control-antibody may negatively impact c-Fos expression in a concentration-dependent manner. Moreover, the c-Fos levels are only marginally increased (10%) by 10 µg/ml of ZEB85-antibody compared to 1 µg/ml, suggesting that the higher concentration has no effect or only a marginal additional effect on c-Fos expression.

In summary, this study shows that ZEB85-antibody leads to the activation of TrkB downstream signaling, as indicated by the increased c-Fos expression.

4.2. ZEB85-Antibody Induces TrkB Activation

Acute stimulation in cultured hippocampal neurons is known to result in a transient activation of the TrkB receptor (Ji et al., 2010; Guo et al., 2014). Western blot analysis revealed that TrkB phosphorylation levels return to baseline levels after a continuous 4 h treatment with BDNF (Ji et al., 2010). In this study, a significant increase in TrkB receptor phosphorylation at site Tyr706/707 was detected via immunocytochemistry after application of BDNF for 60 min. Unlike the BDNF treatment, the 1 µg/ml of ZEB85-antibody did not lead to a detectable TrkB phosphorylation. This result is in agreement with the observation that 1 µg/ml of ZEB85-antibody had a smaller effect on c-Fos expression compared to BDNF. Moreover, it was shown that after stimulation with BDNF, TrkB phosphorylation levels reach their maximum after about 15 min and that after 60 min they are already reduced by 30-50% compared to it (Ji et al., 2010; Guo et al., 2014). Thus, it is possible that part of the effect of the low concentration of 1 µg/ml of ZEB85-antibody on TrkB activation might be already missed after 60 min. However, while a 15 min treatment with BDNF confirmed that a shorter stimulation results in a stronger TrkB phosphorylation a similar treatment with 1 µg/ml of ZEB85-antibody had no effect on TrkB phosphorylation. In contrast, the higher concentration of 10 µg/ml of ZEB85-antibody significantly increased all measured parameters. A possible explanation of why the low concentration of ZEB85-antibody showed no effect, might be that the limited sensitivity of the detection via immunocytochemistry might not be enough to detect small changes in TrkB

phosphorylation. Western blots, that are extremely sensitive and allow for an exact quantification, would be the better suited method in this case.

It as been shown that ZEB85-antibody reproduces the effects of BDNF on TrkB phosphorylation. But it is important to mention that both, the previous experiment on c-Fos expression and this experiment showed that the effect of ZEB85-antibody is lower compared to BDNF. This result confirms the previous study by Merkouris et al. (2018) which examined TrkB phosphorylation in cultured mouse cortical neurons at DIV7 by Western blot, showing that the effect of ZEB85-antibody on TrkB activation was smaller compared to BDNF, even though using a 5 times higher concentration (50 µg/ml vs. 10 µg/ml). However, in a human cell line ZEB85-antibody displayed a similar TrkB activation profile than BDNF (Merkouris et al., 2018). Thus, the human TrkB agonist antibody ZEB85 displays a different potency towards TrkB depending on the species. This could be a result of the small, but significant differences in the sequence of the TrkB ectodomain among mammalian species. While these differences are irrelevant for BDNF signaling, they may influence the potency of TrkB agonist antibodies (Merkouris et al., 2018).

The phosphorylation site Tyr706/707 localized in the activation loop of the catalytic domain of TrkB enhances the integral receptor tyrosine kinase activity thereby increasing the subsequent autophosphorylation at two additional tyrosine residues (Tyr515 and Tyr816). Each of these tyrosine residues induces the activation of specific downstream signaling cascades (Cunningham et al., 1997; McCarty and Feinstein, 1998; Huang and Reichardt, 2003; Obianyo and Ye, 2013). The phosphorylation of TrkB at Tyr515 triggers signaling through the RAS-ERK and PI3K cascades, associated with neuronal survival, differentiation and dendritic development. Phosphorylation of TrkB at Tyr816 elicits activation of the PLCγ pathway, generally involved in synaptic plasticity (Boltaev et al., 2017). So due to the fact that ZEB85-antibody leads to the phosphorylation of Tyr706/707, one could speculate that also the two other tyrosine residues get phosphorylated. This seems likely, as ZEB85-antibody has been also shown to modulate the structure and functional plasticity in hippocampal neurons, as discussed below.

Concluding, this study shows that in mouse hippocampal neurons the ZEB85-antibody leads to TrkB phosphorylation and signaling even at a 5 times lower concentration than the one used in the previous study (Merkouris et al., 2018).

4.3. Dendritic Architecture of Excitatory and Inhibitory Neurons

Neuronal architecture is strictly linked to neuronal function and has been shown to be modulated by BDNF, depending on the developmental time point and cell-type. Therefore, a series of experimental paradigms addressing neuronal morphology and known to be strongly depended on BDNF/TrkB signaling were chosen to further characterize the structural consequences of a treatment with the TrkB agonist antibody ZEB85.

4.3.1. ZEB85-Antibody Increases Neurite Complexity in Developing Neurons

The branching pattern and extent of the dendritic arborization influences the neuronal firing pattern, thereby impacting the processing of neuronal information (Lanoue and Cooper, 2019). As it is well described in the literature that the exogenous application of BDNF to developing neurons promotes neurite growth in different neuronal cell types (Iwasaki et al., 1998; Bosco and Linden, 1999; Sun et al., 2012) including hippocampal neurons (Ji et al., 2005; Kellner et al., 2014), this effect of BDNF was used to further characterize the ZEB85-antibody. This study could reproduce the typical effects seen upon a BDNF treatment on the architecture of developing primary hippocampal neurons, again confirming that this experiment is suitable to analyze if ZEB85-antibody exerts similar functions to BDNF. Indeed, ZEB85-antibody increased the neurite complexity of developing primary hippocampal neurons in a concentration-dependent manner.

BDNF promotes different aspects of neurite architecture, including total neurite length, the number of branch points and the number of primary neurites. Specifically,

application of exogenous BDNF in developing hippocampal neurons (Ji et al., 2005, 2010; Kellner et al., 2014) and, the overexpression of BDNF (Horch et al., 1999; Dijkhuizen and Ghosh, 2005) or TrkB (Yacoubian and Lo, 2000) were shown to specifically promote the growth of primary dendrites in both developing and maturing cortical neurons. In contrast to the direct BDNF manipulations, application of ZEB85-antibody had no effect on the growth of primary neurites, possibly indicating a difference in the elicited TrkB signaling. A previous study found that changes in primary neurite number occurred by a protein synthesis-independent mechanism within hours of treatment, leaving the number of branch points and total neurite length unchanged (Dijkhuizen and Ghosh, 2005). This indicates that BDNF acts via different downstream mechanisms in shaping different aspects of the dendritic tree development. In fact, the inhibition of PI3K or MAPK was shown to completely prevent and, the inhibition of PLCγ to lessen the BDNF induced neurite outgrowth in developing cortical cultures, while the expression of a constitutively active form of PI3K was sufficient to induce primary neurite formation (Dijkhuizen and Ghosh, 2005). Thus, the phosphorylation of TrkB Tyr515 which triggers activation of the RAS-ERK and PI3K pathway might be of importance for this process.

Overall, ZEB85-antibody promotes neuronal architecture of developing hippocampal neurons in a similar manner to BDNF, as shown by the effect on the neurite complexity and length. But due to the fact that ZEB85-antibody has no effect on the primary neurite number, unlike BDNF, the data also indicates that BDNF and ZEB85-antibody may activate different signaling cascades downstream of TrkB, leading to a different activation of subsequent cytoskeletal remodeling molecules which regulate distinct aspects of dendritic development, such as the initiation of dendritic outgrowth, elongation and branching.

4.3.2. The Effect of BDNF on the Dendritic Architecture Depends on the Neuron's Developmental Stage

A treatment with BDNF between DIV3 and DIV7 (as described above) as well as a treatment over the entire culturing time until DIV21 (Zagrebelsky et al., 2018) results in

an increased dendritic complexity of hippocampal neurons. However, a 24 h application of BDNF in mature neurons had no effect (Kellner et al., 2014). Also, BDNF loss-of function experiments had no effect on dendritic architecture in developing neurons (Kellner et al., 2014) nor in mature hippocampal neurons deprived of BDNF at the start of culturing (Zagrebelsky et al., 2018) or over a 24 h period (Kellner et al., 2014). Conditional knockout mice, lacking BDNF throughout the CNS showed only minimal morphological alterations in excitatory pyramidal hippocampal neurons *in vivo* (Rauskolb et al., 2010). In a preliminary experiment it was investigated whether BDNF gain- or loss-of function over a prolonged period in already mature neurons between DIV14 and DIV21 had any influence on neuronal morphology. Also in these experiments neither the knockout of *bdnf* nor the treatment with BDNF in control neurons showed any alterations in dendritic morphology of mature neurons. Taken together, these observations indicate that the effects exerted by BDNF on dendritic architecture depend on the neuron's maturation stage and that alterations in BDNF signaling in mature pyramidal neurons have no effect on dendritic architecture. Indeed, the dendritic arbor in mature neurons is remarkably stable, undergoing only minimal changes under physiological conditions and showing severe remodeling only under pathological conditions (Holtmaat and Svoboda, 2009; Koleske, 2013). It is worth mentioning, that the effects of BDNF on dendritic morphology are region and cell type specific. While pyramidal neurons of the hippocampus show no alterations in response to BDNF loss (Rauskolb et al., 2010; Zagrebelsky et al., 2018), other cell types like the granule cells of the dentate gyrus (Zagrebelsky et al., 2018) or medium spiny neurons of the striatum are severely affected (Baquet et al., 2004; Rauskolb et al., 2010; Baydyuk and Xu, 2014). Indeed, as discussed below GABAergic inhibitory neurons are tightly dependent on BDNF for their normal development.

4.3.3. ZEB85-Antibody Rescues Abnormalities in Dendritic Architecture of BDNF-Deficient PV$^+$ Interneurons

In contrast to mature excitatory neurons in which the effects of BDNF on dendritic architecture are mostly subtle, BDNF/TrkB signaling is crucial for the correct dendritic

development and maintenance of GABAergic interneurons (Mizuno et al., 1994; Kohara et al., 2003; Rauskolb et al., 2010; Zheng et al., 2011; Tan et al., 2018; Zagrebelsky et al., 2018). Mature primary hippocampal GABAergic interneurons, specifically Parvalbumin positive (PV^+) interneurons, deprived of BDNF at the start of culturing were shown to be significantly smaller and less complex than their control counterpart (Zagrebelsky et al., 2018). Due to the fact that the structural deficits of PV^+ interneurons in *bdnf* knockout cultures could be rescued with the application of BDNF during culturing (Zagrebelsky et al., 2018), this experimental model was chosen as a proof of principle to investigate if ZEB85-antibody is also able to rescue the altered phenotype of PV^+ interneurons in *bdnf* knockout cultures. First of all, the severe structural deficits in PV^+ interneuron architecture due to the loss of BDNF could be reproduced in this study. Importantly, treatment with ZEB85-antibody during the entire culturing time was able to completely rescue the deficits seen in dendritic morphology in BDNF-deficient PV^+ interneurons. Moreover, the treatment with ZEB85-antibody in control, non-BDNF depleted neurons also increased dendritic length and complexity.

To sum up, in combination with the promoting effect of ZEB85 on neurite architecture in developing excitatory primary hippocampal neurons, these experiments provide further proof that ZEB85-antibody exerts a similar effect to BDNF on neuronal morphology.

4.4. Dendritic Spine Density in Health and Disease

Unlike the dendritic arbor, dendritic spines are highly dynamic structures that can vary both in shape and number in an activity-dependent manner. Dendritic spine density which gives an estimate about neuronal connectivity and spine morphology which can be an indicator for neuronal strength, are both also modulated by BDNF and hence, these criteria were also analyzed to further characterize the ZEB85-antibody.

4.4.1. Role of ZEB85-Antibody in Modulating Spine Density and Spine Morphology in Mature Neurons

BDNF-dependent TrkB signaling has been shown, via a series of BDNF or TrkB loss-of function experiments to be important for the formation, maturation and maintenance of dendritic spines (Zagrebelsky et al., 2020). In this study, a 24 h treatment with BDNF had no effect on the dendritic spine number of mature hippocampal neurons. While this is in line with previously published studies in mice (Kellner et al., 2014; Zagrebelsky et al., 2018) others have reported an increase in spine density using rat cultures (Tyler and Pozzo-Miller, 2001; Ji et al., 2010). Apart from the different animal species, the spine density in control neurons was approximately 5 times higher in my study and in Kellner et al. (2014) compared to Ji et al. (2010), showing that culture conditions could also play a role in this discrepancy. Surprisingly, in contrast to BDNF, 1 µg/ml of ZEB85-antibody showed a significant increase in spine density compared to control-antibody treated neurons. However, it is important though to mention that the spine number in control neurons was significantly lower than in the control used for the BDNF treatment. This result suggests that the control-antibody might negatively influence spine number in healthy hippocampal neurons under normal culture conditions. In addition, the higher concentration of 10 µg/ml of ZEB85-antibody did not result in a higher spine number. While, the increase in spine density upon a treatment with the low concentration of ZEB85 is indeed interesting, the discrepancy to BDNF and to the higher concentration of the ZEB85-antibody invite to being cautious and indicate the need for further experiments in this context.

Dendritic spines can be categorized in different types depending on their shape, i.e. thin, stubby and mushroom (see Figure 2.2), reflecting their maturation state. The long thin spines are associated with an immature phenotype while stubby and mushroom spines are proposed to be mature (Bonhoeffer and Yuste, 2002). Like for the spine density, a 24 h treatment with BDNF did not lead to any alterations in spine morphology. Again, this was previously reported (Kellner et al., 2014; Zagrebelsky et al., 2018) but does also contradict other published literature (Tyler and Pozzo-Miller, 2001; Ji et al., 2010), possibly due to different culture conditions. In contrast to BDNF, treatment with

1 µg/ml of ZEB85-antibody lead to a shift towards a more mature spine phenotype indicated by an increase in the proportion of mushroom spines and a decrease in the proportion of thin spines. But like for the spine density, the control-antibody differs, although not significantly from the control of BDNF.

The treatment or the depletion of BDNF at the start of culturing has shown to have no influence on spine density in mature hippocampal neurons (Zagrebelsky et al., 2018). Also in this work it was shown that the spine density is not affected in mature neurons of *bdnf* knockout cultures. However, preliminary data indicates that treatment with ZEB85-antibody at the start of culturing might modulate dendritic spine density.

In summary, while still needing further confirmation, ZEB85-antibody might indeed modulate some structural aspects at dendritic spines. This effect seems to differ from BDNF. It can be speculated that ZEB85-antibody activates different targets downstream of TrkB that are involved in the modulation of spine structure. Or that the elicited signal is longer, as it has been reported that binding of some TrkB agonist antibodies result in much longer TrkB activation and further lead to a reduced TrkB internalization and intracellular degradation compared to BDNF (Guo et al., 2019). However no experiment in this study was performed to directly address this hypothesis.

4.4.2. ZEB85-Antibody Restores Amyloid-β Induced Spine Loss

Alzheimer's disease (AD) is the most common form of dementia worldwide, accounting for approximately 60–80% of all cases amongst elderly over 60 years old (Alzheimer's-Association, 2020), causing a progressive decline of cognitive functions (Dorostkar et al., 2015). The progression in AD is reflected by the early loss of synapses (DeKosky and Scheff, 1990; Scheff et al., 2007), followed by progressive neuronal loss (Whitehouse et al., 1981; Dorostkar et al., 2015), leading to brain atrophy in areas such as the hippocampus. One of the described hallmarks of AD is the deposition of extracellular amyloid-β (Aβ) plaques and intracellular neurofibrillary tangles composed of hyperphosphorylated tau protein aggregates. However, the Aβ plaque load correlates poorly with the severity of the disease (Arriagada et al., 1992;

Gomez-Isla et al., 1997; Andrade-Moraes et al., 2013) and soluble Aβ oligomers were found to preferentially associate with synapses, notably dendritic spines, leading to alterations in both presynaptic and postsynaptic structures (Lacor et al., 2004; Wang et al., 2017; He et al., 2019). Therefore, it is generally assumed that diffusible Aβ oligomers and not the plaques are the major toxic species, disrupting normal synaptic function of neurons and hence are responsible for disease development and progression (Hefti et al., 2013). Indeed, soluble Aβ oligomers have been linked to dendritic spine loss (Brouillette, 2014; Dorostkar et al., 2015; Patnaik et al., 2020). And also this study could replicate that a 6 h application of Aβ oligomers leads to a significant dendritic spine loss in primary hippocampal cultures (Lacor et al., 2007; Patnaik et al., 2020).

Accumulating evidence has shown that BDNF and its receptor TrkB are significantly decreased in AD (Phillips et al., 1991; Ferrer et al., 1999; Hock et al., 2000; Ginsberg et al., 2010) and several studies have provided evidence that BDNF can protect neurons against Aβ toxicity and is able to restore spine abnormalities in AD mouse models *in vivo* (de Pins et al., 2019) and *in vitro* (Meng et al., 2013) and, to improve several other phenotypes associated with the disease including impaired cognition (Nagahara et al., 2009). Therefore, it was assessed whether ZEB85-antibody could prevent the Aβ induced loss of dendritic spines. Indeed, the abnormal reduction in spine number was completely prevented by a 6 h application of ZEB85-antibody. Further studies would need to be performed to analyze in detail how this protective effect is archived. However, this is also not really understood for BDNF either and the scientific findings to date suggest a wide variety of possible mechanisms which may cause synapse loss or dysfunction underlying Alzheimer's disease (Dorostkar et al., 2015). One hypothesis would be that BDNF, known to stabilize the local actin cytoskeleton through F-actin assembly (Gallo et al., 2002; Rex et al., 2007; Lin and Koleske, 2010; Dombert et al., 2017), prevents the Aβ mediated F-actin disassembly in dendritic spines (Lin and Koleske, 2010; Tu et al., 2014; Kommaddi et al., 2018). The addition of ZEB85-antibody to untreated control cultures did not alter spine density, again confirming the notion that neurons, even at the level of dendritic spines, are relatively stable under physiological conditions.

4.5. ZEB85-Antibody Rescues Long-Term Potentiation in Heterozygous BDNF Knockout Mice

BDNF/TrkB signaling potentiates basal excitatory synaptic transmission (Kang and Schuman, 1995; Ji et al., 2010) and elicits action potentials just as rapidly as the neurotransmitter glutamate in central neurons of the hippocampus, cortex and cerebellum (Kafitz et al., 1999). And evidence has shown that BDNF is crucial for the induction and maintenance of long-term potentiation (LTP). These roles for BDNF/TrkB signaling were mostly shown by loss-of function experiments (Korte et al., 1995; Patterson et al., 1996; Akaneya et al., 1997; Kang et al., 1997) but several studies also reported promoting effects on LTP with BDNF application in brain slices from wild-type mice. As such, a gradual increase in BDNF concentration with a 1 h pre-treatment before and after theta burst stimulation (TBS) was shown to facilitate early LTP in neonatal hippocampal slices (Ji et al., 2010). Also in other brain regions such as the developing visual cortex, BDNF enhanced the magnitude of LTP induced by tetanic stimulation and the application 5 min before TBS and during recording of LTP was sufficient to induce these changes (Akaneya et al., 1997).

To investigate whether a pre-treatment with ZEB85-antibody leads to changes in LTP, as it has been reported for BDNF, acute brain slices from wild-type mice were pre-treated for 1 h with 1 µg/ml of ZEB85-antibody before the start of the recordings. However, the amplitude of recorded field excitatory postsynaptic potentials (fEPSP), measured in the CA1 region by stimulation of the Schaffer collateral pathway, did not show any difference between slices treated with ZEB85-antibody or control-antibody suggesting that under these experimental conditions ZEB85-antibody did not influence LTP. As it was not proven that ZEB85-antibody actually penetrates the slice, it could be argued that ZEB85-antibody only sticks to the surface of the slice or at least doesn't reach the depth where the electrodes are placed. However, it has been reported that exogenous BDNF penetrates into the whole slice within 5 min of its application in a submerged setup (Akaneya et al., 1997). A submerged recording setup has the advantage over an interface setup that the brain slices are completely immersed into the recording solution and are exposed to a continuous flow of the medium enabling a

better penetration of the tested substance. As a submerged recording setup was also used in this study and slices were pre-treated for 60 min, it could be speculated that penetration might not be the issue, why no changes in LTP could be seen with ZEB85-antibody. However, as it is not known how much of the antibody actually reaches the slice and how much of the antibody might be lost in the recording system due to possible binding of ZEB85-antibody to plastic surfaces, it could simply be that with the low concentration not enough of ZEB85-antibody penetrates into the slice to have an effect on LTP. Further, based on the previous experiments that showed that the higher concentration of 10 µg/ml of ZEB85-antibody had a stronger effect on TrkB activation and on the neurite architecture of developing neurons compared to the low concentration, the higher concentration of ZEB85-antibody would be more likely to have an effect on LTP. Unfortunately, this experimental setup did not allow testing the higher concentration of ZEB85-antibody as too large amounts of antibody would have been required.

To circumvent this issue, instead of using acute slices, organotypic hippocampal slice cultures were prepared that enabled the treatment with the high concentration of ZEB85-antibody. In addition, brain slices from BDNF knockout mice were used as these mice exhibit a deficit in LTP, both in the induction and maintenance (Korte et al., 1995; Patterson et al., 1996). This impairment could be rescued via the application of recombinant BDNF over multiple hours to the hippocampal slices (Patterson et al., 1996). In this study, the organotypic slices were also treated over several days in culture, to make sure that the antibody had enough time to penetrate into the slice. In this work it was shown that organotypic slices from heterozygous BDNF knockout mice displayed a severe impairment in LTP induction. LTP could only be induced in 20% of slices, and if induced could not be maintained. Interestingly, treatment with ZEB85-antibody was able to improve the observed LTP deficits. Especially the induction of LTP was improved (60%) but also the overall maintenance. Thus, this result again shows that ZEB85-antibody exerts a similar function to BDNF and further supports the common notion for a requirement for BDNF/TrkB signaling in ongoing synaptic function in the hippocampus.

4.6. Advantages and Disadvantages of Different Approaches to Increase BDNF/TrkB Signaling - A Short Overview

The attempt has been and is being made to develop compounds and methods that overcome the poor pharmacokinetic profile and challenging delivery of BDNF into the brain. The advantages and disadvantages of some of these different approaches, including those of TrkB agonist antibodies are discussed in short below.

Small-molecule TrkB agonists have the advantage that they are likely to cross the blood-brain barrier (BBB) with high efficiency. However, some studies have reported that these small BDNF mimetics do not fully activate the TrkB receptor or not at all, raising doubts about their specificity and potential therapeutic use. This might be a problem of the size difference between these small molecules and BDNF, e.g. BDNF has been reported to be 100-fold larger in molecular weight than 7,8-DHF, a reported TrkB agonist (Liu et al., 2014). As such, from a structural point of view, small molecule mimetics might be unable to bridge the two TrkB monomers and induce effective TrkB activation (Boltaev et al., 2017) or they are only able to induce the phosphorylation of a few tyrosine residues in the intracellular tyrosine kinase domain of TrkB, leading to only partial imitation of the biological actions of BDNF (Liu et al., 2014).

TrkB agonist antibodies which are more similar to BDNF in size could overcome this hurdle but again have the potential downside of limited BBB penetration. This possible issue could be circumvented by using other compounds that are able to shuttle the TrkB agonist antibodies across the BBB (Clarke et al., 2020). Another possibility would allow a delivery of therapeutics directly into the brain via an infusion device. A recent clinical study developed a drug delivery device, where infusion catheters were inserted into patient's brains in a robot-assisted surgery, allowing the infusion of the compound directly into the affected areas with pinpoint accuracy via a skull-mounted transcutaneous port behind the ear. Although invasive, the drug delivery device had a very high compliance rate (99%) throughout the duration of the study over 80 weeks (Whone et al., 2019a,b). As this method allows for a precise drug delivery into specific brain regions, a "flooding" of the brain with the drug can be prevented (Gimenez et al., 2011). This is important as it has been shown that an indiscriminate overload

("flooding") with BDNF in the brain can have adverse effects such as increased seizure susceptibility (Binder et al., 2001; Fumagalli et al., 2006; Lughetti et al., 2018) or induction of oncogenic effects, e.g. by increasing cancer cell growth (Lai et al., 2010; Radin and Patel, 2017; Meng et al., 2019; Li et al., 2020). In general TrkB agonists have the advantage that they are specific and therefore have no off targets such as the $p75_{NTR}$ pathway. And importantly, typically have better pharmacokinetics and bioavailability than BDNF (Lu et al., 2013; Guo et al., 2019).

Another alternative approach are compounds that increase endogenous production of BDNF (Deogracias et al., 2012; Lu et al., 2013; Bascunana et al., 2020). These compounds usually cross the BBB and limit pharmacology to physiologically relevant BDNF-expressing cells and further enable the regulation at subcellular locations (Lu et al., 2013). However, they could potentially have side effects by leading also to the production of proBDNF (Vidal-Martinez et al., 2016) which can induce opposing effects on cellular physiology by preferentially binding to $P75_{NTR}$ (Buhusi et al., 2017). This could especially be important in disorders where the processing of proBDNF into BDNF is disrupted (You et al., 2020), as it has been reported for AD (Fleitas et al., 2018). Engineered BDNF producing cells represent another promising BDNF modulatory category. Such as the use of mesenchymal stem/stromal cells (MSC) that deliver BDNF into the target tissue (Deng et al., 2016; Pollock et al., 2016; Volkman and Offen, 2017; Scheper et al., 2019) or astrocytes that administer BDNF conditionally and locally depending on the severity of the disease (de Pins et al., 2019).

Most of these methods have shown very promising results and the benefits seem to outweigh possible negative effects. However, there is still the need for further investigations into currently existing compounds/ approaches and of course the development of new ones, with even better characteristics. Further, depending on the disorder and brain areas affected different strategies might have to be applied, which is why it makes sense to develop and investigate different options.

4.7. Conclusion

This work analyzed the recently described fully human TrkB agonist antibody ZEB85, to test whether and how its biological functions compare to those of BDNF as a natural ligand for the TrkB receptor. Proof-of principle experiments in which the modulatory effects of BDNF have been previously confirmed multiple times were performed in addition to experiments where the effects of BDNF are indicated but less certain, as for instance the dendritic spine density of mature neurons.

Like BDNF, the application of ZEB85-antibody to primary hippocampal cultures results in TrkB receptor phosphorylation as well as in the activation of downstream signaling. Indeed, the expression of the immediate early gene c-Fos is increased by ZEB85 application.

Atrophies in dendritic morphology can alter the function of the central nervous system and are the basis of several neurodevelopmental disorders such as neurodegenerative and neuropsychiatric disorders (Kulkarni and Firestein, 2012). Here, ZEB85-antibody has shown promising results as it was shown that the neuronal complexity of developing hippocampal neurons is increased upon its application. Further, BDNF has been shown to be crucial for the correct dendritic development and maintenance of PV^+ interneurons. Interneuron dysfunction in general alters the excitation/ inhibition balance and is a potential pathogenetic mechanism underlying brain dysrhythmias and cognitive dysfunction in many neurological and psychiatric disorders, like schizophrenia and Alzheimer's disease (Cardin, 2018; Mattson, 2020; Xu et al., 2020). And like BDNF the TrkB agonist is able to completely rescue developmental deficits from mature PV^+ interneurons, induced by depleting BDNF at the start of culturing. The promoting effects of ZEB85 on the dendritic architecture could even be observed in control PV^+ interneurons.

Another interesting finding is that ZEB85 increases spine density and shifts spine type distribution toward a more mature spine phenotype in mature hippocampal neurons compared to control-antibody treated neurons. Here, the effect of ZEB85 differs from the one of BDNF, as BDNF treatment did not result in any of these changes. However, it cannot be denied that the observed effects could also be a result of the

control-antibody negatively influencing the dendritic spines. But, preliminary data also indicates that ZEB85-antibody is able to modulate spine number when applied at the start of culturing, with a continuous treatment during the entire culturing time. To further address if ZEB85 is able to induce changes in spine density a pathological model was used. Therefore, cultures were treated with Aβ, resulting in a significant reduction in spine number, which reproduces the results of previous reports (Brouillette, 2014; Dorostkar et al., 2015; Patnaik et al., 2020). And like it has been reported for BDNF, the TrkB agonist antibody completely prevented the Aβ induced dendritic spine loss. This is an important finding and also relevant for a potential use as a therapeutic agent in neurodegenerative diseases, because the disease onset usually starts with the early loss of synapses.

Lastly, synaptic transmission, especially long-term potentiation (LTP) is known to depend on BDNF/TrkB signaling. Therefore, it was attempted to rescue LTP deficits in organotypic slice cultures from *bdnf* knockout mice. And indeed, ZEB85 was able to enhance LTP in brain slices of these mice. This is an important first observation and opens up the potential for many future experiments regarding functional plasticity experiments.

In summary, the fully human TrkB agonist antibody ZEB85 exerts some of the biological functions of BDNF as seen in TrkB activation, c-Fos levels, structural changes at the dendrite and spine level and functional changes at the synapse, by improving deficits in LTP. Taken together, in this study it could be shown that this novel TrkB-agonist antibody shows promising potential and might be of value for therapeutical applications. Nevertheless, ZEB85 still needs further characterization, as discussed in the outlook.

4.8. Outlook

Treatment with ZEB85-antibody results in TrkB phosphorylation at site Tyr706/707. The two additional tyrosine residues Tyr515 and Tyr816 induce activation of specific signaling cascades, associated with distinct functions, such as dendritic development

and synaptic plasticity, respectively. Therefore, it would be interesting and necessary to investigate these two tyrosine phosphorylation sites of the TrkB receptor as well. Further, c-Fos expression was increased also independently of an observed TrkB activation for the low concentration of 1 µg/ml. Thus, either the method to detect changes in TrkB phosphorylation is not sensitive enough or c-Fos levels might be also upregulated in a TrkB-independent manner with ZEB85-antibody. Therefore, besides using immunocytochemistry to detect differences in TrkB phosphorylation, the results need to be confirmed via western blot as well since this method is extremely sensitive and allows for an exact quantification. Further, other downstream targets of TrkB should be investigated such as Erk1/2, Akt and PLCγ allowing the identification which downstream pathways might be preferentially activated.

ZEB85-antibody was shown to promote the neuronal architecture of developing hippocampal neurons in a similar fashion to BDNF. However, unlike BDNF, treatment with ZEB85-antibody did not result in any changes in the number of primary neurites. It has been suggested that the phosphorylation of TrkB at site Tyr515, which triggers activation of the RAS-ERK and PI3K pathway, is involved in the outgrowth of primary neurites (Dijkhuizen and Ghosh, 2005). In this regard as mentioned above, it is interesting to analyze the TrkB phosphorylation site Tyr515 as well. In addition, it could be also interesting to investigate intracellular factors that are regulated by BDNF/TrkB signaling, that shape dendritic arbors such as the small GTPases RhoA, Rac1, and Cdc42 which are also regulated by the PI3K pathway and play a role in various aspects of neuronal development (Dijkhuizen and Ghosh, 2005; Govek et al., 2005; Auer et al., 2011; Campa et al., 2015; Schulz et al., 2016). Specifically, Rac1 and Cdc42 have been implicated in primary dendrite formation (Threadgill et al., 1997; Luo, 2000; Redmond and Ghosh, 2001).

Further, as mentioned above, the effect of BDNF on dendritic morphology is also cell type specific. So apart from the analysis of pyramidal hippocampal neurons, granule cells which seem to be more susceptible to changes in BDNF signaling (Tolwani et al., 2002; Zagrebelsky et al., 2018), should be analyzed as well in *bdnf* knockout cultures treated with ZEB85-antibody. And further different time points during maturation can be chosen for the knockout of *bdnf*.

This study again confirmed the common notion that BDNF/TrkB signaling is crucial for the correct dendritic development and maintenance of GABAergic interneurons. Inhibitory neurons with atrophic dendritic trees may receive less excitatory input, as connections are lost, thereby decreasing their inhibitory outputs. Indeed, it has been shown that cultured cortical neurons from animals in which the sensory experience-dependent induction of BDNF expression is disrupted, form fewer functional inhibitory synapses (Hong et al., 2008). Even a single cell knockout of *bdnf* in excitatory neurons of the visual cortex revealed that the number of GABAergic terminals on the these neurons was smaller than that of neighboring control neurons (Kohara et al., 2007), possibly leading to disrupted neuronal and circuit plasticity, information processing and learning (Palop and Mucke, 2016; He et al., 2018). Therefore, it is also interesting to investigate the number of inhibitory contacts made onto excitatory neurons in *bdnf* knockout cultures and at aiming to rescue a potential deficit with ZEB85-antibody. Further, an altered excitation/ inhibition balance should be analyzed in single cell patch-clamp experiments by measuring the excitatory postsynaptic potential (EPSP) and inhibitory postsynaptic potential (IPSP) in *bdnf* knockout cultures.

Further experiments regarding the effects of ZEB85 on dendritic spines need to be performed. For once experiments with the 24 h application of 10 µg/ml of ZEB85-antibody need to be repeated and the spine types need to be analyzed. What is even more interesting in this regard, is the analysis of dendritic spine dynamics. Even if no changes in spine density are detected, it might very well be that the spine dynamics are changing with ZEB85-antibody application, therefore time-lapse imaging needs to be performed. Further, additional experiments are needed where ZEB85-antibody is applied to hippocampal neurons at the start of culturing. In line with this experiment, the dendritic morphology of hippocampal excitatory neurons should also be analyzed, as it has been previously shown that treatment over the entire culturing time with BDNF increases dendritic complexity. Moreover, Aβ exposure was shown to lead to significant dendritic spine loss. Further, it has been reported that application of Aβ also leads to an aberrant spine shape and also towards a shift of a more immature spine phenotype (Lacor et al., 2007; Patnaik et al., 2020). Therefore, it should be investigated if co-

treatment with ZEB85-antibody in Aβ exposed cells is able to rescue the altered spine phenotype.

Further experiments should be performed in hippocampal organotypic slice cultures prepared from heterozygous *bdnf* knockout mice to increase the number of recorded slices as the variance is high. In addition, instead of treatment over 5 days, a shorter treatment time-course could be performed to investigate at what time point changes in LTP start to occur. In a future experiment it is planned to prepare the organotypic slices from adult mice, instead of mice that are a couple of days old (P5). The thought behind this is that the neuronal network is more developed and stabilized if the organotypic slices are prepared from adult mice and that LTP recordings therefore yield better results. Moreover, other disease mouse models could be used were the disease onset starts later in life, such as the Alzheimer's disease mouse model APP/PS1 (Marjanska et al., 2005; Gengler et al., 2010). Further, the penetration of the antibody into the slice should be confirmed via immunohistochemistry.

In summary, further *in vitro* experiments must be performed to characterize ZEB85 in detail. Ultimately, the goal is of course to test ZEB85-antibody *in vivo*. First it would need to be assessed if the ZEB85-antibody is able to cross the BBB. If not the antibody could be administered via stereotactic injection directly into the desired brain region. Disease mouse models can be utilized to asses if ZEB85-antibody improves some of the particular symptoms, such as memory impairment or neuronal alterations.

A. Bibliography

Aicardi, G., Argilli, E., Cappello, S., Santi, S., Riccio, M., Thoenen, H., and Canossa, M. (2004). Induction of long-term potentiation and depression is reflected by corresponding changes in secretion of endogenous brain-derived neurotrophic factor. *Proc Natl Acad Sci U S A*, 101(44):15788–92.

Akaneya, Y., Tsumoto, T., Kinoshita, S., and Hatanaka, H. (1997). Brain-derived neurotrophic factor enhances long-term potentiation in rat visual cortex. *J Neurosci*, 17(17):6707–16.

Alonso, M., Vianna, M. R., Izquierdo, I., and Medina, J. H. (2002). Signaling mechanisms mediating BDNF modulation of memory formation in vivo in the hippocampus. *Cell Mol Neurobiol*, 22(5-6):663–74.

Alvarez, V. A. and Sabatini, B. L. (2007). Anatomical and physiological plasticity of dendritic spines. *Annu Rev Neurosci*, 30:79–97.

Alzheimer's-Association (2020). 2020 Alzheimer's disease facts and figures. *Alzheimers Dement*.

Amaral, D. G., Scharfman, H. E., and Lavenex, P. (2007). The dentate gyrus: fundamental neuroanatomical organization (dentate gyrus for dummies). *Prog Brain Res*, 163:3–22.

Andersen, P., Morris, R., Amaral, D., Bliss, T., and O'Keefe, J. (2006). *The hippocampus book*. Oxford University Press.

Andrade-Moraes, C. H., Oliveira-Pinto, A. V., Castro-Fonseca, E., da Silva, C. G., Guimaraes, D. M., Szczupak, D., Parente-Bruno, D. R., Carvalho, L. R., Polichiso, L., Gomes, B. V., Oliveira, L. M., Rodriguez, R. D., Leite, R. E., Ferretti-Rebustini, R. E., Jacob-Filho, W., Pasqualucci, C. A., Grinberg, L. T., and Lent, R. (2013). Cell number changes in Alzheimer's disease relate to dementia, not to plaques and tangles. *Brain*, 136(Pt 12):3738–52.

Arriagada, P. V., Growdon, J. H., Hedley-Whyte, E. T., and Hyman, B. T. (1992). Neurofibrillary tangles but not senile plaques parallel duration and severity of Alzheimer's disease. *Neurology*, 42(3 Pt 1):631–9.

Auer, M., Hausott, B., and Klimaschewski, L. (2011). Rho GTPases as regulators of morphological neuroplasticity. *Ann Anat*, 193(4):259–66.

Augustinack, J. C., van der Kouwe, A. J., Salat, D. H., Benner, T., Stevens, A. A., Annese, J., Fischl, B., Frosch, M. P., and Corkin, S. (2014). H.M.'s contributions to neuroscience: a review and autopsy studies. *Hippocampus*, 24(11):1267–86.

Aytan, N., Choi, J. K., Carreras, I., Crabtree, L., Nguyen, B., Lehar, M., Blusztajn, J. K., Jenkins, B. G., and Dedeoglu, A. (2018). Protective effects of 7,8-dihydroxyflavone on neuropathological and neurochemical changes in a mouse model of Alzheimer's disease. *Eur J Pharmacol*, 828:9–17.

Bannerman, D. M., Rawlins, J. N., McHugh, S. B., Deacon, R. M., Yee, B. K., Bast, T., Zhang, W. N., Pothuizen, H. H., and Feldon, J. (2004). Regional dissociations within the hippocampus–memory and anxiety. *Neurosci Biobehav Rev*, 28(3):273–83.

Baquet, Z. C., Gorski, J. A., and Jones, K. R. (2004). Early striatal dendrite deficits followed by neuron loss with advanced age in the absence of anterograde cortical brain-derived neurotrophic factor. *J Neurosci*, 24(17):4250–8.

Barco, A., Pittenger, C., and Kandel, E. R. (2003). CREB, memory enhancement and the treatment of memory disorders: promises, pitfalls and prospects. *Expert Opin Ther Targets*, 7(1):101–14.

Barde, Y. A., Edgar, D., and Thoenen, H. (1982). Purification of a new neurotrophic factor from mammalian brain. *EMBO J*, 1(5):549–53.

Barreda Tomas, F. J., Turko, P., Heilmann, H., Trimbuch, T., Yanagawa, Y., Vida, I., and Munster-Wandowski, A. (2020). BDNF expression in cortical GABAergic interneurons. *Int J Mol Sci*, 21(5).

Bascunana, P., Mohle, L., Brackhan, M., and Pahnke, J. (2020). Fingolimod as a treatment in neurologic disorders beyond multiple sclerosis. *Drugs R D*, 20(3):197–207.

Baseri, B., Choi, J. J., Deffieux, T., Samiotaki, G., Tung, Y. S., Olumolade, O., Small, S. A., Morrison, B., and Konofagou, E. E. (2012). Activation of signaling pathways following localized delivery of systemically administered neurotrophic factors across the blood-brain barrier using focused ultrasound and microbubbles. *Phys Med Biol*, 57(7):N65–81.

Baydyuk, M. and Xu, B. (2014). BDNF signaling and survival of striatal neurons. *Front Cell Neurosci*, 8:254.

Benavides-Piccione, R., Regalado-Reyes, M., Fernaud-Espinosa, I., Kastanauskaite, A., Tapia-Gonzalez, S., Leon-Espinosa, G., Rojo, C., Insausti, R., Segev, I., and DeFelipe, J. (2020). Differential structure of hippocampal CA1 pyramidal neurons in the human and mouse. *Cereb Cortex*, 30(2):730–752.

Berghuis, P., Agerman, K., Dobszay, M. B., Minichiello, L., Harkany, T., and Ernfors, P. (2006). Brain-derived neurotrophic factor selectively regulates dendritogenesis of parvalbumin-containing interneurons in the main olfactory bulb through the PLCgamma pathway. *J Neurobiol*, 66(13):1437–51.

Berry, K. P. and Nedivi, E. (2017). Spine dynamics: are they all the same? *Neuron*, 96(1):43–55.

Binder, D. K., Croll, S. D., Gall, C. M., and Scharfman, H. E. (2001). BDNF and epilepsy: too much of a good thing? *Trends Neurosci*, 24(1):47–53.

Blank, M., Petry, F. S., Lichtenfels, M., Valiati, F. E., Dornelles, A. S., and Roesler, R. (2016). TrkB blockade in the hippocampus after training or retrieval impairs memory: protection from consolidation impairment by histone deacetylase inhibition. *J Neural Transm (Vienna)*, 123(3):159–65.

Bliss, T. V. and Cooke, S. F. (2011). Long-term potentiation and long-term depression: a clinical perspective. *Clinics (Sao Paulo)*, 66 Suppl 1:3–17.

Bliss, T. V. and Lomo, T. (1973). Long-lasting potentiation of synaptic transmission in the dentate area of the anaesthetized rabbit following stimulation of the perforant path. *J Physiol*, 232(2):331–56.

Boltaev, U., Meyer, Y., Tolibzoda, F., Jacques, T., Gassaway, M., Xu, Q., Wagner, F., Zhang, Y. L., Palmer, M., Holson, E., and Sames, D. (2017). Multiplex quantitative assays indicate a need for reevaluating reported small-molecule TrkB agonists. *Sci Signal*, 10(493).

Bonhoeffer, T. and Yuste, R. (2002). Spine motility. phenomenology, mechanisms, and function. *Neuron*, 35(6):1019–27.

Booker, S. A. and Vida, I. (2018). Morphological diversity and connectivity of hippocampal interneurons. *Cell Tissue Res*, 373(3):619–641.

Boots, E. A., Schultz, S. A., Clark, L. R., Racine, A. M., Darst, B. F., Koscik, R. L., Carlsson, C. M., Gallagher, C. L., Hogan, K. J., Bendlin, B. B., Asthana, S., Sager, M. A., Hermann, B. P., Christian, B. T., Dubal, D. B., Engelman, C. D., Johnson, S. C., and Okonkwo, O. C. (2017). BDNF val66met predicts cognitive decline in the wisconsin registry for Alzheimer's prevention. *Neurology*, 88(22):2098–2106.

Bosch, M., Castro, J., Saneyoshi, T., Matsuno, H., Sur, M., and Hayashi, Y. (2014). Structural and molecular remodeling of dendritic spine substructures during long-term potentiation. *Neuron*, 82(2):444–59.

Bosch, M. and Hayashi, Y. (2012). Structural plasticity of dendritic spines. *Curr Opin Neurobiol*, 22(3):383–8.

Bosco, A. and Linden, R. (1999). BDNF and NT-4 differentially modulate neurite outgrowth in developing retinal ganglion cells. *J Neurosci Res*, 57(6):759–69.

Bourne, J. N. and Harris, K. M. (2008). Balancing structure and function at hippocampal dendritic spines. *Annu Rev Neurosci*, 31:47–67.

Brouillette, J. (2014). The effects of soluble abeta oligomers on neurodegeneration in Alzheimer's disease. *Curr Pharm Des*, 20(15):2506–19.

Buchman, A. S., Yu, L., Boyle, P. A., Schneider, J. A., De Jager, P. L., and Bennett, D. A. (2016). Higher brain BDNF gene expression is associated with slower cognitive decline in older adults. *Neurology*, 86(8):735–41.

Buhusi, M., Etheredge, C., Granholm, A. C., and Buhusi, C. V. (2017). Increased hippocampal proBDNF contributes to memory impairments in aged mice. *Front Aging Neurosci*, 9:284.

Burgess, N., Maguire, E. A., and O'Keefe, J. (2002). The human hippocampus and spatial and episodic memory. *Neuron*, 35(4):625–41.

Campa, C. C., Ciraolo, E., Ghigo, A., Germena, G., and Hirsch, E. (2015). Crossroads of PI3K and rac pathways. *Small GTPases*, 6(2):71–80.

Canivet, A., Albinet, C. T., Andre, N., Pylouster, J., Rodriguez-Ballesteros, M., Kitzis, A., and Audiffren, M. (2015). Effects of BDNF polymorphism and physical activity on episodic memory in the elderly: a cross sectional study. *Eur Rev Aging Phys Act*, 12:15.

Cardin, J. A. (2018). Inhibitory interneurons regulate temporal precision and correlations in cortical circuits. *Trends Neurosci*, 41(10):689–700.

Carter, B. D., Zirrgiebel, U., and Barde, Y. A. (1995). Differential regulation of p21ras activation in neurons by nerve growth factor and brain-derived neurotrophic factor. *J Biol Chem*, 270(37):21751–7.

Castello, N. A., Nguyen, M. H., Tran, J. D., Cheng, D., Green, K. N., and LaFerla, F. M. (2014). 7,8-dihydroxyflavone, a small molecule TrkB agonist, improves spatial memory and increases thin spine density in a mouse model of Alzheimer disease-like neuronal loss. *PLoS One*, 9(3):e91453.

Castren, E. and Rantamaki, T. (2010). The role of BDNF and its receptors in depression and antidepressant drug action: Reactivation of developmental plasticity. *Dev Neurobiol*, 70(5):289–97.

Catani, M., Thiebaut de Schotten, M., Slater, D., and Dell'Acqua, F. (2013). Connectomic approaches before the connectome. *Neuroimage*, 80:2–13.

Cazorla, M., Premont, J., Mann, A., Girard, N., Kellendonk, C., and Rognan, D. (2011). Identification of a low-molecular weight TrkB antagonist with anxiolytic and antidepressant activity in mice. *J Clin Invest*, 121(5):1846–57.

Chakravarthy, S., Saiepour, M. H., Bence, M., Perry, S., Hartman, R., Couey, J. J., Mansvelder, H. D., and Levelt, C. N. (2006). Postsynaptic TrkB signaling has distinct roles in spine maintenance in adult visual cortex and hippocampus. *Proc Natl Acad Sci U S A*, 103(4):1071–6.

Chang, Q., Khare, G., Dani, V., Nelson, S., and Jaenisch, R. (2006). The disease progression of Mecp2 mutant mice is affected by the level of BDNF expression. *Neuron*, 49(3):341–8.

Chao, M. V. (2003). Neurotrophins and their receptors: a convergence point for many signalling pathways. *Nat Rev Neurosci*, 4(4):299–309.

Chapleau, C. A. and Pozzo-Miller, L. (2012). Divergent roles of p75NTR and trk receptors in BDNF's effects on dendritic spine density and morphology. *Neural Plast*, 2012:578057.

Chen, A. I., Zang, K., Masliah, E., and Reichardt, L. F. (2016a). Glutamatergic axon-derived BDNF controls GABAergic synaptic differentiation in the cerebellum. *Sci Rep*, 6:20201.

Chen, H., Yang, G. Z., Getachew, H., Acosta, C., Sierra Sanchez, C., and Konofagou, E. E. (2016b). Focused ultrasound-enhanced intranasal brain delivery of brain-derived neurotrophic factor. *Sci Rep*, 6:28599.

Chen, J. G., Jiang, Q. C., Wen, B., Wang, R. Y., Wu, Y. G., and Li, X. (2018). Effects of deoxygedunin on Alzheimer-like pathologic dysfunction induced by D-galactose combined with AlCl3. *Zhongguo Ying Yong Sheng Li Xue Za Zhi*, 34(6):496–500.

Cheng, P. L., Song, A. H., Wong, Y. H., Wang, S., Zhang, X., and Poo, M. M. (2011). Self-amplifying autocrine actions of BDNF in axon development. *Proc Natl Acad Sci U S A*, 108(45):18430–5.

Chowdhury, A. and Caroni, P. (2018). Time units for learning involving maintenance of system-wide cFos expression in neuronal assemblies. *Nat Commun*, 9(1):4122.

Citri, A. and Malenka, R. C. (2008). Synaptic plasticity: multiple forms, functions, and mechanisms. *Neuropsychopharmacology*, 33(1):18–41.

Clarke, E., Sinclair, L., Fletcher, E. J. R., Krawczun-Rygmaczewska, A., Stocki, P., Rutowski, J. L., Doherty, P., and Walsh, F. S. (2020). TrkB agonist antibody delivery to the brain using a TfR1 specific BBB shuttle provides neuroprotection in a mouse model of parkinson's disease (preprint). *bioRxiv*.

Cohen-Cory, S., Kidane, A. H., Shirkey, N. J., and Marshak, S. (2010). Brain-derived neurotrophic factor and the development of structural neuronal connectivity. *Dev Neurobiol*, 70(5):271–88.

Cunha, C., Brambilla, R., and Thomas, K. L. (2010). A simple role for BDNF in learning and memory? *Front Mol Neurosci*, 3:1.

Cunningham, M. E., Stephens, R. M., Kaplan, D. R., and Greene, L. A. (1997). Autophosphorylation of activation loop tyrosines regulates signaling by the TRK nerve growth factor receptor. *J Biol Chem*, 272(16):10957–67.

Danielson, E. and Lee, S. H. (2014). Synpanal: software for rapid quantification of the density and intensity of protein puncta from fluorescence microscopy images of neurons. *PLoS One*, 9(12):e115298.

de Pins, B., Cifuentes-Diaz, C., Farah, A. T., Lopez-Molina, L., Montalban, E., Sancho-Balsells, A., Lopez, A., Gines, S., Delgado-Garcia, J. M., Alberch, J., Gruart, A., Girault, J. A., and Giralt, A. (2019). Conditional BDNF delivery from astrocytes rescues memory deficits, spine density, and synaptic properties in the 5xFAD mouse model of alzheimer disease. *J Neurosci*, 39(13):2441–2458.

DeKosky, S. T. and Scheff, S. W. (1990). Synapse loss in frontal cortex biopsies in Alzheimer's disease: correlation with cognitive severity. *Ann Neurol*, 27(5):457–64.

Deng, P., Anderson, J. D., Yu, A. S., Annett, G., Fink, K. D., and Nolta, J. A. (2016). Engineered BDNF producing cells as a potential treatment for neurologic disease. *Expert Opin Biol Ther*, 16(8):1025–33.

Deogracias, R., Yazdani, M., Dekkers, M. P., Guy, J., Ionescu, M. C., Vogt, K. E., and Barde, Y. A. (2012). Fingolimod, a sphingosine-1 phosphate receptor modulator, increases BDNF levels and improves symptoms of a mouse model of Rett syndrome. *Proc Natl Acad Sci U S A*, 109(35):14230–5.

Devi, L. and Ohno, M. (2012). 7,8-dihydroxyflavone, a small-molecule TrkB agonist, reverses memory deficits and bace1 elevation in a mouse model of Alzheimer's disease. *Neuropsychopharmacology*, 37(2):434–44.

Dijkhuizen, P. A. and Ghosh, A. (2005). BDNF regulates primary dendrite formation in cortical neurons via the PI3-kinase and MAP kinase signaling pathways. *J Neurobiol*, 62(2):278–88.

Dombert, B., Balk, S., Luningschror, P., Moradi, M., Sivadasan, R., Saal-Bauernschubert, L., and Jablonka, S. (2017). BDNF/TrkB induction of calcium transients through cav2.2 calcium channels in motoneurons corresponds to f-actin assembly and growth cone formation on beta2-Chain Laminin (221). *Front Mol Neurosci*, 10:346.

Dong, M., Wu, Y., Fan, Y., Xu, M., and Zhang, J. (2006). c-fos modulates brain-derived neurotrophic factor mRNA expression in mouse hippocampal CA3 and dentate gyrus neurons. *Neurosci Lett*, 400(1-2):177–80.

Dorostkar, M. M., Zou, C., Blazquez-Llorca, L., and Herms, J. (2015). Analyzing dendritic spine pathology in Alzheimer's disease: problems and opportunities. *Acta Neuropathol*, 130(1):1–19.

Eichenbaum, H. (2004). Hippocampus: cognitive processes and neural representations that underlie declarative memory. *Neuron*, 44(1):109–20.

Ernfors, P., Lee, K. F., and Jaenisch, R. (1994). Mice lacking brain-derived neurotrophic factor develop with sensory deficits. *Nature*, 368(6467):147–50.

Ferrer, I., Goutan, E., Marin, C., Rey, M. J., and Ribalta, T. (2000). Brain-derived neurotrophic factor in huntington disease. *Brain Res*, 866(1-2):257–61.

Ferrer, I., Marin, C., Rey, M. J., Ribalta, T., Goutan, E., Blanco, R., Tolosa, E., and Marti, E. (1999). BDNF and full-length and truncated TrkB expression in Alzheimer disease. implications in therapeutic strategies. *J Neuropathol Exp Neurol*, 58(7):729–39.

Figurov, A., Pozzo-Miller, L. D., Olafsson, P., Wang, T., and Lu, B. (1996). Regulation of synaptic responses to high-frequency stimulation and LTP by neurotrophins in the hippocampus. *Nature*, 381(6584):706–9.

Fleitas, C., Pinol-Ripoll, G., Marfull, P., Rocandio, D., Ferrer, I., Rampon, C., Egea, J., and Espinet, C. (2018). proBDNF is modified by advanced glycation end products in Alzheimer's disease and causes neuronal apoptosis by inducing p75 neurotrophin receptor processing. *Mol Brain*, 11(1):68.

Foggetti, A., Baccini, G., Arnold, P., Schiffelholz, T., and Wulff, P. (2019). Spiny and non-spiny parvalbumin-positive hippocampal interneurons show different plastic properties. *Cell Rep*, 27(13):3725–3732 e5.

Fortin, D. A., Davare, M. A., Srivastava, T., Brady, J. D., Nygaard, S., Derkach, V. A., and Soderling, T. R. (2010). Long-term potentiation-dependent spine enlargement requires synaptic Ca2+-permeable AMPA receptors recruited by cam-kinase i. *J Neurosci*, 30(35):11565–75.

Frank, L., Ventimiglia, R., Anderson, K., Lindsay, R. M., and Rudge, J. S. (1996). BDNF down-regulates neurotrophin responsiveness, TrkB protein and TrkB mRNA levels in cultured rat hippocampal neurons. *Eur J Neurosci*, 8(6):1220–30.

Frankland, P. W. and Bontempi, B. (2005). The organization of recent and remote memories. *Nat Rev Neurosci*, 6(2):119–30.

Franzmeier, N., Ren, J., Damm, A., Monte-Rubio, G., Boada, M., Ruiz, A., Ramirez, A., Jessen, F., Duzel, E., Rodriguez Gomez, O., Benzinger, T., Goate, A., Karch, C. M., Fagan, A. M., McDade, E., Buerger, K., Levin, J., Duering, M., Dichgans, M., Suarez-Calvet, M., Haass, C., Gordon, B. A., Lim, Y. Y., Masters, C. L., Janowitz, D., Catak, C., Wolfsgruber, S., Wagner, M., Milz, E., Moreno-Grau, S., Teipel, S.,

Grothe, M. J., Kilimann, I., Rossor, M., Fox, N., Laske, C., Chhatwal, J., Falkai, P., Perneczky, R., Lee, J. H., Spottke, A., Boecker, H., Brosseron, F., Fliessbach, K., Heneka, M. T., Nestor, P., Peters, O., Fuentes, M., Menne, F., Priller, J., Spruth, E. J., Franke, C., Schneider, A., Westerteicher, C., Speck, O., Wiltfang, J., Bartels, C., Araque Caballero, M. A., Metzger, C., Bittner, D., Salloway, S., Danek, A., Hassenstab, J., Yakushev, I., Schofield, P. R., Morris, J. C., Bateman, R. J., and Ewers, M. (2019). The BDNFval66met snp modulates the association between beta-amyloid and hippocampal disconnection in Alzheimer's disease. *Mol Psychiatry*.

Frey, U. and Morris, R. G. (1997). Synaptic tagging and long-term potentiation. *Nature*, 385(6616):533–6.

Fukumoto, N., Fujii, T., Combarros, O., Kamboh, M. I., Tsai, S. J., Matsushita, S., Nacmias, B., Comings, D. E., Arboleda, H., Ingelsson, M., Hyman, B. T., Akatsu, H., Grupe, A., Nishimura, A. L., Zatz, M., Mattila, K. M., Rinne, J., Goto, Y., Asada, T., Nakamura, S., and Kunugi, H. (2010). Sexually dimorphic effect of the val66met polymorphism of BDNF on susceptibility to Alzheimer's disease: New data and meta-analysis. *Am J Med Genet B Neuropsychiatr Genet*, 153B(1):235–42.

Fumagalli, F., Racagni, G., and Riva, M. A. (2006). The expanding role of BDNF: a therapeutic target for Alzheimer's disease? *Pharmacogenomics J*, 6(1):8–15.

Furutani, Y. and Yoshihara, Y. (2018). Proteomic analysis of dendritic filopodia-rich fraction isolated by telencephalin and vitronectin interaction. *Frontiers in synaptic neuroscience*, 10:27.

Gallo, G., Ernst, A. F., McLoon, S. C., and Letourneau, P. C. (2002). Transient pka activity is required for initiation but not maintenance of BDNF-mediated protection from nitric oxide-induced growth-cone collapse. *J Neurosci*, 22(12):5016–23.

Gao, L., Tian, M., Zhao, H. Y., Xu, Q. Q., Huang, Y. M., Si, Q. C., Tian, Q., Wu, Q. M., Hu, X. M., Sun, L. B., McClintock, S. M., and Zeng, Y. (2016). TrkB activation by 7, 8-dihydroxyflavone increases synapse AMPA subunits and ameliorates spatial memory deficits in a mouse model of Alzheimer's disease. *J Neurochem*, 136(3):620–36.

Gao, X., Smith, G. M., and Chen, J. (2009). Impaired dendritic development and synaptic formation of postnatal-born dentate gyrus granular neurons in the absence of brain-derived neurotrophic factor signaling. *Exp Neurol*, 215(1):178–90.

Garaschuk, O., Schneggenburger, R., Schirra, C., Tempia, F., and Konnerth, A. (1996). Fractional ca2+ currents through somatic and dendritic glutamate receptor channels of rat hippocampal CA1 pyramidal neurones. *J Physiol*, 491 (Pt 3):757–72.

Garcia-Diaz Barriga, G., Giralt, A., Anglada-Huguet, M., Gaja-Capdevila, N., Orlandi, J. G., Soriano, J., Canals, J. M., and Alberch, J. (2017). 7,8-dihydroxyflavone ameliorates cognitive and motor deficits in a Huntington's disease mouse model through specific activation of the PLCgamma1 pathway. *Hum Mol Genet*, 26(16):3144–3160.

Gascon, E., Vutskits, L., Zhang, H., Barral-Moran, M. J., Kiss, P. J., Mas, C., and Kiss, J. Z. (2005). Sequential activation of p75 and TrkB is involved in dendritic development of subventricular zone-derived neuronal progenitors in vitro. *Eur J Neurosci*, 21(1):69–80.

Gengler, S., Hamilton, A., and Holscher, C. (2010). Synaptic plasticity in the hippocampus of a app/ps1 mouse model of Alzheimer's disease is impaired in old but not young mice. *PLoS One*, 5(3):e9764.

Gibon, J. and Barker, P. A. (2017). Neurotrophins and proneurotrophins: Focus on synaptic activity and plasticity in the brain. *Neuroscientist*, 23(6):587–604.

Gibon, J., Barker, P. A., and Seguela, P. (2016). Opposing presynaptic roles of BDNF and proBDNF in the regulation of persistent activity in the entorhinal cortex. *Mol Brain*, 9:23.

Gimenez, F., Krauze, M. T., Valles, F., Hadaczek, P., Bringas, J., Sharma, N., Forsayeth, J., and Bankiewicz, K. S. (2011). Image-guided convection-enhanced delivery of GDNF protein into monkey putamen. *Neuroimage*, 54 Suppl 1:S189–95.

Ginsberg, S. D., Alldred, M. J., Counts, S. E., Cataldo, A. M., Neve, R. L., Jiang, Y., Wuu, J., Chao, M. V., Mufson, E. J., Nixon, R. A., and Che, S. (2010). Microarray

analysis of hippocampal CA1 neurons implicates early endosomal dysfunction during Alzheimer's disease progression. *Biol Psychiatry*, 68(10):885–93.

Gomez-Isla, T., Hollister, R., West, H., Mui, S., Growdon, J. H., Petersen, R. C., Parisi, J. E., and Hyman, B. T. (1997). Neuronal loss correlates with but exceeds neurofibrillary tangles in Alzheimer's disease. *Ann Neurol*, 41(1):17–24.

Gomez-Pinilla, F., So, V., and Kesslak, J. P. (2001). Spatial learning induces neurotrophin receptor and synapsin i in the hippocampus. *Brain Res*, 904(1):13–9.

Gooney, M., Shaw, K., Kelly, A., O'Mara, S. M., and Lynch, M. A. (2002). Long-term potentiation and spatial learning are associated with increased phosphorylation of TrkB and extracellular signal-regulated kinase (erk) in the dentate gyrus: evidence for a role for brain-derived neurotrophic factor. *Behav Neurosci*, 116(3):455–63.

Govek, E. E., Newey, S. E., and Van Aelst, L. (2005). The role of the Rho GTPases in neuronal development. *Genes Dev*, 19(1):1–49.

Graves, A. R., Moore, S. J., Bloss, E. B., Mensh, B. D., Kath, W. L., and Spruston, N. (2012). Hippocampal pyramidal neurons comprise two distinct cell types that are countermodulated by metabotropic receptors. *Neuron*, 76(4):776–89.

Guirado, R., Perez-Rando, M., Sanchez-Matarredona, D., Castillo-Gomez, E., Liberia, T., Rovira-Esteban, L., Varea, E., Crespo, C., Blasco-Ibanez, J. M., and Nacher, J. (2014). The dendritic spines of interneurons are dynamic structures influenced by PSA-NCAM expression. *Cereb Cortex*, 24(11):3014–24.

Gulyas, A. I., Megias, M., Emri, Z., and Freund, T. F. (1999). Total number and ratio of excitatory and inhibitory synapses converging onto single interneurons of different types in the CA1 area of the rat hippocampus. *J Neurosci*, 19(22):10082–97.

Guo, W., Ji, Y., Wang, S., Sun, Y., and Lu, B. (2014). Neuronal activity alters BDNF-TrkB signaling kinetics and downstream functions. *J Cell Sci*, 127(Pt 10):2249–60.

Guo, W., Pang, K., Chen, Y., Wang, S., Li, H., Xu, Y., Han, F., Yao, H., Liu, H., Lopes-Rodrigues, V., Sun, D., Shao, J., Shen, J., Dou, Y., Zhang, W., You, H., Wu, W.,

and Lu, B. (2019). TrkB agonistic antibodies superior to BDNF: Utility in treating motoneuron degeneration. *Neurobiol Dis*, 132:104590.

Haddad, Y., Adam, V., and Heger, Z. (2017). Trk receptors and neurotrophin cross-interactions: New perspectives toward manipulating therapeutic side-effects. *Front Mol Neurosci*, 10:130.

Hall, J., Thomas, K. L., and Everitt, B. J. (2000). Rapid and selective induction of BDNF expression in the hippocampus during contextual learning. *Nat Neurosci*, 3(6):533–5.

Hao, L., Yang, Z., and Lei, J. (2018). Underlying mechanisms of cooperativity, input specificity, and associativity of long-term potentiation through a positive feedback of local protein synthesis. *Front Comput Neurosci*, 12:25.

Harms, K. J. and Dunaevsky, A. (2007). Dendritic spine plasticity: looking beyond development. *Brain Res*, 1184:65–71.

Harward, S. C., Hedrick, N. G., Hall, C. E., Parra-Bueno, P., Milner, T. A., Pan, E., Laviv, T., Hempstead, B. L., Yasuda, R., and McNamara, J. O. (2016). Autocrine BDNF-TrkB signalling within a single dendritic spine. *Nature*, 538(7623):99–103.

He, H. Y., Shen, W., Zheng, L., Guo, X., and Cline, H. T. (2018). Excitatory synaptic dysfunction cell-autonomously decreases inhibitory inputs and disrupts structural and functional plasticity. *Nat Commun*, 9(1):2893.

He, J., Yamada, K., and Nabeshima, T. (2002). A role of Fos expression in the CA3 region of the hippocampus in spatial memory formation in rats. *Neuropsychopharmacology*, 26(2):259–68.

He, Y., Wei, M., Wu, Y., Qin, H., Li, W., Ma, X., Cheng, J., Ren, J., Shen, Y., Chen, Z., Sun, B., Huang, F. D., Shen, Y., and Zhou, Y. D. (2019). Amyloid beta oligomers suppress excitatory transmitter release via presynaptic depletion of phosphatidylinositol-4,5-bisphosphate. *Nat Commun*, 10(1):1193.

Hefti, F., Goure, W. F., Jerecic, J., Iverson, K. S., Walicke, P. A., and Krafft, G. A. (2013). The case for soluble abeta oligomers as a drug target in Alzheimer's disease. *Trends Pharmacol Sci*, 34(5):261–6.

Heldt, S. A., Stanek, L., Chhatwal, J. P., and Ressler, K. J. (2007). Hippocampus-specific deletion of BDNF in adult mice impairs spatial memory and extinction of aversive memories. *Mol Psychiatry*, 12(7):656–70.

Hering, H. and Sheng, M. (2001). Dendritic spines: structure, dynamics and regulation. *Nat Rev Neurosci*, 2(12):880–8.

Hock, C., Heese, K., Hulette, C., Rosenberg, C., and Otten, U. (2000). Region-specific neurotrophin imbalances in alzheimer disease: decreased levels of brain-derived neurotrophic factor and increased levels of nerve growth factor in hippocampus and cortical areas. *Arch Neurol*, 57(6):846–51.

Holm, M. M., Nieto-Gonzalez, J. L., Vardya, I., Vaegter, C. B., Nykjaer, A., and Jensen, K. (2009). Mature BDNF, but not proBDNF, reduces excitability of fast-spiking interneurons in mouse dentate gyrus. *J Neurosci*, 29(40):12412–8.

Holtmaat, A. and Svoboda, K. (2009). Experience-dependent structural synaptic plasticity in the mammalian brain. *Nat Rev Neurosci*, 10(9):647–58.

Hong, E. J., McCord, A. E., and Greenberg, M. E. (2008). A biological function for the neuronal activity-dependent component of BDNF transcription in the development of cortical inhibition. *Neuron*, 60(4):610–24.

Horch, H. W. and Katz, L. C. (2002). BDNF release from single cells elicits local dendritic growth in nearby neurons. *Nat Neurosci*, 5(11):1177–84.

Horch, H. W., Kruttgen, A., Portbury, S. D., and Katz, L. C. (1999). Destabilization of cortical dendrites and spines by BDNF. *Neuron*, 23(2):353–64.

Howells, D. W., Porritt, M. J., Wong, J. Y., Batchelor, P. E., Kalnins, R., Hughes, A. J., and Donnan, G. A. (2000). Reduced BDNF mRNA expression in the parkinson's disease substantia nigra. *Exp Neurol*, 166(1):127–35.

Huang, E. J. and Reichardt, L. F. (2001). Neurotrophins: roles in neuronal development and function. *Annu Rev Neurosci*, 24:677–736.

Huang, E. J. and Reichardt, L. F. (2003). Trk receptors: roles in neuronal signal transduction. *Annu Rev Biochem*, 72:609–42.

Huang, Z. J., Kirkwood, A., Pizzorusso, T., Porciatti, V., Morales, B., Bear, M. F., Maffei, L., and Tonegawa, S. (1999). BDNF regulates the maturation of inhibition and the critical period of plasticity in mouse visual cortex. *Cell*, 98(6):739–55.

Iwasaki, K., Isaacs, K. R., and Jacobowitz, D. M. (1998). Brain-derived neurotrophic factor stimulates neurite outgrowth in a calretinin-enriched neuronal culture system. *Int J Dev Neurosci*, 16(2):135–45.

Jahr, C. E. and Stevens, C. F. (1993). Calcium permeability of the n-methyl-d-aspartate receptor channel in hippocampal neurons in culture. *Proc Natl Acad Sci U S A*, 90(24):11573–7.

Jang, S. W., Liu, X., Chan, C. B., France, S. A., Sayeed, I., Tang, W., Lin, X., Xiao, G., Andero, R., Chang, Q., Ressler, K. J., and Ye, K. (2010a). Deoxygedunin, a natural product with potent neurotrophic activity in mice. *PLoS One*, 5(7):e11528.

Jang, S. W., Liu, X., Yepes, M., Shepherd, K. R., Miller, G. W., Liu, Y., Wilson, W. D., Xiao, G., Blanchi, B., Sun, Y. E., and Ye, K. (2010b). A selective TrkB agonist with potent neurotrophic activities by 7,8-dihydroxyflavone. *Proc Natl Acad Sci U S A*, 107(6):2687–92.

Ji, Y., Lu, Y., Yang, F., Shen, W., Tang, T. T., Feng, L., Duan, S., and Lu, B. (2010). Acute and gradual increases in BDNF concentration elicit distinct signaling and functions in neurons. *Nat Neurosci*, 13(3):302–9.

Ji, Y., Pang, P. T., Feng, L., and Lu, B. (2005). Cyclic AMP controls BDNF-induced TrkB phosphorylation and dendritic spine formation in mature hippocampal neurons. *Nat Neurosci*, 8(2):164–72.

Jiang, M., Peng, Q., Liu, X., Jin, J., Hou, Z., Zhang, J., Mori, S., Ross, C. A., Ye, K., and Duan, W. (2013). Small-molecule TrkB receptor agonists improve motor function and extend survival in a mouse model of Huntington's disease. *Hum Mol Genet*, 22(12):2462–70.

Jiao, S. S., Shen, L. L., Zhu, C., Bu, X. L., Liu, Y. H., Liu, C. H., Yao, X. Q., Zhang, L. L., Zhou, H. D., Walker, D. G., Tan, J., Gotz, J., Zhou, X. F., and Wang, Y. J. (2016).

Brain-derived neurotrophic factor protects against tau-related neurodegeneration of Alzheimer's disease. *Transl Psychiatry*, 6(10):e907.

Johnson, R. A., Lam, M., Punzo, A. M., Li, H., Lin, B. R., Ye, K., Mitchell, G. S., and Chang, Q. (2012). 7,8-dihydroxyflavone exhibits therapeutic efficacy in a mouse model of Rett syndrome. *J Appl Physiol (1985)*, 112(5):704–10.

Kafitz, K. W., Rose, C. R., Thoenen, H., and Konnerth, A. (1999). Neurotrophin-evoked rapid excitation through TrkB receptors. *Nature*, 401(6756):918–21.

Kang, H., Welcher, A. A., Shelton, D., and Schuman, E. M. (1997). Neurotrophins and time: different roles for TrkB signaling in hippocampal long-term potentiation. *Neuron*, 19(3):653–64.

Kang, H. J. and Schuman, E. M. (1995). Neurotrophin-induced modulation of synaptic transmission in the adult hippocampus. *J Physiol Paris*, 89(1):11–22.

Kasai, H., Fukuda, M., Watanabe, S., Hayashi-Takagi, A., and Noguchi, J. (2010). Structural dynamics of dendritic spines in memory and cognition. *Trends Neurosci*, 33(3):121–9.

Kauer, J. A. and Malenka, R. C. (2007). Synaptic plasticity and addiction. *Nat Rev Neurosci*, 8(11):844–58.

Kawamoto, Y., Nakamura, S., Nakano, S., Oka, N., Akiguchi, I., and Kimura, J. (1996). Immunohistochemical localization of brain-derived neurotrophic factor in adult rat brain. *Neuroscience*, 74(4):1209–26.

Kelleher, R. J., r., Govindarajan, A., and Tonegawa, S. (2004). Translational regulatory mechanisms in persistent forms of synaptic plasticity. *Neuron*, 44(1):59–73.

Kellner, Y., Godecke, N., Dierkes, T., Thieme, N., Zagrebelsky, M., and Korte, M. (2014). The BDNF effects on dendritic spines of mature hippocampal neurons depend on neuronal activity. *Front Synaptic Neurosci*, 6:5.

Kennedy, K. M., Reese, E. D., Horn, M. M., Sizemore, A. N., Unni, A. K., Meerbrey, M. E., Kalich, A. G., J., and Rodrigue, K. M. (2015). BDNF val66met polymorphism affects aging of multiple types of memory. *Brain Res*, 1612:104–17.

Kerkis, I., Macedo da Silva, J., Wenceslau, C., Mambelli-Lisboa, N., and Frare, E. (2020). *Brain-Derived Neurotrophic Factor and Stem Cell-Based Technologies in Huntington's Disease Therapy*. [Online First], IntechOpen.

Kesslak, J. P., So, V., Choi, J., Cotman, C. W., and Gomez-Pinilla, F. (1998). Learning upregulates brain-derived neurotrophic factor messenger ribonucleic acid: a mechanism to facilitate encoding and circuit maintenance? *Behav Neurosci*, 112(4):1012–9.

Khalin, I., Alyautdin, R., Wong, T. W., Gnanou, J., Kocherga, G., and Kreuter, J. (2016). Brain-derived neurotrophic factor delivered to the brain using poly (lactide-co-glycolide) nanoparticles improves neurological and cognitive outcome in mice with traumatic brain injury. *Drug Deliv*, 23(9):3520–3528.

Kim, J., Lee, S., Kang, S., Kim, S. H., Kim, J. C., Yang, M., and Moon, C. (2017). Brain-derived neurotropic factor and GABAergic transmission in neurodegeneration and neuroregeneration. *Neural Regen Res*, 12(10):1733–1741.

Klausberger, T. and Somogyi, P. (2008). Neuronal diversity and temporal dynamics: the unity of hippocampal circuit operations. *Science*, 321(5885):53–7.

Klein, R., Smeyne, R. J., Wurst, W., Long, L. K., Auerbach, B. A., Joyner, A. L., and Barbacid, M. (1993). Targeted disruption of the TrkB neurotrophin receptor gene results in nervous system lesions and neonatal death. *Cell*, 75(1):113–22.

Knusel, B., Gao, H., Okazaki, T., Yoshida, T., Mori, N., Hefti, F., and Kaplan, D. R. (1997). Ligand-induced down-regulation of Trk messenger rna, protein and tyrosine phosphorylation in rat cortical neurons. *Neuroscience*, 78(3):851–62.

Kohara, K., Kitamura, A., Adachi, N., Nishida, M., Itami, C., Nakamura, S., and Tsumoto, T. (2003). Inhibitory but not excitatory cortical neurons require presynaptic brain-derived neurotrophic factor for dendritic development, as revealed by chimera cell culture. *J Neurosci*, 23(14):6123–31.

Kohara, K., Yasuda, H., Huang, Y., Adachi, N., Sohya, K., and Tsumoto, T. (2007). A local reduction in cortical GABAergic synapses after a loss of endogenous brain-

derived neurotrophic factor, as revealed by single-cell gene knock-out method. *J Neurosci*, 27(27):7234–44.

Koleske, A. J. (2013). Molecular mechanisms of dendrite stability. *Nat Rev Neurosci*, 14(8):536–50.

Kommaddi, R. P., Das, D., Karunakaran, S., Nanguneri, S., Bapat, D., Ray, A., Shaw, E., Bennett, D. A., Nair, D., and Ravindranath, V. (2018). Abeta mediates f-actin disassembly in dendritic spines leading to cognitive deficits in Alzheimer's disease. *J Neurosci*, 38(5):1085–1099.

Korte, M. and Bonhoeffer, T. (1997). Activity-dependent synaptic plasticity: a new face of action for neurotrophins. *Mol Psychiatry*, 2(3):197–9.

Korte, M., Carroll, P., Wolf, E., Brem, G., Thoenen, H., and Bonhoeffer, T. (1995). Hippocampal long-term potentiation is impaired in mice lacking brain-derived neurotrophic factor. *Proc Natl Acad Sci U S A*, 92(19):8856–60.

Korte, M., Griesbeck, O., Gravel, C., Carroll, P., Staiger, V., Thoenen, H., and Bonhoeffer, T. (1996). Virus-mediated gene transfer into hippocampal CA1 region restores long-term potentiation in brain-derived neurotrophic factor mutant mice. *Proc Natl Acad Sci U S A*, 93(22):12547–52.

Korte, M., Kang, H., Bonhoeffer, T., and Schuman, E. (1998). A role for BDNF in the late-phase of hippocampal long-term potentiation. *Neuropharmacology*, 37(4-5):553–9.

Korte, M. and Schmitz, D. (2016). Cellular and system biology of memory: timing, molecules, and beyond. *Physiological reviews*, 96(2):647–693.

Kovacs, K. J. (2008). Measurement of immediate-early gene activation- c-fos and beyond. *J Neuroendocrinol*, 20(6):665–72.

Kulkarni, V. A. and Firestein, B. L. (2012). The dendritic tree and brain disorders. *Mol Cell Neurosci*, 50(1):10–20.

Kumar, A. (2011). Long-term potentiation at CA3-CA1 hippocampal synapses with special emphasis on aging, disease, and stress. *Front Aging Neurosci*, 3:7.

Kwon, H. B. and Sabatini, B. L. (2011). Glutamate induces de novo growth of functional spines in developing cortex. *Nature*, 474(7349):100–4.

Lacor, P. N., Buniel, M. C., Chang, L., Fernandez, S. J., Gong, Y., Viola, K. L., Lambert, M. P., Velasco, P. T., Bigio, E. H., Finch, C. E., Krafft, G. A., and Klein, W. L. (2004). Synaptic targeting by Alzheimer's-related amyloid beta oligomers. *J Neurosci*, 24(45):10191–200.

Lacor, P. N., Buniel, M. C., Furlow, P. W., Clemente, A. S., Velasco, P. T., Wood, M., Viola, K. L., and Klein, W. L. (2007). Abeta oligomer-induced aberrations in synapse composition, shape, and density provide a molecular basis for loss of connectivity in Alzheimer's disease. *J Neurosci*, 27(4):796–807.

Lai, P. C., Chiu, T. H., and Huang, Y. T. (2010). Overexpression of BDNF and TrkB in human bladder cancer specimens. *Oncol Rep*, 24(5):1265–70.

Lanoue, V. and Cooper, H. M. (2019). Branching mechanisms shaping dendrite architecture. *Dev Biol*, 451(1):16–24.

Laske, C., Stellos, K., Hoffmann, N., Stransky, E., Straten, G., Eschweiler, G. W., and Leyhe, T. (2011). Higher BDNF serum levels predict slower cognitive decline in Alzheimer's disease patients. *Int J Neuropsychopharmacol*, 14(3):399–404.

Lee, F. S., Kim, A. H., Khursigara, G., and Chao, M. V. (2001). The uniqueness of being a neurotrophin receptor. *Curr Opin Neurobiol*, 11(3):281–6.

Lewin, G. R. and Barde, Y. A. (1996). Physiology of the neurotrophins. *Annu Rev Neurosci*, 19:289–317.

Li, T., Yu, Y., Song, Y., Li, X., Lan, D., Zhang, P., Xiao, Y., and Xing, Y. (2020). Activation of BDNF/TrkB pathway promotes prostate cancer progression via induction of epithelial-mesenchymal transition and anoikis resistance. *FASEB J*, 34(7):9087–9101.

Li, W., Bellot-Saez, A., Phillips, M. L., Yang, T., Longo, F. M., and Pozzo-Miller, L. (2017). A small-molecule TrkB ligand restores hippocampal synaptic plasticity and object location memory in Rett syndrome mice. *Dis Model Mech*, 10(7):837–845.

Li, X. H., Dai, C. F., Chen, L., Zhou, W. T., Han, H. L., and Dong, Z. F. (2016). 7,8-dihydroxyflavone ameliorates motor deficits via suppressing alpha-synuclein expression and oxidative stress in the mptp-induced mouse model of parkinson's disease. *CNS Neurosci Ther*, 22(7):617–24.

Lim, Y. Y., Villemagne, V. L., Laws, S. M., Ames, D., Pietrzak, R. H., Ellis, K. A., Harrington, K. D., Bourgeat, P., Salvado, O., Darby, D., Snyder, P. J., Bush, A. I., Martins, R. N., Masters, C. L., Rowe, C. C., Nathan, P. J., Maruff, P., Australian Imaging, B., and Lifestyle Research, G. (2013). BDNF val66met, abeta amyloid, and cognitive decline in preclinical Alzheimer's disease. *Neurobiol Aging*, 34(11):2457–64.

Lin, P. Y., Kavalali, E. T., and Monteggia, L. M. (2018). Genetic dissection of presynaptic and postsynaptic BDNF-TrkB signaling in synaptic efficacy of CA3-CA1 synapses. *Cell Rep*, 24(6):1550–1561.

Lin, Y. C. and Koleske, A. J. (2010). Mechanisms of synapse and dendrite maintenance and their disruption in psychiatric and neurodegenerative disorders. *Annu Rev Neurosci*, 33:349–78.

Linnarsson, S., Bjorklund, A., and Ernfors, P. (1997). Learning deficit in BDNF mutant mice. *Eur J Neurosci*, 9(12):2581–7.

Lisman, J. (1989). A mechanism for the hebb and the anti-hebb processes underlying learning and memory. *Proc Natl Acad Sci U S A*, 86(23):9574–8.

Liu, X., Obianyo, O., Chan, C. B., Huang, J., Xue, S., Yang, J. J., Zeng, F., Goodman, M., and Ye, K. (2014). Biochemical and biophysical investigation of the brain-derived neurotrophic factor mimetic 7,8-dihydroxyflavone in the binding and activation of the TrkB receptor. *J Biol Chem*, 289(40):27571–84.

Lom, B. and Cohen-Cory, S. (1999). Brain-derived neurotrophic factor differentially regulates retinal ganglion cell dendritic and axonal arborization in vivo. *J Neurosci*, 19(22):9928–38.

Lu, B., Nagappan, G., Guan, X., Nathan, P. J., and Wren, P. (2013). BDNF-based synaptic repair as a disease-modifying strategy for neurodegenerative diseases. *Nat Rev Neurosci*, 14(6):401–16.

Lu, Y., Christian, K., and Lu, B. (2008). BDNF: a key regulator for protein synthesis-dependent LTP and long-term memory? *Neurobiol Learn Mem*, 89(3):312–23.

Lughetti, L., Lucaccioni, L., Fugetto, F., Predieri, B., Berardi, A., and Ferrari, F. (2018). Brain-derived neurotrophic factor and epilepsy: a systematic review. *Neuropeptides*, 72:23–29.

Luikart, B. W., Nef, S., Virmani, T., Lush, M. E., Liu, Y., Kavalali, E. T., and Parada, L. F. (2005). TrkB has a cell-autonomous role in the establishment of hippocampal schaffer collateral synapses. *J Neurosci*, 25(15):3774–86.

Luo, L. (2000). Rho GTPases in neuronal morphogenesis. *Nat Rev Neurosci*, 1(3):173–80.

Maccaferri, G. and Lacaille, J. C. (2003). Interneuron diversity series: Hippocampal interneuron classifications–making things as simple as possible, not simpler. *Trends Neurosci*, 26(10):564–71.

Mammen, A. L., Kameyama, K., Roche, K. W., and Huganir, R. L. (1997). Phosphorylation of the alpha-amino-3-hydroxy-5-methylisoxazole4-propionic acid receptor glur1 subunit by calcium/calmodulin-dependent kinase ii. *J Biol Chem*, 272(51):32528–33.

Marjanska, M., Curran, G. L., Wengenack, T. M., Henry, P. G., Bliss, R. L., Poduslo, J. F., Jack, C. R., J., Ugurbil, K., and Garwood, M. (2005). Monitoring disease progression in transgenic mouse models of Alzheimer's disease with proton magnetic resonance spectroscopy. *Proc Natl Acad Sci U S A*, 102(33):11906–10.

Markram, H., Toledo-Rodriguez, M., Wang, Y., Gupta, A., Silberberg, G., and Wu, C. (2004). Interneurons of the neocortical inhibitory system. *Nat Rev Neurosci*, 5(10):793–807.

Marty, S., Carroll, P., Cellerino, A., Castren, E., Staiger, V., Thoenen, H., and Lindholm, D. (1996). Brain-derived neurotrophic factor promotes the differentiation of various hippocampal nonpyramidal neurons, including cajal-retzius cells, in organotypic slice cultures. *J Neurosci*, 16(2):675–87.

Massa, S. M., Yang, T., Xie, Y., Shi, J., Bilgen, M., Joyce, J. N., Nehama, D., Rajadas, J., and Longo, F. M. (2010). Small molecule BDNF mimetics activate TrkB signaling and prevent neuronal degeneration in rodents. *J Clin Invest*, 120(5):1774–85.

Matsuzaki, M., Honkura, N., Ellis-Davies, G. C., and Kasai, H. (2004). Structural basis of long-term potentiation in single dendritic spines. *Nature*, 429(6993):761–6.

Mattson, M. P. (2020). Involvement of GABAergic interneuron dysfunction and neuronal network hyperexcitability in Alzheimer's disease: Amelioration by metabolic switching. *Int Rev Neurobiol*, 154:191–205.

Mayr, B. and Montminy, M. (2001). Transcriptional regulation by the phosphorylation-dependent factor CREB. *Nat Rev Mol Cell Biol*, 2(8):599–609.

McAllister, A. K., Katz, L. C., and Lo, D. C. (1997). Opposing roles for endogenous BDNF and NT-3 in regulating cortical dendritic growth. *Neuron*, 18(5):767–78.

McAllister, A. K., Katz, L. C., and Lo, D. C. (1999). Neurotrophins and synaptic plasticity. *Annu Rev Neurosci*, 22:295–318.

McAllister, A. K., Lo, D. C., and Katz, L. C. (1995). Neurotrophins regulate dendritic growth in developing visual cortex. *Neuron*, 15(4):791–803.

McCarty, J. H. and Feinstein, S. C. (1998). Activation loop tyrosines contribute varying roles to TrkB autophosphorylation and signal transduction. *Oncogene*, 16(13):1691–700.

Meeker, R. B. and Williams, K. S. (2015). The p75 neurotrophin receptor: at the crossroad of neural repair and death. *Neural Regen Res*, 10(5):721–5.

Meier, C., Anastasiadou, S., and Knoll, B. (2011). Ephrin-a5 suppresses neurotrophin evoked neuronal motility, erk activation and gene expression. *PLoS One*, 6(10):e26089.

Meng, C., He, Z., and Xing, D. (2013). Low-level laser therapy rescues dendrite atrophy via upregulating BDNF expression: implications for Alzheimer's disease. *J Neurosci*, 33(33):13505–17.

Meng, L., Liu, B., Ji, R., Jiang, X., Yan, X., and Xin, Y. (2019). Targeting the BDNF/TrkB pathway for the treatment of tumors. *Oncol Lett*, 17(2):2031–2039.

Merkouris, S., Barde, Y. A., Binley, K. E., Allen, N. D., Stepanov, A. V., Wu, N. C., Grande, G., Lin, C. W., Li, M., Nan, X., Chacon-Fernandez, P., DiStefano, P. S., Lindsay, R. M., Lerner, R. A., and Xie, J. (2018). Fully human agonist antibodies to TrkB using autocrine cell-based selection from a combinatorial antibody library. *Proc Natl Acad Sci U S A*, 115(30):E7023–E7032.

Messaoudi, E., Ying, S. W., Kanhema, T., Croll, S. D., and Bramham, C. R. (2002). Brain-derived neurotrophic factor triggers transcription-dependent, late phase long-term potentiation in vivo. *J Neurosci*, 22(17):7453–61.

Michaelsen-Preusse, K., Kellner, Y., Korte, M., and Zagrebelsky, M. (2014). *Analysis of Actin Turnover and Spine Dynamics in Hippocampal Slice Cultures*, pages 189–217. Springer New York, New York, NY.

Minichiello, L. (2009). TrkB signalling pathways in LTP and learning. *Nat Rev Neurosci*, 10(12):850–60.

Mizuno, K., Carnahan, J., and Nawa, H. (1994). Brain-derived neurotrophic factor promotes differentiation of striatal GABAergic neurons. *Dev Biol*, 165(1):243–56.

Mizuno, M., Yamada, K., Olariu, A., Nawa, H., and Nabeshima, T. (2000). Involvement of brain-derived neurotrophic factor in spatial memory formation and maintenance in a radial arm maze test in rats. *J Neurosci*, 20(18):7116–21.

Mogi, M., Togari, A., Kondo, T., Mizuno, Y., Komure, O., Kuno, S., Ichinose, H., and Nagatsu, T. (1999). Brain-derived growth factor and nerve growth factor concentrations are decreased in the substantia nigra in parkinson's disease. *Neurosci Lett*, 270(1):45–8.

Mowla, S. J., Farhadi, H. F., Pareek, S., Atwal, J. K., Morris, S. J., Seidah, N. G., and Murphy, R. A. (2001). Biosynthesis and post-translational processing of the precursor to brain-derived neurotrophic factor. *J Biol Chem*, 276(16):12660–6.

Mu, J. S., Li, W. P., Yao, Z. B., and Zhou, X. F. (1999). Deprivation of endogenous brain-derived neurotrophic factor results in impairment of spatial learning and memory in adult rats. *Brain Res*, 835(2):259–65.

Muller, W. and Connor, J. A. (1991). Dendritic spines as individual neuronal compartments for synaptic Ca2+ responses. *Nature*, 354(6348):73–6.

Mullner, F. E., Wierenga, C. J., and Bonhoeffer, T. (2015). Precision of inhibition: Dendritic inhibition by individual GABAergic synapses on hippocampal pyramidal cells is confined in space and time. *Neuron*, 87(3):576–89.

Murer, M. G., Yan, Q., and Raisman-Vozari, R. (2001). Brain-derived neurotrophic factor in the control human brain, and in Alzheimer's disease and parkinson's disease. *Prog Neurobiol*, 63(1):71–124.

Murphy, D. D., Cole, N. B., and Segal, M. (1998). Brain-derived neurotrophic factor mediates estradiol-induced dendritic spine formation in hippocampal neurons. *Proc Natl Acad Sci U S A*, 95(19):11412–7.

Murray, A. J., Sauer, J. F., Riedel, G., McClure, C., Ansel, L., Cheyne, L., Bartos, M., Wisden, W., and Wulff, P. (2011). Parvalbumin-positive CA1 interneurons are required for spatial working but not for reference memory. *Nat Neurosci*, 14(3):297–9.

Murray, K. D., Gall, C. M., Jones, E. G., and Isackson, P. J. (1994). Differential regulation of brain-derived neurotrophic factor and type ii calcium/calmodulin-dependent protein kinase messenger RNA expression in Alzheimer's disease. *Neuroscience*, 60(1):37–48.

Nagahara, A. H., Merrill, D. A., Coppola, G., Tsukada, S., Schroeder, B. E., Shaked, G. M., Wang, L., Blesch, A., Kim, A., Conner, J. M., Rockenstein, E., Chao, M. V., Koo, E. H., Geschwind, D., Masliah, E., Chiba, A. A., and Tuszynski, M. H. (2009). Neuroprotective effects of brain-derived neurotrophic factor in rodent and primate models of Alzheimer's disease. *Nat Med*, 15(3):331–7.

Nagappan, G., Zaitsev, E., Senatorov, V. V., J., Yang, J., Hempstead, B. L., and Lu, B. (2009). Control of extracellular cleavage of proBDNF by high frequency neuronal activity. *Proc Natl Acad Sci U S A*, 106(4):1267–72.

Narisawa-Saito, M., Carnahan, J., Araki, K., Yamaguchi, T., and Nawa, H. (1999). Brain-derived neurotrophic factor regulates the expression of AMPA receptor proteins in neocortical neurons. *Neuroscience*, 88(4):1009–14.

Neves, G., Cooke, S. F., and Bliss, T. V. (2008). Synaptic plasticity, memory and the hippocampus: a neural network approach to causality. *Nat Rev Neurosci*, 9(1):65–75.

Niesmann, K., Breuer, D., Brockhaus, J., Born, G., Wolff, I., Reissner, C., Kilimann, M. W., Rohlmann, A., and Missler, M. (2011). Dendritic spine formation and synaptic function require neurobeachin. *Nat Commun*, 2:557.

Nimchinsky, E. A., Sabatini, B. L., and Svoboda, K. (2002). Structure and function of dendritic spines. *Annu Rev Physiol*, 64:313–53.

Nykjaer, A., Willnow, T. E., and Petersen, C. M. (2005). p75NTR–live or let die. *Curr Opin Neurobiol*, 15(1):49–57.

Obianyo, O. and Ye, K. (2013). Novel small molecule activators of the trk family of receptor tyrosine kinases. *Biochim Biophys Acta*, 1834(10):2213–8.

Ohba, S., Ikeda, T., Ikegaya, Y., Nishiyama, N., Matsuki, N., and Yamada, M. K. (2005). BDNF locally potentiates GABAergic presynaptic machineries: target-selective circuit inhibition. *Cereb Cortex*, 15(3):291–8.

Palop, J. J. and Mucke, L. (2016). Network abnormalities and interneuron dysfunction in alzheimer disease. *Nat Rev Neurosci*, 17(12):777–792.

Parain, K., Murer, M. G., Yan, Q., Faucheux, B., Agid, Y., Hirsch, E., and Raisman-Vozari, R. (1999). Reduced expression of brain-derived neurotrophic factor protein in parkinson's disease substantia nigra. *Neuroreport*, 10(3):557–61.

Park, H. and Poo, M. M. (2013). Neurotrophin regulation of neural circuit development and function. *Nat Rev Neurosci*, 14(1):7–23.

Park, H. Y., Kim, G. Y., Hyun, J. W., Hwang, H. J., Kim, N. D., Kim, B. W., and Choi, Y. H. (2012). 7,8-dihydroxyflavone exhibits anti-inflammatory properties by downregulating the NF-kappaB and MAPK signaling pathways in lipopolysaccharide-treated raw264.7 cells. *Int J Mol Med*, 29(6):1146–52.

Park, H. Y., Park, C., Hwang, H. J., Kim, B. W., Kim, G. Y., Kim, C. M., Kim, N. D., and Choi, Y. H. (2014). 7,8-dihydroxyflavone attenuates the release of pro-inflammatory mediators and cytokines in lipopolysaccharide-stimulated bv2 microglial cells through the suppression of the nf-kappab and MAPK signaling pathways. *Int J Mol Med*, 33(4):1027–34.

Park, M. (2018). AMPA receptor trafficking for postsynaptic potentiation. *Front Cell Neurosci*, 12:361.

Patnaik, A., Zagrebelsky, M., Korte, M., and Holz, A. (2020). Signaling via the p75 neurotrophin receptor facilitates amyloid-beta-induced dendritic spine pathology. *Sci Rep*, 10(1):13322.

Patterson, S. L., Abel, T., Deuel, T. A., Martin, K. C., Rose, J. C., and Kandel, E. R. (1996). Recombinant BDNF rescues deficits in basal synaptic transmission and hippocampal LTP in BDNF knockout mice. *Neuron*, 16(6):1137–45.

Pelkey, K. A., Chittajallu, R., Craig, M. T., Tricoire, L., Wester, J. C., and McBain, C. J. (2017). Hippocampal GABAergic inhibitory interneurons. *Physiol Rev*, 97(4):1619–1747.

Petzold, A., Psotta, L., Brigadski, T., Endres, T., and Lessmann, V. (2015). Chronic BDNF deficiency leads to an age-dependent impairment in spatial learning. *Neurobiol Learn Mem*, 120:52–60.

Phillips, H. S., Hains, J. M., Armanini, M., Laramee, G. R., Johnson, S. A., and Winslow, J. W. (1991). BDNF mRNA is decreased in the hippocampus of individuals with Alzheimer's disease. *Neuron*, 7(5):695–702.

Pizzorusso, T., Ratto, G. M., Putignano, E., and Maffei, L. (2000). Brain-derived neurotrophic factor causes camp response element-binding protein phosphorylation

in absence of calcium increases in slices and cultured neurons from rat visual cortex. *J Neurosci*, 20(8):2809–16.

Poduslo, J. F. and Curran, G. L. (1996). Permeability at the blood-brain and blood-nerve barriers of the neurotrophic factors: NGF, CNTF, NT-3, BDNF. *Brain Res Mol Brain Res*, 36(2):280–6.

Pollock, K., Dahlenburg, H., Nelson, H., Fink, K. D., Cary, W., Hendrix, K., Annett, G., Torrest, A., Deng, P., Gutierrez, J., Nacey, C., Pepper, K., Kalomoiris, S., J, D. A., McGee, J., Gruenloh, W., Fury, B., Bauer, G., Duffy, A., Tempkin, T., Wheelock, V., and Nolta, J. A. (2016). Human mesenchymal stem cells genetically engineered to overexpress brain-derived neurotrophic factor improve outcomes in Huntington's disease mouse models. *Mol Ther*, 24(5):965–77.

Porcher, C., Medina, I., and Gaiarsa, J. L. (2018). Mechanism of BDNF modulation in GABAergic synaptic transmission in healthy and disease brains. *Front Cell Neurosci*, 12:273.

Qian, M. D., Zhang, J., Tan, X. Y., Wood, A., Gill, D., and Cho, S. (2006). Novel agonist monoclonal antibodies activate TrkB receptors and demonstrate potent neurotrophic activities. *J Neurosci*, 26(37):9394–403.

Radin, D. P. and Patel, P. (2017). BDNF: An oncogene or tumor suppressor? *Anticancer Res*, 37(8):3983–3990.

Raus Balind, S., Mago, A., Ahmadi, M., Kis, N., Varga-Nemeth, Z., Lorincz, A., and Makara, J. K. (2019). Diverse synaptic and dendritic mechanisms of complex spike burst generation in hippocampal CA3 pyramidal cells. *Nat Commun*, 10(1):1859.

Rauskolb, S., Zagrebelsky, M., Dreznjak, A., Deogracias, R., Matsumoto, T., Wiese, S., Erne, B., Sendtner, M., Schaeren-Wiemers, N., Korte, M., and Barde, Y. A. (2010). Global deprivation of brain-derived neurotrophic factor in the cns reveals an area-specific requirement for dendritic growth. *J Neurosci*, 30(5):1739–49.

Rauti, R., Cellot, G., D'Andrea, P., Colliva, A., Scaini, D., Tongiorgi, E., and Ballerini, L. (2020). BDNF impact on synaptic dynamics: extra or intracellular long-term release differently regulates cultured hippocampal synapses. *Mol Brain*, 13(1):43.

Redmond, L. and Ghosh, A. (2001). The role of notch and Rho GTPase signaling in the control of dendritic development. *Curr Opin Neurobiol*, 11(1):111–7.

Rex, C. S., Lin, C. Y., Kramar, E. A., Chen, L. Y., Gall, C. M., and Lynch, G. (2007). Brain-derived neurotrophic factor promotes long-term potentiation-related cytoskeletal changes in adult hippocampus. *J Neurosci*, 27(11):3017–29.

Rochefort, N. L. and Konnerth, A. (2012). Dendritic spines: from structure to in vivo function. *EMBO Rep*, 13(8):699–708.

Rose, C. R., Blum, R., Kafitz, K. W., Kovalchuk, Y., and Konnerth, A. (2004). From modulator to mediator: rapid effects of BDNF on ion channels. *Bioessays*, 26(11):1185–94.

Sakane, T. and Pardridge, W. M. (1997). Carboxyl-directed pegylation of brain-derived neurotrophic factor markedly reduces systemic clearance with minimal loss of biologic activity. *Pharm Res*, 14(8):1085–91.

Scalzo, P., Kummer, A., Bretas, T. L., Cardoso, F., and Teixeira, A. L. (2010). Serum levels of brain-derived neurotrophic factor correlate with motor impairment in parkinson's disease. *J Neurol*, 257(4):540–5.

Scheff, S. W., Price, D. A., Schmitt, F. A., DeKosky, S. T., and Mufson, E. J. (2007). Synaptic alterations in CA1 in mild alzheimer disease and mild cognitive impairment. *Neurology*, 68(18):1501–8.

Scheper, V., Schwieger, J., Hamm, A., Lenarz, T., and Hoffmann, A. (2019). BDNF-overexpressing human mesenchymal stem cells mediate increased neuronal protection in vitro. *J Neurosci Res*, 97(11):1414–1429.

Schulz, J., Franke, K., Frick, M., and Schumacher, S. (2016). Different roles of the small GTPases Rac1, Cdc42, and RhoG in CALEB/NGC-induced dendritic tree complexity. *J Neurochem*, 139(1):26–39.

Sconce, M. D., Churchill, M. J., Moore, C., and Meshul, C. K. (2015). Intervention with 7,8-dihydroxyflavone blocks further striatal terminal loss and restores motor deficits in a progressive mouse model of parkinson's disease. *Neuroscience*, 290:454–71.

Sholl, D. A. (1953). Dendritic organization in the neurons of the visual and motor cortices of the cat. *J Anat*, 87(4):387–406.

Shouval, H. Z., Bear, M. F., and Cooper, L. N. (2002). A unified model of nmda receptor-dependent bidirectional synaptic plasticity. *Proc Natl Acad Sci U S A*, 99(16):10831–6.

Simmons, D. A., Belichenko, N. P., Yang, T., Condon, C., Monbureau, M., Shamloo, M., Jing, D., Massa, S. M., and Longo, F. M. (2013). A small molecule TrkB ligand reduces motor impairment and neuropathology in R6/2 and BACHD mouse models of Huntington's disease. *J Neurosci*, 33(48):18712–27.

Soderquist, R. G., Milligan, E. D., Sloane, E. M., Harrison, J. A., Douvas, K. K., Potter, J. M., Hughes, T. S., Chavez, R. A., Johnson, K., Watkins, L. R., and Mahoney, M. J. (2009). Pegylation of brain-derived neurotrophic factor for preserved biological activity and enhanced spinal cord distribution. *J Biomed Mater Res A*, 91(3):719–29.

Squire, L. R. (2009). The legacy of patient h.m. for neuroscience. *Neuron*, 61(1):6–9.

Stewart, M. G., Medvedev, N. I., Popov, V. I., Schoepfer, R., Davies, H. A., Murphy, K., Dallerac, G. M., Kraev, I. V., and Rodriguez, J. J. (2005). Chemically induced long-term potentiation increases the number of perforated and complex postsynaptic densities but does not alter dendritic spine volume in CA1 of adult mouse hippocampal slices. *Eur J Neurosci*, 21(12):3368–78.

Stoppini, L., Buchs, P. A., and Muller, D. (1991). A simple method for organotypic cultures of nervous tissue. *J Neurosci Methods*, 37(2):173–82.

Sun, Y., Lim, Y., Li, F., Liu, S., Lu, J. J., Haberberger, R., Zhong, J. H., and Zhou, X. F. (2012). ProBDNF collapses neurite outgrowth of primary neurons by activating RhoA. *PLoS One*, 7(4):e35883.

Sweatt, J. D. (1999). Toward a molecular explanation for long-term potentiation. *Learn Mem*, 6(5):399–416.

Takata, K., Kitamura, Y., Umeki, M., Tsuchiya, D., Kakimura, J., Taniguchi, T., Gebicke-Haerter, P. J., and Shimohama, S. (2003). Possible involvement of small oligomers of

amyloid-beta peptides in 15-deoxy-delta 12,14 prostaglandin J2-sensitive microglial activation. *J Pharmacol Sci*, 91(4):330–3.

Tan, S., Xiao, Y., Yin, H. H., Chen, A. I., Soong, T. W., and Je, H. S. (2018). Postnatal TrkB ablation in corticolimbic interneurons induces social dominance in male mice. *Proc Natl Acad Sci U S A*, 115(42):E9909–E9915.

Tanaka, J., Horiike, Y., Matsuzaki, M., Miyazaki, T., Ellis-Davies, G. C., and Kasai, H. (2008). Protein synthesis and neurotrophin-dependent structural plasticity of single dendritic spines. *Science*, 319(5870):1683–7.

Tanaka, T., Saito, H., and Matsuki, N. (1997). Inhibition of gabaa synaptic responses by brain-derived neurotrophic factor (BDNF) in rat hippocampus. *J Neurosci*, 17(9):2959–66.

Teng, H. K., Teng, K. K., Lee, R., Wright, S., Tevar, S., Almeida, R. D., Kermani, P., Torkin, R., Chen, Z. Y., Lee, F. S., Kraemer, R. T., Nykjaer, A., and Hempstead, B. L. (2005). ProBDNF induces neuronal apoptosis via activation of a receptor complex of p75NTR and sortilin. *J Neurosci*, 25(22):5455–63.

Threadgill, R., Bobb, K., and Ghosh, A. (1997). Regulation of dendritic growth and remodeling by Rho, Rac, and Cdc42. *Neuron*, 19(3):625–34.

Todd, D., Gowers, I., Dowler, S. J., Wall, M. D., McAllister, G., Fischer, D. F., Dijkstra, S., Fratantoni, S. A., van de Bospoort, R., Veenman-Koepke, J., Flynn, G., Arjomand, J., Dominguez, C., Munoz-Sanjuan, I., Wityak, J., and Bard, J. A. (2014). A monoclonal antibody TrkB receptor agonist as a potential therapeutic for Huntington's disease. *PLoS One*, 9(2):e87923.

Tolwani, R. J., Buckmaster, P. S., Varma, S., Cosgaya, J. M., Wu, Y., Suri, C., and Shooter, E. M. (2002). BDNF overexpression increases dendrite complexity in hippocampal dentate gyrus. *Neuroscience*, 114(3):795–805.

Tongiorgi, E. (2008). Activity-dependent expression of brain-derived neurotrophic factor in dendrites: facts and open questions. *Neurosci Res*, 61(4):335–46.

Tu, S., Okamoto, S., Lipton, S. A., and Xu, H. (2014). Oligomeric abeta-induced synaptic dysfunction in Alzheimer's disease. *Mol Neurodegener*, 9:48.

Turner, B. A., Sparrow, J., Cai, B., Monroe, J., Mikawa, T., and Hempstead, B. L. (2006). TrkB/BDNF signaling regulates photoreceptor progenitor cell fate decisions. *Dev Biol*, 299(2):455–65.

Tyler, W. J. and Pozzo-Miller, L. D. (2001). BDNF enhances quantal neurotransmitter release and increases the number of docked vesicles at the active zones of hippocampal excitatory synapses. *J Neurosci*, 21(12):4249–58.

Udakis, M., Pedrosa, V., Chamberlain, S. E. L., Clopath, C., and Mellor, J. R. (2020). Interneuron-specific plasticity at parvalbumin and somatostatin inhibitory synapses onto CA1 pyramidal neurons shapes hippocampal output. *Nat Commun*, 11(1):4395.

Van Harreveld, A. and Fifkova, E. (1975). Swelling of dendritic spines in the fascia dentata after stimulation of the perforant fibers as a mechanism of post-tetanic potentiation. *Exp Neurol*, 49(3):736–49.

Vidal-Martinez, G., Vargas-Medrano, J., Gil-Tommee, C., Medina, D., Garza, N. T., Yang, B., Segura-Ulate, I., Dominguez, S. J., and Perez, R. G. (2016). Fty720/fingolimod reduces synucleinopathy and improves gut motility in A53T mice: Contributions of pro-brain-derived neurotrophic factor (pro-BDNF) and mature BDNF. *J Biol Chem*, 291(39):20811–21.

Volkman, R. and Offen, D. (2017). Concise review: Mesenchymal stem cells in neurodegenerative diseases. *Stem Cells*, 35(8):1867–1880.

von Bohlen und Halbach, O. (2010). Involvement of BDNF in age-dependent alterations in the hippocampus. *Front Aging Neurosci*, 2.

Wang, S., Yao, H., Xu, Y., Hao, R., Zhang, W., Liu, H., Huang, Y., Guo, W., and Lu, B. (2020). Therapeutic potential of a TrkB agonistic antibody for Alzheimer's disease. *Theranostics*, 10(15):6854–6874.

Wang, Z., Jackson, R. J., Hong, W., Taylor, W. M., Corbett, G. T., Moreno, A., Liu, W., Li, S., Frosch, M. P., Slutsky, I., Young-Pearse, T. L., Spires-Jones, T. L., and Walsh,

D. M. (2017). Human brain-derived abeta oligomers bind to synapses and disrupt synaptic activity in a manner that requires app. *J Neurosci*, 37(49):11947–11966.

Waterhouse, E. G., An, J. J., Orefice, L. L., Baydyuk, M., Liao, G. Y., Zheng, K., Lu, B., and Xu, B. (2012). BDNF promotes differentiation and maturation of adult-born neurons through GABAergic transmission. *J Neurosci*, 32(41):14318–30.

Weissmiller, A. M. and Wu, C. (2012). Current advances in using neurotrophic factors to treat neurodegenerative disorders. *Transl Neurodegener*, 1(1):14.

Whitehouse, P. J., Price, D. L., Clark, A. W., Coyle, J. T., and DeLong, M. R. (1981). Alzheimer disease: evidence for selective loss of cholinergic neurons in the nucleus basalis. *Ann Neurol*, 10(2):122–6.

Whone, A., Luz, M., Boca, M., Woolley, M., Mooney, L., Dharia, S., Broadfoot, J., Cronin, D., Schroers, C., Barua, N. U., Longpre, L., Barclay, C. L., Boiko, C., Johnson, G. A., Fibiger, H. C., Harrison, R., Lewis, O., Pritchard, G., Howell, M., Irving, C., Johnson, D., Kinch, S., Marshall, C., Lawrence, A. D., Blinder, S., Sossi, V., Stoessl, A. J., Skinner, P., Mohr, E., and Gill, S. S. (2019a). Randomized trial of intermittent intraputamenal glial cell line-derived neurotrophic factor in Parkinson's disease. *Brain*, 142(3):512–525.

Whone, A. L., Boca, M., Luz, M., Woolley, M., Mooney, L., Dharia, S., Broadfoot, J., Cronin, D., Schroers, C., Barua, N. U., Longpre, L., Barclay, C. L., Boiko, C., Johnson, G. A., Fibiger, H. C., Harrison, R., Lewis, O., Pritchard, G., Howell, M., Irving, C., Johnson, D., Kinch, S., Marshall, C., Lawrence, A. D., Blinder, S., Sossi, V., Stoessl, A. J., Skinner, P., Mohr, E., and Gill, S. S. (2019b). Extended treatment with glial cell line-derived neurotrophic factor in parkinson's disease. *J Parkinsons Dis*, 9(2):301–313.

Woo, N. H., Teng, H. K., Siao, C. J., Chiaruttini, C., Pang, P. T., Milner, T. A., Hempstead, B. L., and Lu, B. (2005). Activation of p75NTR by proBDNF facilitates hippocampal long-term depression. *Nat Neurosci*, 8(8):1069–77.

Xenos, D., Kamceva, M., Tomasi, S., Cardin, J. A., Schwartz, M. L., and Vaccarino,

F. M. (2018). Loss of TrkB signaling in parvalbumin-expressing basket cells results in network activity disruption and abnormal behavior. *Cereb Cortex*, 28(10):3399–3413.

Xie, H., Leung, K. L., Chen, L., Chan, Y. S., Ng, P. C., Fok, T. F., Wing, Y. K., Ke, Y., Li, A. M., and Yung, W. H. (2010a). Brain-derived neurotrophic factor rescues and prevents chronic intermittent hypoxia-induced impairment of hippocampal long-term synaptic plasticity. *Neurobiol Dis*, 40(1):155–62.

Xie, Y., Hayden, M. R., and Xu, B. (2010b). BDNF overexpression in the forebrain rescues Huntington's disease phenotypes in yac128 mice. *J Neurosci*, 30(44):14708–18.

Xu, Y., Zhao, M., Han, Y., and Zhang, H. (2020). GABAergic inhibitory interneuron deficits in Alzheimer's disease: Implications for treatment. *Front Neurosci*, 14:660.

Yacoubian, T. A. and Lo, D. C. (2000). Truncated and full-length TrkB receptors regulate distinct modes of dendritic growth. *Nat Neurosci*, 3(4):342–9.

Yamada, M. K., Nakanishi, K., Ohba, S., Nakamura, T., Ikegaya, Y., Nishiyama, N., and Matsuki, N. (2002). Brain-derived neurotrophic factor promotes the maturation of GABAergic mechanisms in cultured hippocampal neurons. *J Neurosci*, 22(17):7580–5.

Yamashita, T., Fujitani, M., Hata, K., Mimura, F., and Yamagishi, S. (2005). Diverse functions of the p75 neurotrophin receptor. *Anat Sci Int*, 80(1):37–41.

Yang, G., Pan, F., and Gan, W. B. (2009). Stably maintained dendritic spines are associated with lifelong memories. *Nature*, 462(7275):920–4.

Yoshimoto, Y., Lin, Q., Collier, T. J., Frim, D. M., Breakefield, X. O., and Bohn, M. C. (1995). Astrocytes retrovirally transduced with BDNF elicit behavioral improvement in a rat model of parkinson's disease. *Brain Res*, 691(1-2):25–36.

You, H., Mizui, T., Kiyosue, K., Takao, K., Miyakawa, T., Kato, K., Otsuka, M., Bai, T., Xia, K., Lu, B., and Kojima, M. (2020). Inhibiting proBDNF to mature BDNF conversion leads to autism-like phenotypes in vivo (preprint). *BioRxiv*.

Yuan, Q., Yang, F., Xiao, Y., Tan, S., Husain, N., Ren, M., Hu, Z., Martinowich, K., Ng, J. S., Kim, P. J., Han, W., Nagata, K. I., Weinberger, D. R., and Je, H. S. (2016). Regulation of brain-derived neurotrophic factor exocytosis and gamma-aminobutyric acidergic interneuron synapse by the schizophrenia susceptibility gene dysbindin-1. *Biol Psychiatry*, 80(4):312–322.

Yuste, R. and Denk, W. (1995). Dendritic spines as basic functional units of neuronal integration. *Nature*, 375(6533):682–4.

Zagrebelsky, M., Godecke, N., Remus, A., and Korte, M. (2018). Cell type-specific effects of BDNF in modulating dendritic architecture of hippocampal neurons. *Brain Struct Funct*, 223(8):3689–3709.

Zagrebelsky, M., Holz, A., Dechant, G., Barde, Y. A., Bonhoeffer, T., and Korte, M. (2005). The p75 neurotrophin receptor negatively modulates dendrite complexity and spine density in hippocampal neurons. *J Neurosci*, 25(43):9989–99.

Zagrebelsky, M. and Korte, M. (2014). Form follows function: BDNF and its involvement in sculpting the function and structure of synapses. *Neuropharmacology*, 76 Pt C:628–38.

Zagrebelsky, M., Tacke, C., and Korte, M. (2020). BDNF signaling during the lifetime of dendritic spines. *Cell Tissue Res*.

Zanin, J. P., Montroull, L. E., Volosin, M., and Friedman, W. J. (2019). The p75 neurotrophin receptor facilitates TrkB signaling and function in rat hippocampal neurons. *Front Cell Neurosci*, 13:485.

Zhang, Y. P., Holbro, N., and Oertner, T. G. (2008). Optical induction of plasticity at single synapses reveals input-specific accumulation of alphacamkii. *Proc Natl Acad Sci U S A*, 105(33):12039–44.

Zhang, Z., Liu, X., Schroeder, J. P., Chan, C. B., Song, M., Yu, S. P., Weinshenker, D., and Ye, K. (2014). 7,8-dihydroxyflavone prevents synaptic loss and memory deficits in a mouse model of Alzheimer's disease. *Neuropsychopharmacology*, 39(3):638–50.

Zheng, K., An, J. J., Yang, F., Xu, W., Xu, Z. Q., Wu, J., Hokfelt, T. G., Fisahn, A., Xu, B., and Lu, B. (2011). TrkB signaling in parvalbumin-positive interneurons is critical for gamma-band network synchronization in hippocampus. *Proc Natl Acad Sci U S A*, 108(41):17201–6.

Zhou, Q., Homma, K. J., and Poo, M. M. (2004). Shrinkage of dendritic spines associated with long-term depression of hippocampal synapses. *Neuron*, 44(5):749–57.

Zuccato, C. and Cattaneo, E. (2009). Brain-derived neurotrophic factor in neurodegenerative diseases. *Nat Rev Neurol*, 5(6):311–22.

Zuccato, C., Ciammola, A., Rigamonti, D., Leavitt, B. R., Goffredo, D., Conti, L., MacDonald, M. E., Friedlander, R. M., Silani, V., Hayden, M. R., Timmusk, T., Sipione, S., and Cattaneo, E. (2001). Loss of huntingtin-mediated BDNF gene transcription in Huntington's disease. *Science*, 293(5529):493–8.

Zuccato, C., Marullo, M., Conforti, P., MacDonald, M. E., Tartari, M., and Cattaneo, E. (2008). Systematic assessment of BDNF and its receptor levels in human cortices affected by Huntington's disease. *Brain Pathol*, 18(2):225–38.

B. Supplementary Data

Table B.1.: Referring to Figure 3.1.
Number of c-Fos positive neurons. "N" = number of coverslips (CS) analyzed. Per CS 7 fields of view were analyzed. Data is obtained from 4 independent experiments. Figure 3.1 A; One-way ANOVA $F_{2, 33} = 5.856$, $p = 0.0067$. Figure 3.1 B; One-way ANOVA $F_{3, 44} = 25.95$, $p < 0.0001$.

Number of c-Fos positive neurons						
	DMSO (Fig.A)	7,8-DHF	BDNF	DMSO (Fig.B)	ANA-12	ANA-12 + BDNF
Mean	6.875	6.933	13.55	5.450	0.3250	1.983
SEM	1.297	1.297	2.045	0.9512	0.1338	0.4830
N	12	12	12	12	12	12

Table B.2.: Referring to Figure 3.2 B and C.
Number of c-Fos positive neurons. "N" = number of coverslips (CS) analyzed. Per CS 7 fields of view were analyzed. Data is obtained from 4-5 independent experiments. Figure 3.2 B; One-way ANOVA $F_{2, 30} = 8.772$, $p = 0.001$. Figure 3.2 C; t-test $p = 0.036$.

Number of c-Fos positive neurons					
	CTRL-Ab 1 µg/ml	ZEB85-Ab 1 µg/ml	BDNF	CTRL-Ab 10 µg/ml	ZEB85-Ab 10 µg/ml
Mean	0.9909	2.2750	3.167	1.007	0.7500
SEM	0.1719	0.3380	0.3974	0.07333	0.09124
N	11	12	12	15	14

Table B.3.: Referring to Figure 3.2 D.
Number of c-Fos positive neurons. "N" = number of coverslips (CS) analyzed. Per CS 7 fields of view were analyzed. Data is obtained from 4 independent experiments. Figure 7 D. One-way ANOVA $F_{3, 38} = 4.5$, $p = 0.0085$.

Number of c-Fos positive neurons				
	CTRL-Ab 1 µg/ml	ZEB85-Ab 1 µg/ml	CTRL-Ab 10 µg/ml	ZEB85-Ab 10 µg/ml
Mean	40.75	39.80	32.62	43.62
SEM	2.739	1.483	2.546	1.907
N	10	11	10	11

Table B.4.: Referring to Figure 3.3.
"N" = number of dendrites/neurons. Data is obtained from 2 independent experiments. Figure 3.3 A; One-way ANOVA $F_{3, 101} = 16.85$, $p < 0.0001$. Figure 3.3 B; One-way ANOVA $F_{3, 101} = 6.768$, $p = 0.0003$. Figure 3.3 C; One-way ANOVA $F_{3, 101} = 20.01$, $p < 0.0001$.

TrkB phosphorylation (1 h)					
		CTRL	BDNF	CTRL-Ab 1 µg/ml	ZEB85-Ab 1 µg/ml
Fluorescence intensity	Mean	672.0	1089	538.6	559.6
	SEM	36.66	88.90	52.00	57.79
Puncta Area	Mean	0.1543	0.1825	0.1300	0.1289
	SEM	0.0075	0.0106	0.0093	0.0110
Puncta/µm	Mean	2.251	3.628	2.100	1.945
	SEM	0.1251	0.1955	0.1371	0.2181
	N	28	28	22	27

Table B.5.: Referring to Figure 3.4.
"N" = number of dendrites/neurons. Data is obtained from 2 independent experiments. Figure 3.4 A; t-test $p = 0.0002$. Figure 3.4 C; t-test p ¡ 0.0001. Figure 3.4 B; t-test $p = 0.065$.

TrkB phosphorylation (15 min)			
		CTRL-Ab 10 µg/ml	ZEB85-Ab 10 µg/ml
Fluorescence intensity	Mean	532.1	808.7
	SEM	47.73	48.96
Puncta Area	Mean	0.1332	0.1559
	SEM	0.0099	0.0067
Puncta/µm	Mean	1.958	3.083
	SEM	0.1991	0.1057
	N	28	27

Table B.6.: Referring to Figure 3.5.
"N" = number of dendrites/neurons. Data is obtained from 2 independent experiments. Figure 3.5 B; One-way ANOVA $F_{5, 120}$ = 46.60, $p < 0.0001$. Figure 3.5 C; One-way ANOVA $F_{5, 120}$ = 19.22, $p < 0.0001$. (Figure 3.5 D; One-way ANOVA $F_{5, 120}$ = 30.92, $p < 0.0001$.

TrkB phosphorylation (15 min)							
		CTRL	BDNF	CTRL-Ab 1 µg/ml	ZEB85-Ab 1 µg/ml	CTRL-Ab 10 µg/ml	ZEB85-Ab 10 µg/ml
Fluorescence intensity	Mean	514.8	1139	524.0	420.2	475.5	716.6
	SEM	35.53	75.23	26.10	16.05	23.27	29.20
Puncta Area	Mean	0.1267	0.1686	0.1195	0.1071	0.1176	0.1448
	SEM	0.0061	0.0053	0.0050	0.0040	0.0051	0.0049
Puncta/µm	Mean	1.824	2.894	1.725	1.670	1.605	2.477
	SEM	0.1058	0.1306	0.08108	0.07696	0.08149	0.08154
	N	21	21	21	21	21	21

Table B.7.: Referring to Figure 3.6.
"N" = number of neurons. Data is obtained from 3 independent experiments. One-way ANOVA was used to compare BDNF to 1 µg/mlZEB85-antibody and the respective controls. A t-test was used to compare 10 µg/ml ZEB85-antibody to its respective control. Figure 3.6 B; One-way ANOVA $F_{3, 559}$ = 25.75, $p < 0.0001$; 10 µg/ml: t-test p = 0.0023. Figure 3.6 C; One-way ANOVA $F_{3, 559}$ = 25.75, $p < 0.0001$. 10 µg/ml: t-test p = 0.0041. Figure 3.6 D; One-way ANOVA $F_{3, 559}$ = 23.43, $p < 0.0001$; 10 µg/ml: t-test p = 0.0007. Figure 3.6 E; One-way ANOVA $F_{3, 559}$ = 19.86, $p < 0.0001$.

Neurite complexity							
		CTRL	BDNF	CTRL-Ab 1 µg/ml	ZEB85-Ab 1 µg/ml	CTRL-Ab 10 µg/ml	ZEB85-Ab 10 µg/ml
Total intersections	Mean	39.23	49.71	39.56	43.01	44.97	52.06
	SEM	0.8051	1.173	0.9299	0.8841	1.562	1.690
Branch points	Mean	5.043	8.043	4.752	5.738	7.597	9.899
	SEM	0.3048	0.3804	0.2617	0.2834	0.5163	0.6038
Total neurite length [µm]	Mean	448.9	565.5	444.4	500.0	512.5	612.0
	SEM	10.12	14.04	10.80	11.33	19.29	21.77
Primary neurites	Mean	6.518	7.907	6.496	6.652	6.983	6.916
	SEM	0.1299	0.1861	0.1419	0.1455	0.2015	0.1764
	N	140	141	141	141	119	119

Table B.8.: Referring to Figure 3.7 B.
"N" = number of dendrites/ neurons. Data is obtained for BDNF and CTRL: from 4 independent experiments and for 1 µg/ml ZEB85-Ab and CTRL-Ab: from 6 neurons independent and for 10 µg/ml ZEB85-Ab and CTRL-Ab: from one experiment. Figure 3.7 B; One-way ANOVA $F_{3,\ 288}$ = 6.979, p = 0.0002.

Spine density						
	CTRL	BDNF	CTRL-Ab 1 µg/ml	ZEB85-Ab 1 µg/ml	CTRL-Ab 10 µg/ml	ZEB85-Ab 10 µg/ml
Mean	0.9500	0.9527	0.8851	0.9890	0.9753	0.9467
SEM	0.0232	0.0214	0.0136	0.0159	0.0545	0.0517
N	58	60	88	86	15	15

Table B.9.: Referring to Figure 3.7 C .
"N" = number of dendrites neurons. Data is obtained for BDNF and CTRL: from 3 independent experiments and for 1 µg/ml ZEB85-Ab and CTRL-Ab: from 4 independent experiments. Figure 3.7 C; Two-way ANOVA $F_{3,\ 531}$ = 0.0010, $p < 0.9999$.

Spine types					
		CTRL	BDNF	CTRL-Ab 1 µg/ml	ZEB85-Ab 1 µg/ml
Mushroom	Mean	60.869	59.930	57.607	64.030
	SEM	2.478	2.050	1.761	1.914
Thin	Mean	26.622	26.808	27.765	20.605
	SEM	2.223	2.012	1.741	1.566
Stubby	Mean	12.435	13.263	14.423	15.347
	SEM	1.300	1.345	1.180	1.072
	N	40	37	52	52

Table B.10.: Referring to Figure 3.8.
"N" = number of dendrites neurons. Data is obtained from 3 independent experiments. Figure 3.8 B; One-way ANOVA $F_{3,\ 187}$ = 10.89, $p < 0.0001$.

Spine density				
	CTRL-Ab	CTRL-Ab + oAβ	ZEB85-Ab	ZEB85-Ab + oAβ
Mean	0.8687	0.7516	0.8777	0.8525
SEM	0.0175	0.0182	0.0184	0.0170
N	47	49	47	48

Table B.11.: Referring to Figure 3.9 C.
"N" = number of neurons. Data is obtained from 3 independent experiments. Figure 3.9 C; Two-way ANOVA $F_{=3,13063} = 234.4$, $p < 0.0001$.

Parvalbumin interneuron Sholl analysis								
	CTRL-Ab		BDNFΔ + CTRL-Ab		ZEB85-Ab		BDNFΔ +ZEB85-Ab	
µm	Mean	SEM	Mean	SEM	Mean	SEM	Mean	SEM
50	8.56	0.25	7.88	0.27	8.28	0.31	8.06	0.34
100	11.62	0.36	9.81	0.36	11.35	0.34	11.35	0.39
150	8.86	0.48	6.45	0.42	10.27	0.45	9.55	0.46
200	4.77	0.47	2.34	0.29	7.05	0.46	4.95	0.40
250	1.81	0.28	0.56	0.10	3.17	0.36	1.67	0.25
300	0.49	0.13	0.08	0.04	0.91	0.16	0.37	0.08
350	0.05	0.03	0.01	0.01	0.18	0.06	0.08	0.03
400	0	0	0	0	0.04	0.02	0	0
440	0	0	0	0	0.02	0.01	0	0
N	75		75		74		74	

Table B.12.: Referring to Figure 3.9 D-F.
Data is obtained from 3 independent experiments. Figure 3.9 D; One-way ANOVA $F_{3,\,293} = 24.55$, $p < 0.0001$. Figure 3.9; One-way ANOVA $F_{3,\,293} = 10.05$, $p < 0.0001$. Figure 2 3.9; One-way ANOVA $F_{3,\,294} = 22.55$, $p < 0.0001$.

Parvalbumin interneuron dendritic complexity					
		CTRL-Ab	BDNFΔ + CTRL-Ab	ZEB85-Ab	BDNFΔ + ZEB85-Ab
Total intersections	Mean	181.6	139.9	211.5	187.1
	SEM	6.172	5.183	6.259	6.400
Branch points	Mean	18.89	13.56	19.32	19.66
	SEM	1.012	0.7353	0.8618	1.013
Total dendritic length [µm]	Mean	2313	1722	2633	2361
	SEM	85.12	66.47	84.97	85.67
	N	75	75	74	73

Table B.13.: Referring to Figure 3.10.
"N" = number of dendrites neurons. Data is obtained from 1 experiment. Figure 3.10 B One-way ANOVA $F_{3, 53} = 1.724$, $p = 0.1733$.

Spine density				
	CTRL-Ab	BDNFΔ + CTRL-Ab	ZEB85-Ab	BDNFΔ + ZEB85-Ab
Mean	0.9179	0.9150	1.071	0.9164
SEM	0.0346	0.0672	1.0710	0.0516
N	14	14	15	14

Table B.14.: Referring to Figure 3.11.
"N" = number of dendrites neurons. Data is obtained from 1 experiment. Figure 3.11 B; One-way ANOVA $F_{3, 36} = 0.6039$, $p = 0.6167$. Figure 3.11 C; One-way ANOVA $F_{3, 36} = 0.9205$, $p = 0.4407$. Figure 3.11 D; One-way ANOVA $F_{3, 36} = 1.192$, $p = 0.3264$. Figure 3.11 E; One-way ANOVA $F_{3, 36} = 0.5228$, $p = 0.6694$.

Dendritic morphology and spine density - BDNFΔ					
		CTRL-Ab	BDNFΔ + CTRL-Ab	ZEB85-Ab	BDNFΔ + ZEB85-Ab
Total intersections	Mean	271.1	252.4	244.3	223.9
	SEM	23.25	29.22	25.45	22.17
Branch points	Mean	23.90	26.40	21.50	20.30
	SEM	2.541	4.031	2.491	1.680
Total dendritic length [µm]	Mean	3167	2969	2899	2642
	SEM	270.6	337.6	321.8	263.9
Primary dendrites	Mean	8.800	8.500	8.800	6.900
	SEM	0.8000	1.014	0.9522	0.4583
Spine density	Mean	0.9680	0.8625	1.130	1.323
	SEM	0.0466	0.0427	0.0514	0.0867
	N	10	10	10	10

Table B.15.: Referring to Figure 3.12 A.
"N" = number of recorded slices. Only every 5th minute/value is depicted. Two-way ANOVA $F_{1, 35} = 0.3307$, $p = 0.5689$

Electrophysiology ZEB85-Ab acute slices				
	CTRL-Ab 1 µg/ml		**ZEB85-Ab 1 µg/ml**	
Time [min]	Mean	SEM	Mean	SEM
0	100.42	0.37	100.58	0.27
5	99.90	0.48	100.43	0.43
10	100.12	0.41	99.39	0.37
15	100.20	0.45	99.01	0.30
20	151.18	9.90	144.94	9.12
25	192.01	17.71	193.63	14.26
30	169.86	11.01	177.73	12.05
35	158.20	7.78	166.70	9.58
40	153.06	6.04	159.03	8.19
45	147.04	5.71	153.15	6.68
50	145.97	6.71	149.59	6.21
55	139.23	4.65	147.03	5.62
60	137.06	4.65	141.57	5.56
65	134.78	4.34	140.07	5.17
70	133.51	4.11	139.54	4.52
75	131.49	4.49	134.63	4.29
80	131.09	4.42	134.49	4.11
N	18		19	

Table B.16.: Referring to Figure 3.12 B.
"N" = number of recorded slices.

Electrophysiology ZEB85-Ab acute slices				
	CTRL-Ab 1 µg/ml		**ZEB85-Ab 1 µg/ml**	
Time [min]	Mean	SEM	Mean	SEM
20-25	175.43	13.17	175.83	11.21
75-80	131.18	4.45	134.40	4.25
N	18		19	

Table B.17.: Referring to Figure 3.12 D.
"N" = number of recorded slices. Only every 5th minute/value is depicted.Two-way ANOVA $F_{1, 18}$ = 4.036, p = 0.0598.

Electrophysiology OHCs				
	CTRL-Ab 10 µg/ml		**ZEB85-Ab 10 µg/ml**	
Time [min]	Mean	SEM	Mean	SEM
0	101.30	2.77	104.39	2.87
5	102.60	3.80	95.15	3.29
10	131.60	34.64	340.22	90.49
15	93.10	6.53	263.05	75.01
20	85.40	10.40	211.47	65.21
25	93.40	13.29	199.63	62.44
30	75.9	12.72	223.80	71.01
35	76.50	12.16	202.77	66.38
40	78.60	12.87	195.50	56.02
N	10		10	

Table B.18.: Referring to Figure 3.12 E.
"N" = number of recorded slices.

Electrophysiology OHCs				
	CTRL-Ab 10 µg/ml		**ZEB85-Ab 10 µg/ml**	
Time [min]	Mean	SEM	Mean	SEM
10-15	114.8	19.5	311.6	88.9
35-40	79.3	13.9	183.4	51.0
N	10		10	

C. List of Figures

D. List of Tables

E. Abbreviations

ACSF	Artificial cerebrospinal fluid
CaMKII	$Ca2^{+}$/calmodulin - dependent protein kinase
AD	Alzheimr's disease
AMPA	α-amino-3-hydroxy-5-methyl-4-isoxazole propionic acid
AMPAR	α-amino-3-hydroxy-5-methyl-4-isoxazole propionic acid receptor
ANOVA	Analysis of variance
Aβ	Amyloid-β
BBB	Blood brain barrier
BDNF	Brain-derived neurotrophic factor
CA	Cornu ammonis
CNS	Central nervous system
CTRL	Control
CTRL-Ab	Control-antibody
DAPI	4',6-diamidino-2-phenylindole
DIV	Days in vitro (post transplantation)
DG	Dentate gyrus
DMSO	Dimethyl sulfocide
EC	Enthorhinal cortex
Erk	Extracellular signal-regulated kinase
fEPSP	Field excitatory post synaptic potential
FOV	Field of view
GABA	γ-aminobutyric acid
GBSS	Gey's balanced salt solution
GFP	Green fluorescent protein
KO	Knockout
LTP	Long-term potentiation
MAP2	Microtubule-associated protein 2
NA	Numerical aperture
NB^{-}/ NB^{+}	Neurobasal-/ Neurobasal+ medium

NMDA	N-methyl-D-aspartate
NT	Neurotrophin
NTR	Neurotrophin receptor
NMDAR	N-methyl-D-aspartate receptor
PB	Phosphate buffer
PBS	Phosphate buffered saline
PSD	Postsynaptic density
PV$^+$	Parvalbumin positive
ROI	Region of interest
RT	Room temperature
TBS	Theta burst stimulation
TrkB	Tropomyosin receptor kinase B
WT	Wild-type
7,8-DHF	7,8-Dihydroxyflavone